# Using Nanotechnology in the Finishing of Cellulosic Fabrics

## Dissertation

zur Erlangung des akademischen Grades eines
Doktors der Naturwissenschaften
– Dr. rer. nat. –

vorgelegt von

**Asmaa Farouk Ahmed Saleh**

geboren in Cairo, Ägypten

Deutsches Textilforschungszentrum Nord-West e.V.,
Institut an
der
Universität Duisburg-Essen

**2011**

Die vorliegende Arbeit wurde im Zeitraum von Dezember 2006 bis Dezember 2010 im Arbeitskreis von Prof. Dr. E. Schollmeyer am Deutsches Textilforschungszentrum Nord-West e.V., Institut an der Universität Duisburg-Essen durchgeführt.

Tag der Disputation: 02-03-2011

Gutachter: Prof. Dr. E. Schollmeyer
Prof. Dr. M. Ulbricht

Vorsitzender: Prof. Dr. Alfred V. Hirner

# Using Nanotechnology in the Finishing of Cellulosic Fabrics

Thesis submitted to
chemistry department, University of Duisburg-Essen
in order to fulfill the requirements for the academic degree

**Doctor rerum naturalium (Dr. rer. nat)**

Thesis presented

by

***Asmaa Farouk Ahmed Saleh***

born
on 04. March 1978 in Cairo - Egypt

First referee: **Prof. Dr. E. Schollmeyer**
Second referee: **Prof. Dr. M. Ulbricht**

Day of promotion: 02.03.2011

# *Acknowledgement*

*All praises and thanks are to Allah, the Lord of the world, the most Beneficent, the most kind for helping me to finish this work.*

*I feel grateful to a number of people in German Textile Research Institute, Krefeld, Germany, who supported me to carry out this work. First and foremost, my heartily deep thanks, gratitude and pleasure to advisor* ***Prof. Dr. E. Schollmeyer*** *for his encouragement, kind support, his invaluable technical and leader advice, suggestions, discussions and guidance were a real support to complete this thesis.*

*Deepest gratefulness and indebtedness to* ***Prof. Dr. M. Ulbricht,*** *University of Duisburg-Essen, for his benevolent supervision as referee, enthusiastic attention, and kindly guidance throughout this work.*

*I owe deepest thanks to my co-advisor* ***Dr. T. Textor*** *for supporting me during my work, his critical reading and discussions and also the useful suggestions to my thesis. He not only provided me with the knowledge, but also teaches me how to acquire it, crack problems, and express ideas. His personality has really influenced me.*

*I am deeply grateful for* ***Prof. Dr. A. Marija Grancacic,*** *faculty of Textile Technology, University of Zagreb, Croatia, for measuring the ultraviolet protection factor in her lab for the protection measurements in this thesis.*

*I would like to thank all staff members of German Textile Research Institute, especially* ***Dr.D. Knittel****,* ***Dr. K.Opwis, Vahid Ameri*** *and* ***Mrs. Leonie Derksen*** *for their concern and kindly support.*

*Very special thanks to the Textile Research Division, National Research Centre, Dokki, Cairo, and the Egyptian Missions Department for giving me the opportunity and the financial support to pursue my Ph.D degree in Germany.*

*Last but not least I wish to acknowledge* ***my husband*** *for his patience and understanding during the different phases of my work, whose immeasurable love and supports are always my source of power to overcome all difficulties. He spared no effort until this work comes to existence.*

***Asmaa Farouk Ahmed Saleh***

*To my family and my husband*

# Abstract

By nanoparticles coating on textile surfaces, mechanical, physical and chemical properties of the textiles can be modified, leading to creation of unique functions. For example, UV protection of some kinds of textile substrates can be achieved through coating a substrate with thin layer of ZnO or $TiO_2$ nanoparticles. This thesis aims to the synthesis and characterization of nanosized zinc oxide particles of different concentrations and various sizes that highly absorb UV light and provide textiles with added functionality such as UV-protection, antibacterial, hydrophobicity, self-cleaning and good dyeability properties. In textile finishing field the washing durability of the finishing agent is very important factor depends on the affinity of the finishing agent or, in the case of polymer coatings, on how well the polymers can bind with the textile surface. Theoretically, the chemical bond between the finishing agent and the textile surface is the best way to achieve durability.

In this study, sol-gel based inorganic-organic hybrid polymers were modified/filled with ZnO nanoparticles and were applied to cellulosic cotton (100%) and cotton/polyester (65/35%) fabrics. These modified inorganic-organic hybrid polymers were based on 3-glycidyloxypropyltrimethoxysilane (GPTMS).

ZnO nanoparticles sol has long stability for further processing. Complete finishing ZnO/GPTMS sols prepared in this work were stable for several hours which is also sufficient for an industrial application. The most important results are:

- The effectiveness of the novel finishing as UV-protection was determined by UV-Vis spectroscopy and by evaluation of the ultraviolet protection factor (UPF). The influences of the finishing for some general textile properties e.g. tensile strength, elongation, air permeability, and degree of whiteness, wear-resistance, stiffness as well as the durability of the treatments were investigated.
- The antibacterial performance of these sol-gel derived hybrid materials was investigated against Gram-negative bacterium *Escherichia coli DSMZ 498* and Gram-positive *Micrococcus lutues ATCC 9341*. The effect of particle size and concentration on the antibacterial performance is examined. Bacteriological tests such as Zone of inhibition test, AATTC Test Method 100-200 and Tetrazolium/formazan test (TTC) were performed in nutrient agar media on solid agar plates and in liquid broth systems using different concentrations and different particle size of ZnO nanoparticles. In this part of thesis a lot of experiments were

carried out to be able to understand the ZnO nanoparticle action as antibacterial finish. This study showed the enhanced antibacterial activity of different concentration and different particle sizes of ZnO nanoparticles against a Gram-negative bacterium and a Gram–positive *Micrococcus lutues* in repeated experiments. This demonstrated that the antibacterial activity of ZnO nanoparticles increases with increasing the concentration of ZnO nanoparticles and also with decreasing the particle size of ZnO nanoparticles.

- Also the antibacterial performance of sol-gel derived inorganic-organic hybrid polymers (GPTMS) filled with ZnO nanoparticles-chitosan composite against a Gram-negative bacterium and a Gram–positive bacterium has been investigated. Chitosan also in this thesis has been used as antimicrobial coating agent, since different concentrations of three different molecular weights (MW) of chitosan with equal degree of deacetylation (DD, 85%) were examined. The influences of the finishing composite for some general textile properties as e.g. crease recovery angle, tensile strength, elongation, air permeability, and degree of whiteness, stiffness as well as the durability of the treatments were investigated. The antibacterial activity of textile treated with hybrid polymers modified with both ZnO nanoparticles and chitosan increases with decreasing the molecular weight of chitosan.
- Hydrophilic cellulosic fabrics pretreated with ZnO-containing hybrid polymers were made superhydrophobic after surface hydrophobization with stearic acid. Drop penetration time (TEGEWA test) and contact angle for cotton and cotton/polyester fabrics before and after treatment with stearic acid as hydrophobic additive were examined. For the cellulosic fabrics treated with stearic acid only, the water contact angle on the fabric surface remained lower than 50°, treatment with ZnO nanoparticle only did not change the hydrophilic surface of cellulosic fabrics used. However, for the fabrics treated with both inorganic-organic hybrid polymers (GPTMS) filled with ZnO nanoparticle and stearic acid, a contact angle higher than 150° can be obtained.
- Photocatalytic degradation of methylene blue by different ZnO nanoparticles concentrations was also studied. Self-cleaning properties of different ZnO concentrations/GPTMS coated fabrics was also investigated. Photocatalytic activity of ZnO nanoparticles was evaluated in normal laboratory environment, under dark condition and after UV-irradiation.

Photocatalytic activity of fabrics coated with different ZnO concentrations within the

coating layer was evaluated.

- Dyeing processes were carried out combining the ZnO-modified hybrid polymers with an exemplarily chosen reactive dyestuff (Intracron red BF-3RM 150%). The result of the dyeing process has been improved by increasing the amount of ZnO nanoparticles or reducing the particle size. The color strength (K/S) and the UV-protection property of the dyed fabrics were also investigated.

The use of hybrid polymers modified with ZnO is therefore a promising approach for the development of highly UV-protecting textiles. The inorganic UV-absorber ZnO is highly stable against degradation and it is non-toxic. Literature discusses various (active) species and processes responsible for the antibacterial action of ZnO. Therefore a particular attention is paid to investigate active species available in the described systems as well as to observe possible interaction between the nanoparticles and bacteria. The sol-gel approach used here for the preparation of the coating materials guarantees a simple processing easily transferred to textile industry. Furthermore the principles of sol-gel technique allow combining additional properties in a single coating material e.g. UV-protection, abrasion resistance, antibacterial activity, hydrophobic and even self-cleaning properties.

# Contents

# List of Figures

# List of Tables

# Chapter 1

# 1. Introduction

## 1.1. Introduction to chemical finishing

It is well known that conventional textile wet processes namely: pretreatments, coloration and chemical finishes, are costly, environmentally unfriendly and adversely affect the overall performance properties of the treated textiles [1].

In recent years, there has been increasing interest in exploring new eco-friendly textile processing techniques e.g. nano-, bio-, plasma technologies, which could cut the materials/water/energy consumptions, lower the cost, upgrade the performance and the functional properties, improve life time, cope with the increasing awareness of environmental protection as well as satisfy the consumer demands [2].

Therefore in order to achieve improved fabric functionalities and performance properties, e.g. UV-protection, antimicrobial activity, water and oil repellency ect. nanotechnology applications have become a very important technique in textile industry especially in textile finishing. Figure 1 shows some of nanosol based textile functionalisation possibilities.

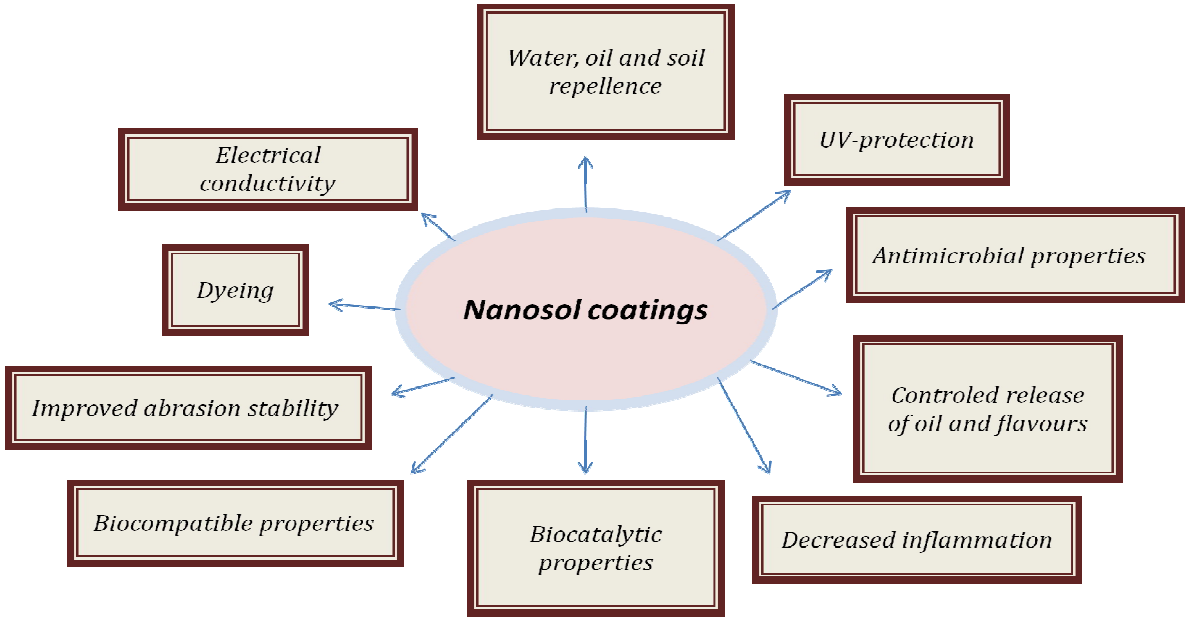


**Figure.1:** Some possibilities of textile functionalisation by modified nanosol [3]

## 1.2. Nanotechnology

Nanotechnology is an innovative tool of fabricating materials smaller than 100 nanometers (one nanometer = $10^{-9}$ meter) [1]. There are different approaches for classification of nanomaterials such as dimension (1, 2 or 3 dimensions < 100 nm), phase composition (single phase, multi-phase solids or systems) as well as manufacturing process (gas phase or liquid phase reaction, mechanical procedures) [1, 3, 4].

The main classes of nanoscale structures are: nanoparticles, e.g. nano metal oxides, nano wire or tubes e.g. carbon nano tubes, nano layers, and nanopores, e.g. aerogel.

Both top-down and bottom-up processes can be used for manufacturing nanostructures, compare Figure 2.

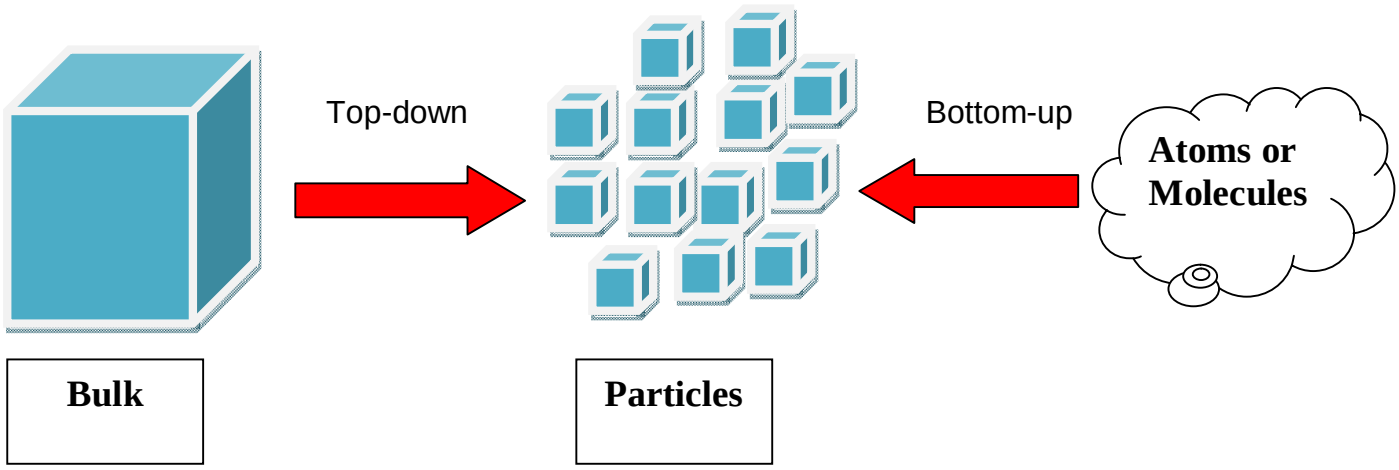


**Figure 2:** Two basic approaches to nanoparticles production: top-down (from lifte to right), and bottom-up (from right to lifte) [5]

Inorganic-based nano-structured materials can be categorized in two main groups namely: **i)** inorganic nanoparticles and their nanocomposites, e.g. $TiO_2$, $Al_2O_3$, ZnO, Ag, Cu nanoparticles, carbon nano tubes, nano layer clay and their nano composites and **ii)** inorganic nano-structured loaded organic carriers, e.g. cyclodextrin loaded with or nano- and micro- capsules having inorganic nanoparticles [6].

Nowadays, nanotechnology has become one of the most important emerging technologies in the textile industry for many reasons such as: more effective, less water/energy/chemicals consumption and cost, less changes to physico-mechanical

properties of the treated textiles, better quality, functionality and durability of important properties, and the most important is less environmental impacts [4].

## 1.3. Nanotechnology in textile finishing

As the use of high performance textiles and the increasing concern over environmental and ecological issues have grown, the urgent need for innovative finishing technologies, e.g. nanotechnology, to impart the demanded functional properties and to cope with the need for revolutionary textile products to face the great challenges in the global market without adversely affecting the environment has grown accordingly.

The imparted functional properties of textile products are determined by: type of substrate, finishing formulation, finishing technique, available equipments, and performance requirements as well as economical and ecological aspects.

The wave of nanotechnology has shown a great potential in textile finishing to improve existing textile performances as well as to develop and impart extraordinary functions such as antimicrobial, UV protection properties, oil and water repellency, maintaining fabric breathability, flam-retardant functionality and self cleaning properties [1].

### 1.3.1. UV protective finish

Over exposure to UV radiation (Table 1), especially UV-B (280-320 nm) can cause premature ageing and sunburn of the skin as well as degradation of textile materials [7]. Therefore there is a great demand for the UV-protection textiles materials. The enhancement in UV-protection functionality depends on nature of textile fibres, fabric construction, dyeing and finishing conditions, using of certain additives such as UV-absorbers and brightening agents, as well as laundering conditions of the garments [8]. Reducing the exposure time to UV-radiation along with using protective clothes with high UPF (ultraviolet protection factor) values in addition to sunscreens are the main options of protection [9].

Table 1 shows the characteristics of solar radiation striking the earth's surface.

**Table 1:** Spectrum of the sun light

| Spectrum of the Sunlight | Wave length range [nm] | Fraction of the total energy [%] | Energy [W/m$^2$] |
|---|---|---|---|
| UV-C<br>UV-B<br>UV-A | 200-285<br>285-320<br>320-400 | 0<br>0.4<br>3.9 | -<br>4<br>44 |
| visible light | 400-800 | 51.8 | 580 |
| infrared | 800-3000 | 43.9 | 492 |

Nano-structured materials based on ZnO-nanoparticles (having some advantages such as lower cost, white appearance, UV-blocking property and not harmful) can be used to impart outstanding UV-blocking property to the finished textiles [10].

When straight light falls onto a textile, part of the radiation is reflected, the material absorbs another part and the remainder transmitted through it as shown in Figure. 3.

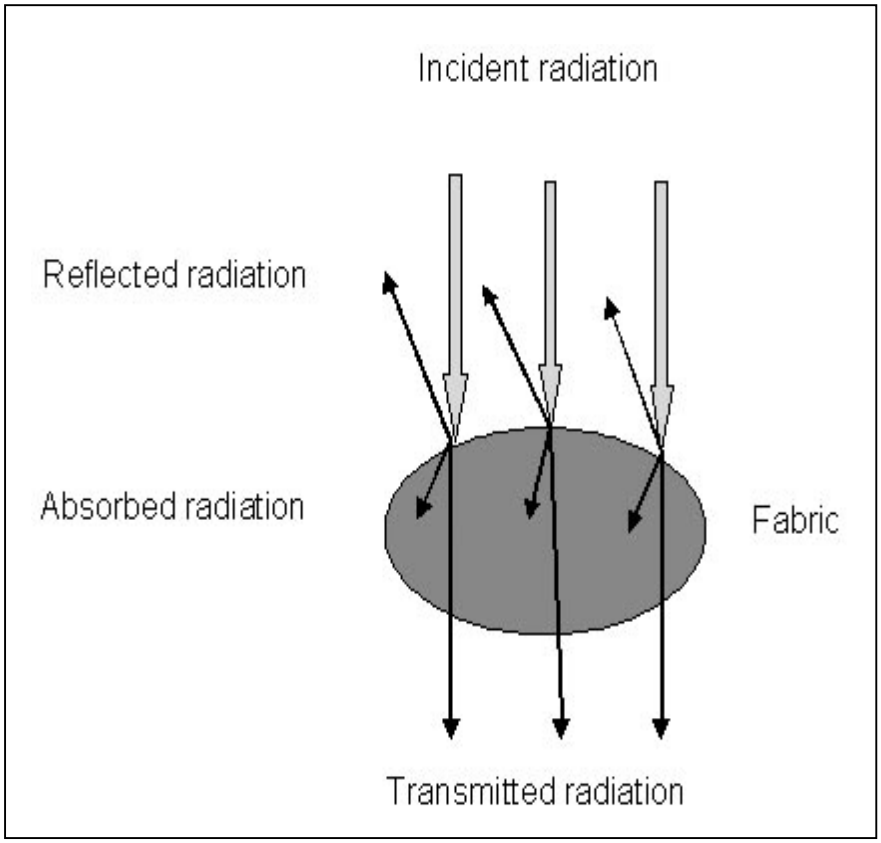


**Figure 3:** Radiation irradiating a textile surface

### 1.3.1.1. Evaluation of UV protection finishes

UPF is the abrevation of the ultraviolet protection factor. It indicates how much longer a person wearing the textile can stay in the sun before the start of skin reddening occurs compared to an unprotected person [11-13]. UPF has been adopted to create awareness among the end users of the negative impacts and effects of UV-radiation. The UV protection factor is determined by using the following equation [11, 12].

$$UPF = \frac{\sum_{\lambda = 280\ nm}^{400\ nm} E_\lambda \, S_\lambda \, \Delta\lambda}{\sum_{\lambda = 280\ nm}^{400\ nm} E_\lambda \, S_\lambda \, T_\lambda \, \Delta\lambda}$$

where:

E(λ) = the solar irradiance [W $m^{-2}$ $nm^{-1}$],

S(λ) = the erythema action spectrum,describing the harmfulness of the different wavelengths,

T(λ) = the spectral transmittance through specimen at wavelength **λ,**

Δλ = the wavelength interval of the measurements [nm].

As described the UPF [14] of a textile material is determined by the transmission of the UV radiation through the textile material. Transmission of a given material is depending on [14]:

- the specific fiber material,
- structural characteristics of the fabric,
- moisture content,
- the color and dyeing intensity,
- presence of optical brightening agents,
- specific finishing products, e.g. UV absorbers,
- laundering conditions of the garments.

## 1.3.2. Antibacterial finish

### 1.3.2.1. Necessity of antibacterial finishes

The growth of microorganisms on textiles, especially natural fibres-based textiles, could be discussed in terms of large receptive surface area along with availability of proper conditions for growing, i.e. temperature, oxygen, moisture and nutrients [15]. The growth of microorganism has negative effects not only on textiles but also on the wearer (in case of clothes), since it results in biodegradation of textile materials along with their dissemination as a health risk.

### 1.3.2.2. Requirements for antibacterial finishes

An effective antimicrobial finish should be: quick acting to be effective, able to kill or stop the growth of microorganisms, it has to be durable to wash or dry cleaning, compatible with other ingredients in the finishing formulation, has minimal impacts on both the environment and the product quality, easy to apply for low cost and low toxicity criteria [16].

### 1.3.2.3. Mechanism of antibacterial finishes

Antimicrobial products can be classified into: i) bacteriostats, i.e. that stop the growth and spread of microbes, and ii) bacteriocides, i.e. that actually kill microbes. An effective biocide must reach and interact with its microbial target sites.

The bacteriostatic mechanisms of action of antimicrobial finishes are including preventing cell production, blocking of enzymes, damaging cell membrane, and/or destruction of the cell wall and poising of the cell from within [1].

The antimicrobial efficiency of biocide formulations varies greatly between different types of microorganisms. Resistance to disinfection follows the decreasing order:

Mycobacterium > Gram -ve bacteria > Gram +ve bacteria.

### 1.3.2.4. Antibacterial finishes and their effect

Chemistry of some antimicrobial finishes as well as their mode of action could be summarized as follows [16]:

- Oxidizing agents such as aldehydes, halogens and peroxy compounds, these compounds can attack the cell membrane, arrive the cytoplasm and change/inactivate the microorganism's enzymes.
- Natural herbal products can be used for antimicrobial finishes.
- Chitosan is an effective natural antimicrobial agent derived from Chitin, an important component in crustacean shells.
- Radical formers like halogens, isothiazones and peroxo compounds; these are source risks to nucleic acids, since they are very reactive (also at low concentration level) due to the presence of free electrons.
- Complexing metallic compounds based on metals like cadmium, silver, copper and mercury cause inhibition of the metabolism.
- Triclosan 5-chloro-2-(2,4-dichloro phenoxyl) phenol products. Triclosan inhibits growth of microorganisms by penetrating and disturbing their cell.
- Quaternary ammonium compounds (polycationic properties). Fabrics finished with these substances lead finally to the breakdown of the cell.

### 1.3.2.5. Evaluation of antibacterial activity

Various tests have been used to determine the effectiveness of the antibacterial activity of textiles. Some of these tests are [1]:

- **Zone of inhibition test:** Rapid qualitative method for determining antibacterial activity of treated textile materials against both Gram-positive and Gram-negative bacteria. In this test, by showing the inhibition zone around the tested sample, it can be shown if a tested finishing agent is protecting the textile from microorganisms or not.
- **AATTC Test Method 100-2004:** It is quantitative method for determining the degree of antibacterial activity of treated textiles. The bacterial growth amount in inoculated and incubated textiles is determined by using serial dilutions which followed by inoculations in sterile agar plate.
- **Tetrazolium/formazan test (TTC):** TTC- test method is considered a rapid method for evaluating the antibacterial activity of the finished fabrics. The red

formazan obtained indicates the activity and viability of the cells. Since, in the presence of bacteria, tetrazolium salts (TTC) is reduced to red formazan.

### 1.3.3. Water repellent finishes

Water-repellent finish should in the best case protect textile fabrics from wetting, without adversely affecting the air permeability of the finished fabrics, through reducing the free energy at the fibre surface. A surface tension of fabric surface is lower than that of the liquid is necessary to active repellent surfaces [1].

#### 1.3.3.1. Mechanisms of repellency

By reducing the free energy at textile fabric surfaces, repellent finishes achieve their properties. Surfaces that exhibit low interactions with liquids are referred to as low energy surfaces, i.e. if the bonding forces between the fabric surface and the liquid are less than the internal cohesive interactions within the liquid, the drop will not spread [17]. Low energy surfaces can be applied to textiles through the chemical reaction of the repellent material with the fabric surface. Examples of these are fatty acid resins, waxes and fluorinated.

#### 1.3.3.2. Super-hydrophobic coatings

A preparation of superhydrophobic surfaces is an important topic in recent years for both technological and scientific concern. Lotus leaf is the best example for a self-cleaning superhydrophobic surface, since water drops bead up and roll off the surface of the leaf without wetting it. The binary micro–nanoscale surface roughnesses together with the presence of hydrophobic epicuticular wax crystals cause the superhydrophobicity of the lotus leaf surface [18]. Wenzel model [19] and Cassie–Baxter model [20] are two theoretical models for the study of superhydrophobic surface. Wenzel model states that water droplet penetrates a rough surface while the water droplet suspends on the top of it for Cassie–Baxter model. A mixture of silane hydrophobes (such as long-chain alkyltrialkoxysilanes) and silane crosslinkers as a non-fluorine silane can be used for getting hydrophobic surfaces [21], for example Daoud et al. [22], made treatment for cotton surface using a mixture of silanes, and obtained a water contact angle of 141°. For superhydrophobic surfaces preparation, a lot of work was done [23–28], and different approaches have been done to get superhydrophobic textiles [29-35]. Wang et al [32] incorporate gold particles into cotton

fabrics and induce a dual-size surface topology.

Mechanical and chemical surface modifications done by Michielsen and Lee [36] through the grafting of 1H,1H-perfluorooctylamine or octadecylamine to poly(acrylic acid) chains, which was previously grafted onto a Nylon 6,6 woven fabric surface, to prepare artificial superhydrophobic surfaces.

Li et al. [35] prepared superhydrophobic cotton surfaces from water glass and nonfluorinated alkylsilane. Several techniques, including the most important sol–gel processes have been used for the preparation of superhydrophobic surfaces.

Coating of textile fabrics with silica nanosols containing perfluoroalkyl compounds has been used to achieve ultra-hydrophobic, oleophobic as well as soil repellent functional properties [37-39]. Moreover, many attempts have tried to increase the hydrophobic properties of textiles by using inorganic sols based on silica or titanium dioxide along with other hydrophobic additives, e.g. polysiloxanes [40,41].

Non-fluorinated hydrophobic nanosols based on long chain alkylsilane additives have been used to avoid the negative environmental impacts of fluorinated compounds as well as to attain coated fabrics with ultra-hydrophobic properties [42].

#### 1.3.3.3. Evaluation of textiles treated with water repellent finishes

Water repellency can be evaluated using the water drop test (method standardised by TEGEWA) [43], contact angles (CA) and the spray test.

### 1.3.4. Photocatalytic activity

A merged word Photocatalysis is referred to two parts, “photo” and “catalysis”. Photocatalysis is a reaction which uses light (photo) to activate a substance which modifies the rate of a chemical reaction without being included itself (catalysis) [44]. As an attractive multi-functional material, nanosized $TiO_2$ or ZnO have been attracted attention for their photocatalytic activities thereby enhancing the extent of degradation of organic pollutants, i.e. self cleaning and environmental purification under UV-irradiation from sun light or illuminated light sources [45].

#### 1.3.4.1. Mechanism of photocatalysis

When photocatalyst e.g. semiconductor $TiO_2$ or ZnO was irradiated with UV-light, electron ($e^-$) from the valence band was excited to the conduction band resulting in the formation of holes ($h^+$) in the valence band. Both excited state electrons (in

conduction band) and holes (in valence band) can recombine, but if suitable scavenger for electrons or holes is available, recombination is prevented [44]. Example, in an air environment, the photogenerated holes and electrons can react with water molecule which adsorbed on the surface or react with oxygen molecule to form hydroxyl and superoxide radicals as shown in the following equations:

$$ZnO + h\nu \rightarrow ZnO\ (e+h)$$

$$h^+ + H_2O \rightarrow OH^{\cdot} + H^+$$

$$e^- + O_2 \rightarrow O_2^-$$

$$[OH^{\cdot} + \text{dye} \rightarrow \text{degradation the of dye}]$$

These radicals are able to oxidize most organic compound due to their high reactivity. Photocatalyst of ZnO as an example for the photocatalysis mechanism was illustrated in Figure 4.

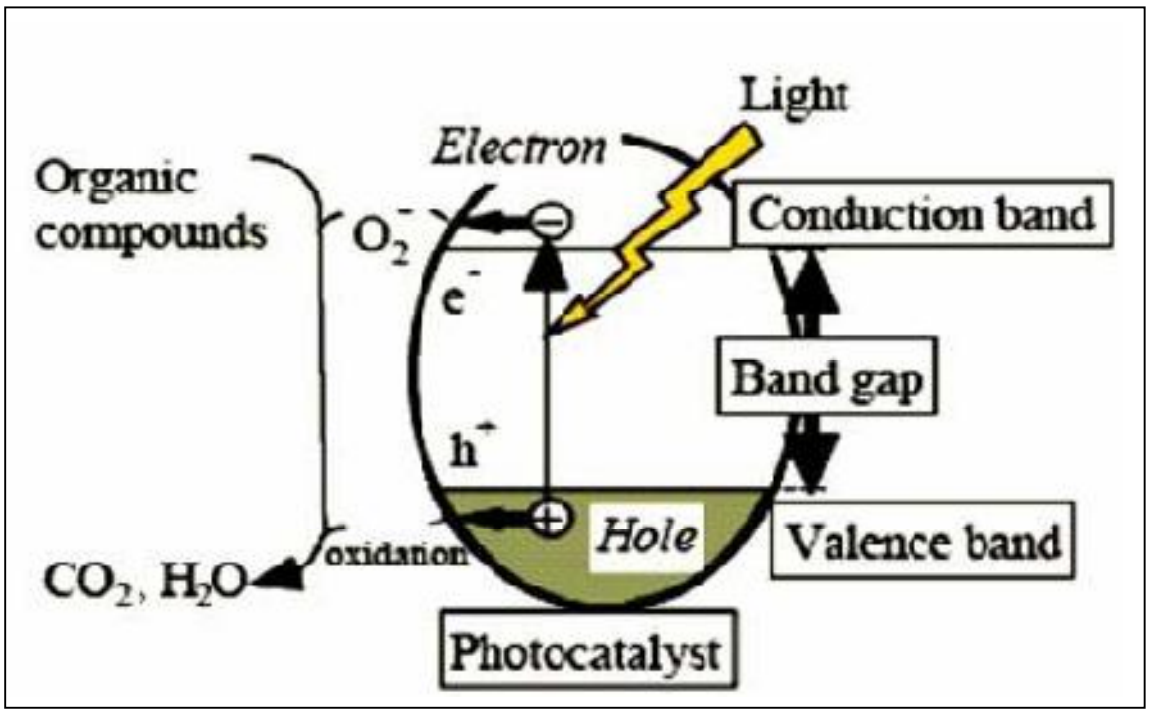


**Figure 4:** schematic illustration of photocatalysis mechanism [44] (reproduced by permission from Indian Journal of Science and Technology)

### 1.3.5. Dyeability of nano-sol coatings

It has been reported that the sol-gel method can lead to improvements in the wash fastness of direct dyes with silica sol [46,47], improving the wash fastness of direct dyes on cotton by Si/Ti composite nanosol using pad-dry-cure method was also reported [48]. The dyes used to color the fabric can have a great influence of fabric UPF. In order to achieve a color, dyes must selectively absorb visible radiation. The absorption band for some dyes extends into the UV spectral region so that such dyes act as UV absorbers. These dyes will therefore increase the fabric UPF value.

Some of the surface dyeing methods which depend on the use of large surface areas of the porous nanohybride for achieving high level capturing of the dyestuff molecules was established [49]. An evaluation of the dyeing behaviour of sol-gel silica doped with direct dyes on cotton fabrics through investigation of color strength (K/S) was reported [50].

## 1.4. Objectives of this thesis

The main task of the present thesis is to search for the proper finishing formulation as well as treatment conditions for attaining innovative multi-functional properties, i.e. UV-protection, antibacterial, superhydrophobic and photocatalytic properties of cellulosic fabrics in addition to improve the dyeability without adversely affecting the physico-mechanical performance properties of the treated substrates necessary for the industrial needs. In this work, sol-gel based inorganic-organic hybrid polymers which based on 3-glycidyloxypropyltrimethoxysilane (GPTMS) were modified/filled with ZnO nanoparticles and were applied to cellulosic cotton (100%) and cotton/polyester (65/35%) fabrics. By nanoparticle coating on textile surfaces both the chemical and physical properties of the fabrics can be improved, giving unique functions.

In this study, the effect of ZnO nanoparticles as UV-protection finish was evaluated by determination of the ultraviolet protection factor (UPF) of the treated fabrics. Also the antibacterial activity of the coated fabrics using ZnO/GPTMS and GPTMS/ZnO-CTS composite against Gram-negative bacterium *Escherichia coli* and a Gram – positive *Micrococcus lutues* has been evaluated. Hydrophobic fabric surface can be obtained after surface hydrophobization using stearic acid. Photocatalytic degradation of methylene blue using ZnO nanoparticles was also studied. Dyeing of ZnO/GPTMS nanosol coating with reactive dye was carried out using ZnO of different concentrations and different particle size, also the UV-protection of the treated fabrics was evaluated after the dyeing process.

# 1.5. Literature overview

## 1.5.1. Why Nano?

Materials in the nanometre scale show new behaviour and allow the creation of new properties not previously possible when compared to bulk material. Since decreasing the size of the particles to nanometre scale they become very active and their properties fundamentally changed [44]. For example: 50 kg of 1 mm-size $SiO_2$ particles which has a surface of 120 $m^2$, after decreasing to 1 nm the surface area become 120.000.000 $m^2$, since after decreasing the particle size the number of molecules in the surface increased compared to the bulk material and this lead to the creation of new unexpected properties [44]. This idea could be clear in the following schematically illustration in Figure 5.

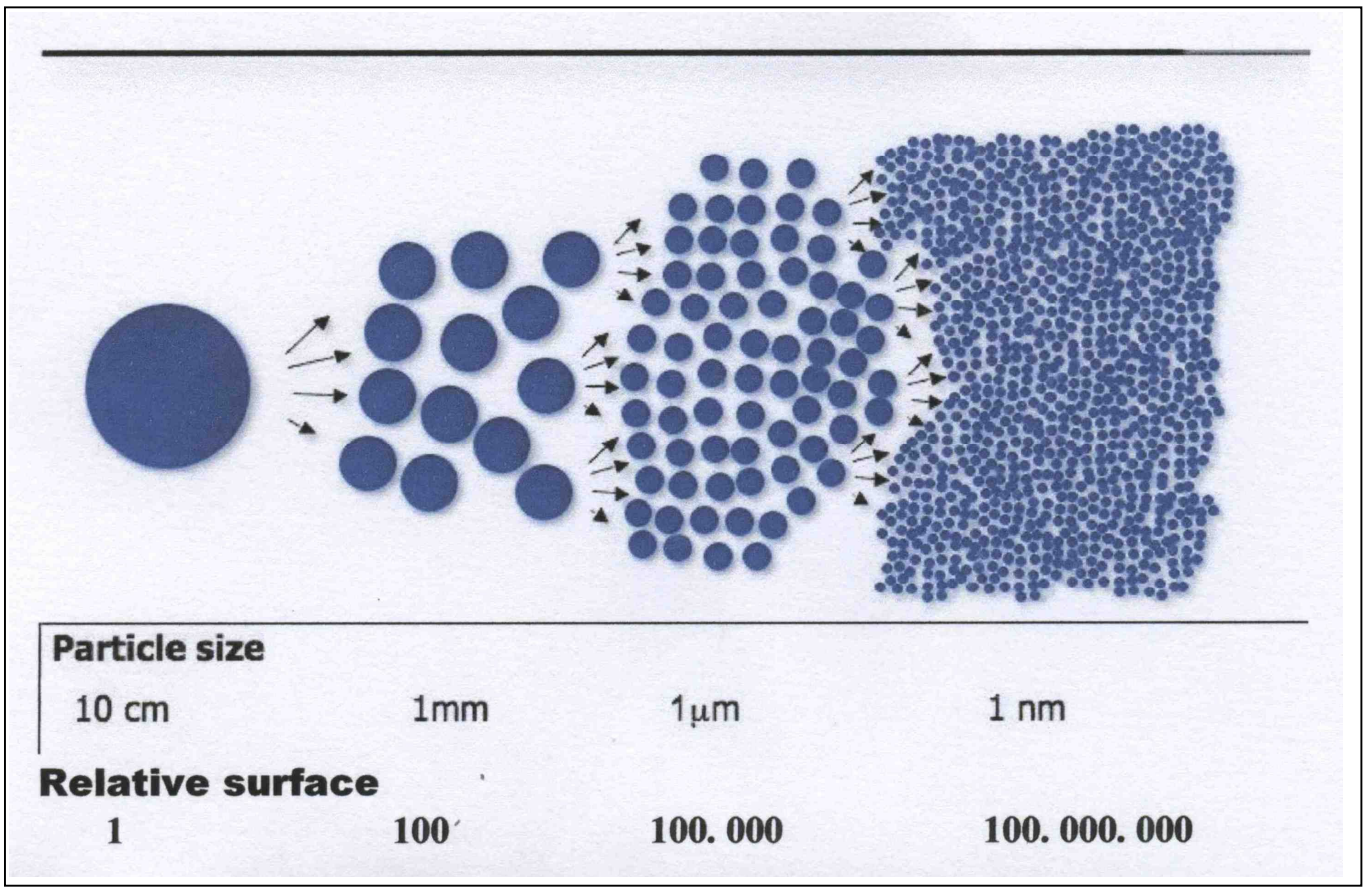


**Figure 5:** schematic illustration of the relation between the particle size and the corresponding specific surface area [44] (reproduced by permission from Indian Journal of Science and Technology)

### 1.5.2. Sol-gel process

Nanoparticles can be produced from atoms or molecules (bottom-up method) using chemical processes which based on the transformation in solution e.g. sol-gel processing (liquid-phase synthesis). The sol-gel process is a low temperature approach for synthesizing solid state oxide materials, this leads to safe, cost-effective and versatile process [3]. The sol-gel process is a wet-chemical technique that uses the colloidal particles (sol) to produce a network (gel).
The size and the shape of the particles can be controlled depending on factors such as, the solution composition, pH, temperature of the reaction, kind of the precursor and the solvent type. Since, it was reported that the type of solvent affected the shape of some metal oxide primary particle [51].

By starting with the precursor such as metal alkoxide and after the hydrolysis and the polycondensation processes the oxide particle is formed. The resulting nanoparticles can be used to prepare nanocoatings or can be separated and processed to form nanopowders with unique properties [52]. The chemical aspects of the sol-gel process can be illustrated as follows:

- Starting e.g. with metal alkoxide as precursor.
- Hydrolysis of precursors (usually multiple steps).

$$M(OR)_x + H_2O \rightarrow M(OR)_{x-1}OH + ROH \qquad \textbf{(Hydrolysis)}$$

- Condensation of the precursors to form metal oxide in the end

$$2M(OR)_{x-1}OH \rightarrow (OR)_{x-1}M\text{-}O\text{-}M(OR)_{x-1} + H_2O \qquad \textbf{(Polycondensation)}$$

**M:** metal species (Si, Al, Ti, Zn, …)
**R:** organic species

For the cellulosic fabric coating process as application method, the high level of adhesion between the metal oxide and cellulosic fabric is due to the condensation reaction between the hydroxyl group of the cellulose and the uncondensed hydroxyl

group of metal species [53].

The sol-gel method has been used to synthesize metal oxide nanostructures, such as $TiO_2$, $ZrO_2$, $CeO_2$, $SnO_2$, SiO2, CuO, $Al_2O_3$ [54-59]. Some mixed metal oxides such as $Ti_{1-x}Sn_xO_2$, $BaTiO_3$, $BaZrO_3$ [55], and CaSnO3 have also been produced [59-64].

### 1.5.3. Introduction of the status of the research about ZnO

The application of nanoparticles to textile materials aimed to produce finished fabrics with different, unique, new and multi-function properties [65]. For example, ZnO nanoparticles can be used for antibacterial and UV-blocking properties, since the inorganic UV blockers has additional preferable properties than organic UV blockers such as chemical stability at high temperature and non toxicity [66].

Moreover, nanoparticles have great effect due to having a large surface area to-volume ratio that results in a major increasing of the effectiveness in blocking UV radiation when compared to bulk materials [65].Therefore, nanoparticles could grant high durability for finished fabrics, with respect to conventional materials, because they have large surface area and high surface energy that ensure enhanced affinity for fabrics and lead to an increase in durability property [65]. Since fabric treated with nanoparticles have excellent UV blocking properties after 55 home laundering [67].

Most important fabric properties like tensile strength, bursting strength, bending rigidity, air permeability, dyeing capacity, and abrasion resistance that play a vital role in textile industries are changed after nanoparticle coating process [65].

Air permeability of the fabric is reduced after coating process with bulk-ZnO [65], while it is improved when nano-ZnO is used [14]. Compared to bulk-ZnO treated fabric, fabric treated with nano-ZnO result in lowering of the friction [68].

Zinc oxide is a wide-bandgap semiconductor (3.3 eV) with a large exciton binding energy (60 meV) at room temperature [69] is considered one of the best biofriendly absorbers of UV radiation [70], also it has been widely used in different fields because of its unique dermatological, photocatalytic, electronic, optical, electrical, and antibacterial properties [65,71-74].

Also, it is one of the few oxides that within the quantum property, allowing variation of the location of the electronic bands in an experimentally available size range [75].

Different methods have been reported for the preparation of ZnO nanocrystal with different size and shape, such as sol-gel method [76], spray pyrolysis [77], pulsed laser deposition [78], template method [79], vapour synthesis [80], wet chemical route [81],

emulsion/microemulsion [82], hydrothermal [83], polymer precursor (so-called Pechini method) [84], thermal decomposition [85], microwave methods [86] etc. Zinc oxide particles have been synthesized under different synthesis method and condition with abundant morphologies e.g. individual ZnO nanoparticles [85,87], nanowires [64,83] and dendritic nanowires [89], nanobelts [90], nanorods [91], nanotubes [92], and nanocantilevers [93].

As antibacterial agent, there are many studies investigating the antibacterial effect of ZnO nanoparticles. For example, some of the authors reported that ZnO particles considered antibacterial activity against both Gram-positive and Gram-negative bacteria [74]. Also at high pressure and temperature it has antibacterial activity against spores, while higher temperature leads to lower activity [94-96]. Yamamoto et al. reported that the surface area and the concentration play an important role in the antibacterial activity consideration, while the particle shape and crystalline structure have lower impact [97]. Yamamoto also reported that the antibacterial activity increased as the particle size decreased [98]. Adams et al., Brayner et al. and Jeng et al. reported that ZnO behaves in a different way towards microorganisms rather than other metal oxides such as $SiO_2$, MgO, $TiO_2$ and CaO [99-101]. All observations reported by the researchers were explained by a number of mechanisms, these mechanisms include production of active oxygen species due to the existence of the nanoparticles [102], damage of membrane cell wall because of the binding of the particles on the bacteria surface due to the electrostatic forces [103], penetration through the cell membrane [83], interaction between the active oxygen species and the cell [104], both the direct nanoparticle-cell membrane interaction and generation of active oxygen species (all the antibacterial tests of this work were done under dark condition) [105], and cellular internalization of ZnO nanoparticles. Since this study suggests that small particle are able to penetrate and accumulate in the bacterial membrane and cytoplasm region of the cell [100].

Hydrophobic modification of ZnO films has been carried out with appling long-chain fatty acids or their sodium salts [101]. Tang et al. have modified ZnO nanorods using sodium oleate as the capping agent, hydrophobicity of ZnO nanorods was found to increase with increase in the amount of sodium oleate.

Wu et al [107] studied the surface wettability of micro-structured ZnO surfaces with different alkanoic acids (C8–C18) and found that the greater the chain lengths of fatty acids the more stable superhydrophobicity was obtained. Badre et al. have studied

the superhydrophobicity of electrochemically deposited ZnO films [108]. They found that after treating the ZnO nanorod films with a linear saturated long-chain fatty acid like stearic acid, higher contact angles were obtained compared to the treatment with other unsaturated fatty acids of the same chain length. Electrodeposited ZnO nanowire array film treated with stearic acid has a highly water-repellent surface [109]. Modification of ZnO films with compounds other than fatty acids has also been reported [110,111]. Guo et al. have reported the superhydrophobicity of ZnO nanorod array films obtained by a hydrothermal method after surface modification using octadecanethiol [112]. Li et al. have prepared conductive hydrophobic ZnO thin films by electrochemical deposition and made it superhydrophobic by (fluoro-alkyl) silane modification [111].

# Chapter 2

# 2. Experimental part

## 2.1. Preparation methods

### 2.1.1. Preparation of ZnO nanoparticles

The preparation procedure was basically similar to that of Spanhel [113]. The procedure consists of two major steps. First the suspension of the precursor and second the hydrolysis of the precursor to form the zinc oxide nanoparticles. Zinc acetate (ZnAc) and isopropanol, were used to prepare the precursor before lithium hydroxide ($LiOH \cdot H_2O$) was used to hydrolyze the precursor.

A two neck round bottom distillation flask was used to suspend 2.8 g of ($ZnAc \cdot 2H_2O$) in 100 ml 2-propanol by reflux heating 82°C (boiling point) for three hours. 0.75 g lithium hydroxide was dissolved in 100 ml isopropanol at room temperature by magnetic stirring. The ZnAc suspension was cooled down to 0 °C before the lithium hydroxide solution was added drop wise under vigorous stirring. The mixture was treated in an ultrasonic bath (SONOREX TK 52H) at room temperature for about 2h. The resulting sol theoretically contains 0.675 wt. % ZnO. Higher amounts of ZnAc and lithium hydroxides were used (using constant amounts of solvent) to prepare colloidal solution of higher concentration, as shown in Table 2. Table 2 indicates the theoretical amount of ZnO wt. % as a result of increasing the amount of both Zinc acetate and lithium hydroxide to get higher ZnO nanoparticles concentrations.

In this method isopropanol solvent can be used to get different ZnO nanoparticles concentrations. The solvent was also changed into ethanol or methanol to control the particle size preparation of ZnO, since preparation was carried out by reflux heating; the corresponding preparations were carried out at different temperatures.

For separating ZnO nanoparticles and to remove the residual materials, high-speed centrifugation 5000 rpm/20 min was used followed by several alcoholic washes to remove the undesirable byproducts, then drying to get the powder which can be weighted ( ZnO wt.% experimentally) and finally resuspended in alcohol to be ready for application.

**Table 2:** Preparation of higher ZnO nanoparticle concentrations

| Isopropanol (ml) | Zinc acetate (g) | Lithum hydroxide (g) | Isopropanol (ml) | ZnO wt.% (theortically) | ZnO wt.% (experimentally) |
|---|---|---|---|---|---|
| 100 | 2.8 | 0.75 | 100 | 0.675 | 0.499 |
| 100 | 5.6 | 1.5 | 100 | 1.35 | 1.145 |
| 100 | 8.4 | 2.25 | 100 | 2.025 | 1.964 |
| 100 | 11.2 | 3 | 100 | 2.70 | 2.497 |
| 100 | 14 | 3.75 | 100 | 3.375 | 3.012 |

For the characterization, the size of the ZnO nanoparticles was measured by dynamic light scattering (DLS), using Zetasizer, Nano-S, produced by Malvern as shown in Figure 6.

**Figure 6:** DLS instrument used for measuring ZnO particle sizes.

### 2.1.2. Preparation of GPTMS-sol

10 ml GPTMS (3-Glycidyloxypropyltrimethoxysilan) are dissolved in 100 ml isopropanol before hydrolysis using (1.22 ml) 0.01M hydrochloric acid. The resulting sol is stirred for at least 3h to form the basis sol (concentration of GPTMS 9,1 vol.%).

### 2.1.3. Preparation and application of GPTMS-ZnO-sol

After the preparation of both ZnO nanoparticles solution and GPTMS sol, the zinc oxide and the GPTMS sol were mixed in different ratios. 1-methylimidazol (0.5 ml/10 ml GPTMS) was added as a catalyst for the cross-linking reaction of the epoxy group of the GPTMS. Table 3 indicate the amount of ZnO in GPTMS to get different ZnO concentration (%) in GPTMS.

**Table 3:** Percentage of ZnO in GPTMS to get different ZnO concentrations

| ZnO-sol (ml) | ZnO (g) | GPTMS-sol (ml) | GPTMS (g) | ZnO (%) |
|---|---|---|---|---|
| 100 | 1 | 110 | 10 | 10% |
| 100 | 2 | 110 | 10 | 20% |
| 100 | 3 | 110 | 10 | 30% |
| 100 | 4 | 110 | 10 | 40% |
| 100 | 5 | 110 | 10 | 50% |

The stability of different concentrations of complete finishing prepared ZnO/GPTMS sols was measured by turbidimetric measurements (NTU...Normal-Turbidity-Unit) Model 2100N laboratory Turbidimeter (HACH).

The final formulation was applied to the fabrics by a pad-cure-method. The coating was carried out by a padding process with a laboratory padder (Werner Mathis AG, Switzerland) to a wet pick up of 100%. After padding samples were dried in a labcoater LTS-S (Werner Mathis AG) at 130°C for 30 min. Finally the fabric were washed and dried at ambient temperature. A laboratory laundering machine was

used to remove the residual material. Laundering was performed in a laboratory washing machine (Linitest, ATLAS in accordance on DIN EN ISO 105-C06 for 2 washing cycles using standard ECE detergent) at 40°C for 20 min.

### 2.1.4. Preparation and application of GPTMS-ZnO-chitosan Composite

0.1, 0.5 and 1% (wt/v) of chitosan was dissolved in 1% (v/v) aqueous acetic acid solution by stirring for 2-3 h. Three different molecular weights (MW) of chitosan $1.36.10^5$, $2.2.10^5$ and $3.0.10^5$ Da with equal degree of deacetylation (DD, 85%) (Coded as: S 85-60, He 85-250, and He 85-500) were tested. The finishing solutions were prepared: Zinc oxide nanoparticle (0.675 wt.%/32 nm) solution, GPTMS sol (110 ml) and solutions of 100 ml 0.1/ 0.5 and 1% chitosan were mixed together and sonicated for 2 h. The pH of the solution containing chitosan was adjusted to be 5.5. To the finishing solution 50 µl of non-ionic detergent was added to improve the wettability. 1-methylimidazol (0.5 ml/10 ml GPTMS) was added as a catalyst for the cross-linking reaction of the epoxy group of the GPTMS. The final formulation was applied to the fabrics by a pad-cure-method at 130°C for 30 min. Finally the fabric were washed and dried at ambient temperature. A laboratory laundering machine was used to remove the residual material. The laundry conditions were the same as described in 2.1.3. The same experiment was done in case of fabric treated with only chitosan/GPTMS but without the addition of ZnO nanoparticle.

### 2.1.5. Stearic acid modification of fabrics finished GPTMS-ZnO composites

In this work, stearic acid was used to lower the surface energy of the fabrics or ZnO-nano coated fabrics. The fabric finished with ZnO/GPTMS as described in 2.1.3 was immersed in 1 wt.% stearic acid solution of acetone for 10 min, before it was padded, and cured at 110 °C for 45 min [114]. The samples were then washed with acetone to remove residues materials not fixed to the fabric and dried. Finally the samples were washed 2 laundering cycles. The laundry conditions were the same as described in 2.1.3.

### 2.1.6. Dyeability of fabrics finished with GPTMS-ZnO Composites

Intracron red BF-3RM 150% 1 g was dissolved in 500 ml water, fabric samples treated with different particle size of ZnO /GPTMS as described in 2.1.3 were immersed in this solution at temperature 60°C, 1 ml sodium sulphate (50 g/l), 1 ml sodium carbonate (5 g/l) and 1 ml sodium hydroxide (1 M) were added with continues stirring for 30 min. then the samples were washed several times with boiling water and 0.1 wt. % Marlipal®, and finally washed with cold water and dried at ambient conditions. The chemical structure of the dyestuff is given in Figure 7.

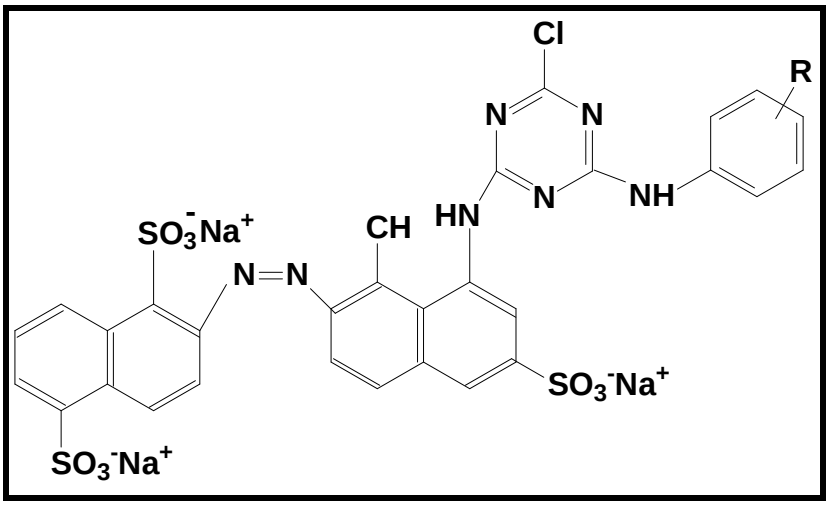


**Figure 7:** Structure of Intracron red® reactive dye, R: as vinylsulfonic acid anchor.

## 2.2. Investigation of antibacterial properties

### 2.2.1. Zone of inhibition method

To evaluate the antibacterial activity of textiles treated with the different finishes; zone of inhibition test as qualitative test was used. The results were evaluated by the existence of halos around the treated samples, and the size of the halos depends on the antibacterial activity and the diffusion degree of the finishing chemicals into the culture medium of the agar plate. In this test, a sterile agar plate was prepared, and then the suspension microbial solution which was freshly prepared was spread by a swab over the face of the agar plate. Fabric treated with the antimicrobial finish is applied to the surface of the agar plate and incubated. The activity of the finishing agent is represented by the presence of halos around the treated fabrics, which

indicate that this area is free from the growth of microbes.

Zone of inhibition test has good advantages, e.g. fast, low costs relative to other tests and most of antimicrobial finishes can be evaluated using this test, but on the other hand, it didn't indicate whether the microbes was killed or only prevented from growing.

### 2.2.2. AATTC test method 100-2004

This test method is bacterial count test (quantitative method) used to evaluate the antibacterial activity of textile finishes [115]. In this test, both blank and treated textile materials are inoculating at 37 °C with 1-2* $10^6$ CFU (colony forming units)/ml in known amounts of nutrient broth for 24 h using vigorous shaking. First, 6 cm diameter circular test samples were placed in wide necked flasks which were sealed with aluminium foil and sterilized, then 3 ml of inoculums, with concentrations of 1-2 × $10^6$ CFU / ml were added. Samples where then taken directly after 24 hours. Add 100 ml 0.9 % NaCl and then shaking them vigorously for 1 minute, followed by extracting 1.5 ml of the solution and then adding 500 µl to agar plates in logarithmic dilutions 0, 1, 2 (except the blanks after 24 hours, which were plated up to 6 logarithmic dilutions). By using agar plating, the number of the bacteria in the liquid was determined [96]. The plates were incubated at 37°C for approximately 48 hours, after which they were removed from the incubator and the formed colonies were counted. After the bacterial count, the reduction rate of the bacteria was calculated as follows:

$$R\% = \frac{B - P}{B} \cdot 100$$

Where:

R = reduction in percentage

B = CFU/ml for test sample in blank

P = CFU/ml for the flask containing the treated samples

### 2.2.3. Tetrazolium/formazan-test method (TTC)

The TTC-test method is used in this thesis to measure the antibacterial efficiency of fabric treated with ZnO/GPTMS sol and ZnO nanoparticle/GPTMS/chitosan composite. Tetrazolium salts as TTC and formazans have been known in chemistry for about a hundred years [116]. Tetrazolium salts and formazan are not only applied in chemistry and industrial technology, but also in histochemistry, biochemistry and biological science e.g. botany, medicine, immunology and pharmacology [11]. The TTC-test method is considered a quick method for evaluating the antibacterial activity of fabrics finished with ZnO nanoparticle and ZnO nanoparticle/chitosan composite, since the absorbance of formazan, measured at 480 nm, is directly proportional to the viable active cells. Therefore, the red formazan obtained indicates the activity and viability of the cell.

The tetrazolium/formazan couple is a special redox system as described below in Figure 8 [117]. Since, in the presence of bacteria, TTC is reduced to red formazan.

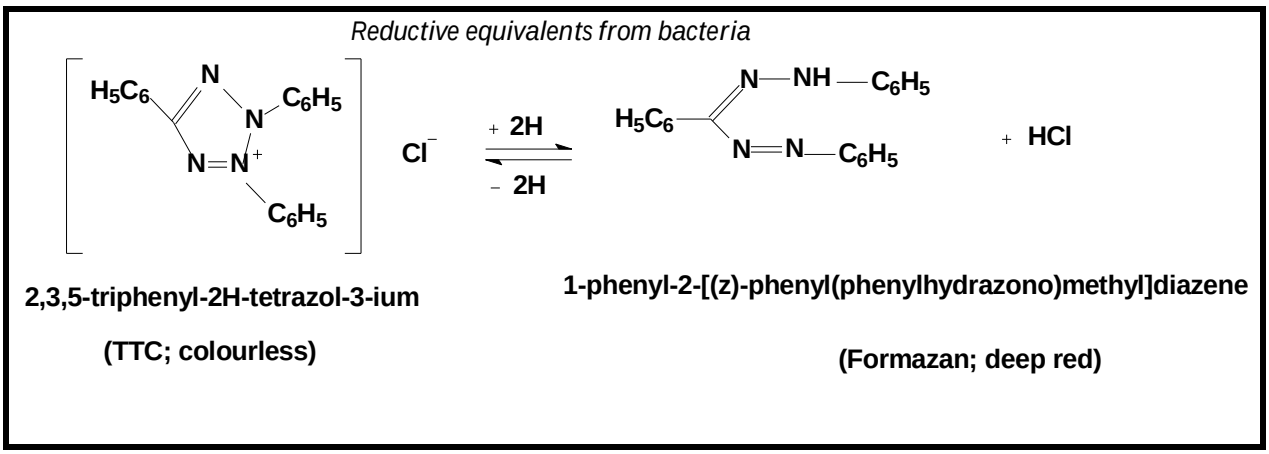


**Figure 8:** Mechanism of the tetrazolium/formazan system

In this test, both control and finished fabrics were cut into small size of a diameter 3.8 ± 0.1 cm of circular shape. The number of circular sample to be used was 6. Before incubation, both the control and the treated samples were sterilized at 110 °C, then all samples were placed in 40 ml nutrient broth medium flask which containing 10 µl of microorganism ($10^8$ CFU/ml), then all flasks were incubated with shaking at 37 °C/200 rpm for 3 h, then 1 ml from each flask which containing the control and the

finished samples was added to sterilized test tubes containing 100 µl TTC (0.5 % w/v). All tubes were incubated at 37 °C for 20 min. The resulted formazan was centrifuged at 4000 rpm for 3 min followed by decantation of the supernatants. The obtained pellets were resuspended and centrifugated again in ethanol. The activity and viability of the cells was determined by the formazan absorbance value which was measured by photometer at 480 nm [117].

### 2.2.4. Antibacterial test carried out with FITC labelled ZnO-particle

In this experiment 20 mg of FITC (Fluorescein isothiocyanate) was dissolved in 100 ml of ZnO nanoparticles (0.1 g/100 ml) which was previously prepared, centrifuged, washed and resuspended in isopropanol, then the mixture was stirred for 1 h. After that 100 µl of ZnO/FITC solution was added to 50 ml of $10^8$ CFU/ml *E.coli* cultures which were grown overnight at 37°C in nutrient broth medium, also 50 ml of $10^8$ CFU/ml of *E.coli* culture was prepared as control solution. Because ZnO and FITC solution was chemically linked, then ZnO nanoparticles can be worked as a fluorescent agent for bacterial cell labelling through the green fluorescence observed after using ZnO/FITC solution. Finally the reduction of the bacterial culture with the time under the flurecence microscope was notice since; the number of fluorescing particles goes down indicating that more and more cells are decomposed. The stained bacteria were observed using the microscope (KEYENCE all-in-one- Type Fluorescence Microscope, BZ-Analyzer 8100E, Japan).

### 2.2.5. Use of DPPH for detecting radical species in ZnO dispersions

The antibacterial activity of ZnO nanoparticles was also explained by the generation of oxyradicals or hydroxyl radicals by using 2,2-Diphenyl-1-pikrylhydrazyl (DPPH• ) stable free radical dye. In this experiment 20 mg of DPPH was added to 100 ml (1 g/l) ZnO nanoparticle sol of the same concentration but with different particle sizes. The mixture was stirred for 10 min under the dark condition. After that UV-Vis Spectrum measurments of DPPH / different ZnO nanoparticle sizes were obtained and the particle size influences on the degree of decomposition of DPPH were also studied. The structure of DPPH dye was shown in Figure 9.

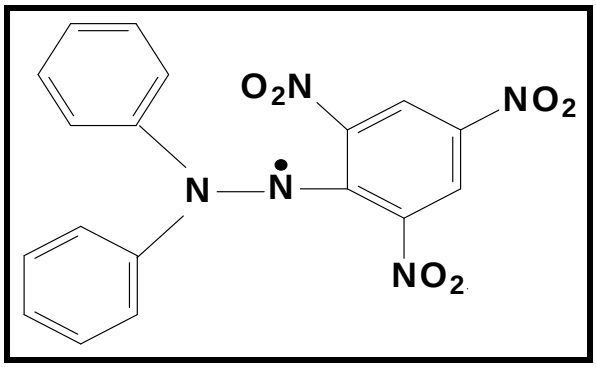


**Figure 9:** Chemical structure of DPPH dye

### 2.2.6. Preparation of ZnO/ catalase enzyme

The antibacterial activity of ZnO/catalase enzyme solution was tested as indication to the generation of $H_2O_2$ due to the presence of ZnO nanoparticles. In this test, 20 mg of catalase enzyme was dissolved in 100 ml water and 0.1 g ZnO nanoparticle (30 nm) which prepared as described in 2.1.1 was resuspended in 100 ml water. Then the two solutions were mixed together with adjusting the pH using buffer pH 7. Zone of inhibition test for both only ZnO nanoparticle solution and ZnO/catalase enzyme solutions were done by adding 10 µl of both ZnO nanoparticle and ZnO/catalase solution on agar plate containing *E.coli*.

## 2.3. UV-protection

Transmissions of UV radiation were measured in Faculty of Textile Technology, University of Zagreb, Croatia according to AS/NZS 4399:1996 – Sun Protective Clothing – Evaluation and Classification using a Cary 50 Solarscreen transmission spectrophotometer. Figure 10 shows the spectrophotometer used for the measurements.

**Figure 10:** Transmission spectrophotometer Cary 50/Solascreen (VARIAN)

UF values were calculated automatically according to (1) and classified according to Table 4 [12].

**Table 4:** UV Protection and classification according to AS/NZS 4399:1996

| UV Protection | UPF classification | Transmitted UV radiation |
|---|---|---|
| excellent | 40, 45, 50,50+ | ≤ 2,5 % |
| very good | 25, 30, 35 | 4,1 – 2,6 % |
| good | 15, 20 | 6,7 – 4,2 % |
| non-rateable | 0, 5, 10 | > 6,7 % |

## 2.4. Wettability measurements

Textile surfaces are not ideal flat surfaces, so only hydrophobic property measurements can be tested on textile surfaces. In this study hydrophobicity were measured by two tests, TEGAWA and contact angle measurements. The wettability test according to TEGAWA was applied [43], in this test the wettability was determined by recording the drop penetration time of the drop penetration test which was done by using an aqueous dye solution based on TEGEWA condition. Since a drop of certain volume (0.05 ml of 2% solution of the dye amino blue V-PW) from a height of 40 mm dropped on the treated sample then the penetration time was recorded as complete dipping of the drop. Contact angles (CA) were measured with 5 µl deionized water using a manual Krüss (G-1) instrument at room temperature. All the contact angles were determined by averaging the values obtained at six different points on each sample surface.

## 2.5. Photocatalytic activity

This study aimed on the use of the stable and durable product of inorganic-organic hybrid polymer modified with ZnO nanoparticles with a focus on the photocatalytic properties of ZnO nanoparticles as textile finishes. The influence of surface coating on the photocatalytic degradation of methylene blue was studied, since the photocatalytic activity of ZnO nanoparticles in form of both colloidal solution and textile coating material was evaluated in normal laboratory environment and after UV-irradiation.

### 2.5.1. Investigation of dyestuff degradation by active samples

On different concentrations of the resuspended solution of ZnO nanoparticles (in case of colloidal solution) and after coating process of fabrics with different concentrations of ZnO/GPTMS sol (in case of textile samples), 10 ml queous suspensions of methylene blue (MB) 20 mg/l was added to 40 ml of the resuspended ZnO nanoparticles (0.1, 0.5 and 1g) and also 100 µl from MB with added to the treated sample surface, then both colloidal solution and coating material was evaluated in normal laboratory environment and/or after UV-irradiation.

The ZnO/MB solution was analyzed with a UV-vis spectrophotometer by recording variations of the absorption band maximum (640 nm) in the UV-vis spectrum of MB. Also we follow the disappearance of the colour by time in case of treated fabric samples after UV-irradiation. Figure 11 shows the chemical structure of MB dye.

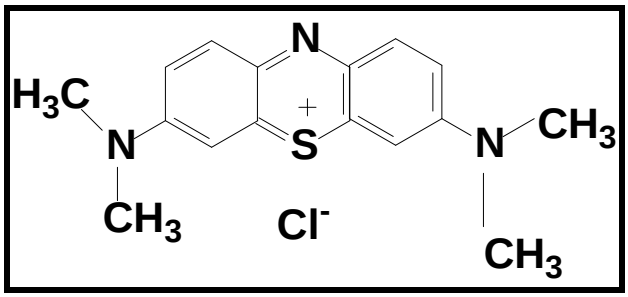


**Figure 11:** Chemical structure of methylen blue (MB)

Photochemical reactor (UV-reactor AN), model RPR-100, Ultraviolet company (Rayonet) was used as UV-irradiation source. It operates on 110/277V, 50/60 cycle. Total current consumption is approximately 400 watts as shown in Figure 12,


**Figure 12:** Photochemical reactor (Model RPR-100).

Absorbance of UV radiation was measured using a Cary 5E UV-vis. Spectrophotometer, Varian Deutschland GmbH.

## 2.6. Further investigation methods/textile parameter

### 2.6.1. Polyelectrolyte titration method

In order to determine the amount of cationic charged group on textile surface, the polyelectrolyte titration was used. Polyelectrolyte titration system, Particle charge detector (PCD 03 PH), was from Mütek Analytic GmbH, Herrsching, Germany.

Polyelectrolyte titrations are done with cationic charged solutions of polydiallyl-methyl-ammonium-chloride (PDADMAC) in case of anionic systems and with anionic poly-ethylensulfonic acid, sodium salt (PESNa) in case of cationic systems as shown in Figure 13. The concentration used is 0.001 N. In this test 1 g of treated sample was immersed in 100 ml acetate buffer solution (pH 4.7), after that 100 µl Marlipal was added, then the samples were left with shaking for 2-3 h. With distilled water the sample were washed then dried at ambient conditions. 50 ml (0.001 N) anionic polyelectrolyte (PES-Na) and 100 µl Marlipal were added to the samples with stirring for 3 h. After that the solution of the samples were filtered out. Then 10 ml from the filtrate was titrated against cationic polyelectrolyte (PDADMAC). The volume consumed during the titration was called ($V_1$). For calibration, 10 ml (PESNa) was titrated against (PDADMAC), the volume determined was called ($V_2$) [116].

The amount of titre consumption at the end point of titration can be used for the calculation of accessible charges according to the following equation:

$$\text{Equivalent (eq.)} = [(V_2\text{-}V_1) \times 0.001]/0.2$$

i.e., $V_1$ = Consumption of (PDADMAC) which is equivalent to the unreacted (PESNa) (eq/ml), and

$V_2$ = Consumption of (PDADMAC) equivalent to 10 ml (PESNa) (eq/ml).

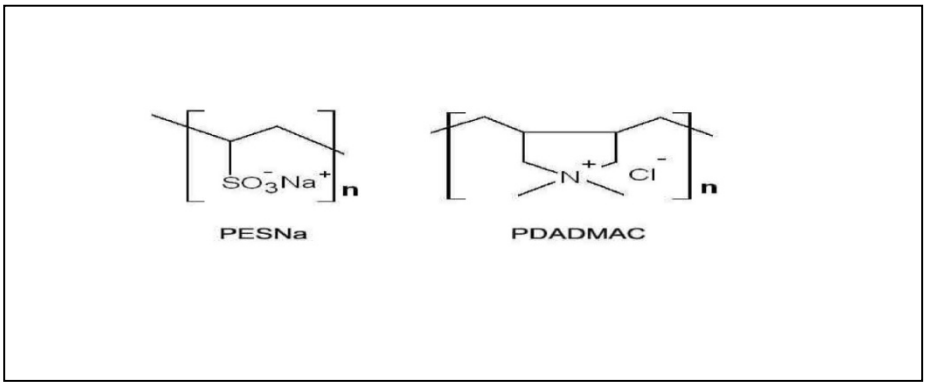


**Figure 13:** Unit structure of cationic and anionic polyelectrolyte

## 2. 6.2. HPAEC-PAD measurements

The generation of $H_2O_2$ from ZnO were detected using a HPAEC-PAD (High Performance Anion Exchange Chromatography-pulsed amperometric detection) system from DIONEX (Idstein, Germany) with a column Carbo Pac PA 1 and eluent 0.5 M NaOH.

In this test, different concentrations of $H_2O_2$ (0.2, 0.1, 0.08, 0.06, 0.04, 0.02, 0.01, 0.005, and 0.0025, 0.0012 g/l) were prepared to draw the calibration curve as relation between the concentration and the corresponding peak surface area which recorded at the retention time for every concentration measurement, since the surface area of the peak used for calibration curve is the average area of three repeated measurements.

After that different concentration of aqueous resuspended ZnO nanoparticles (30 nm) (0.5, 0.8, and 1 g/l) which generate unknown concentration of $H_2O_2$ were injected to be able to determine the unknown $H_2O_2$ amount.

Figure 14 illustrate the calibration curve of $H_2O_2$; suggest that measurements may be weak since, it only gives hint to the expected $H_2O_2$ amounts, in this curve the expected amount of $H_2O_2$ is in the end of accuracy point. Figure 14 shows the $H_2O_2$ calibration curve of different concentrations of $H_2O_2$ (0.2, 0.1, 0.08, 0.06, 0.04, 0.02, 0.01, 0.005, and 0.0025, 0.0012 g/l) and the corresponding peak surface areas.

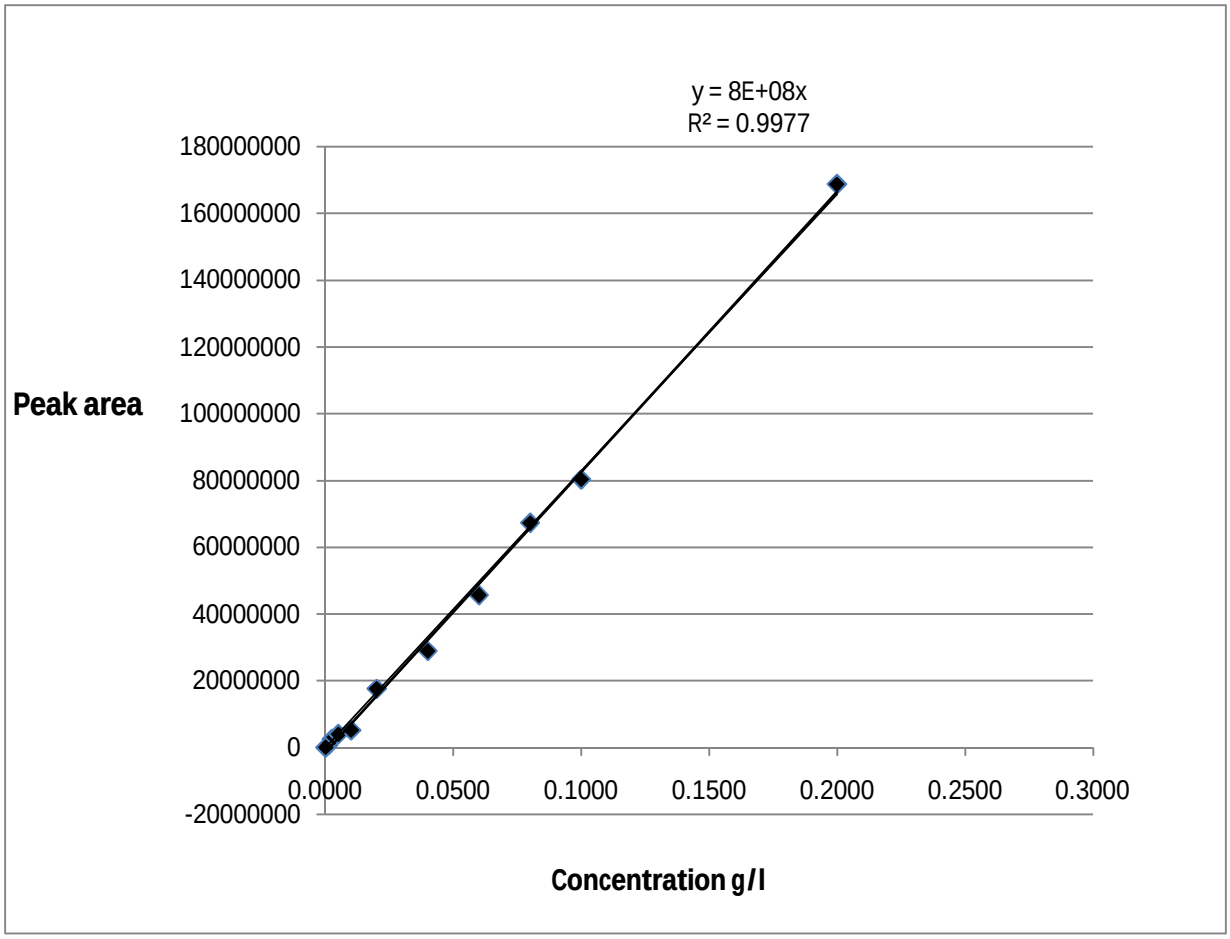


**Figure 14:** $H_2O_2$ calibration curve

## 2. 6.3. Textile testing and instrumentation analysis

Investigation of the coated textiles was carried out by means of the following procedures:

- Investigation of the mechanical properties (tensile strength and elongation) was carried out according to DIN 53857 1 using a Zwick 1445 Testing System, from this test we can determine the strength of the treated fabrics along with the elongation after certain tension test.
- Air permeability was tested using air permeability tester (21443, FRANK) according to DIN 53887. Air permeability is an important feature in the performance of textile materials used to provide an indication of the breathability of the coated fabrics, in this test a circle sample of the fabric was fixed into the tester and by using high air pressure through the fabric, then the rate of air flow was used to determine the air permeability of the tested fabric.

- Treated fabrics were analyzed by scanning electron microscopy (SEM), Topcon-Microscope (ATB-55) to investigate morphological changes of the surface structure.
- Wear resistance was investigated by a Martindale test (James H. Heal & company limited) tests were carried out according to DIN EN ISO 12947-3, from this test we can determine the degree of fabric resistance to the abrasion when this fabric subject to rubbing motion using certain weight.
- Changes in the degree of whiteness of the treated fabrics were evaluated with a Datacolor spectrophotometer 3880 (cocos Manual Version 2, 3). The degree of whiteness is given according to Berger (light source D65/10).
- Stiffness of the fabric was tested using Shirley stiffness tester according to DIN 53362, this test able to determine the degree of fabric rigidity after the coating process.
- Transmittance of UV radiation was measured using a Cary 5E UV-vis. Spectrophotometer, Varian Deutschland GmbH.
- Nitrogen content of the treated samples was determined according to Kjeldahl method [118]. In this test 1 g of the tested fabric was immersed in 10 ml concentrated sulphuric acid with the addition of catalyst (5 g potassium sulphate, 0.15 g copper sulphate and 0.15 g titanium dioxide). Chemical decomposition of the sample is complete when the medium has become clear and colorless. Then the solution was distilled with sodium hydroxide which converts the ammonium salt to ammonia. The amount of ammonia present (hence the amount of nitrogen present in the sample) is determined by back titration. The end of the condenser is dipped into a solution of HCl. The ammonia reacts with the acid and the remainder of the acid is then titrated with a sodium hydroxide solution using phenolphthalein indicator. The nitrogen percentage (N%) of the sample was calculated as follows:

$$N\% = \frac{0.014\ (N \times V)}{W} \times 100$$

Where: W= sample weight (gram).

N = normality of HCl.

V = volume of HCl (ml).

- Crease recovery angles (CRA) of the treated and untreated samples were measured according to DIN 53890 standard test method [119], since the Crease Recovery Tester is used to determine the crease resistance of fabrics by measuring the angle of recovery on a specific scale under specific weight.
- ATR-FTIR instrument was from SHIMADZU, Model IR prestige-21, Germany.
- Ninhydrin test for the characterization of amino groups of chitosan, this test is qualitative test for determination of the present degree of the $-NH_2$ group in the chitosan, since Ninhydrin reacts with the free amino group of chitosan and develops a violet color.
- Colour measurements as K/S were carried out using Datacolor spectrophotometer 3880 (cocos Manual Version 2, 3). The colour degree is given according to Berger (light source D65/10).
- The concentration of zinc on the fabric was measured. To evaluate the metal quantitatively, 0.1 g of the treated samples were digested with 10 ml nitric acid (65%) in a microwave digester (MarsXpress, CEM, Kamp-Lintfort) at 180 $^{\circ}$C. After complete digestion of the samples, the residual clear solutions were transferred to 100 ml flasks and filled with deionised water to dilute the solutions. Finally, the diluted solutions were evaluated using an inductively coupled plasma optical emission spectrometer (ICP/OES; Varian 720-ES, Kamp-Lintfort) to calculate the metal concentration.

# 2. 7. Chemicals and materials

## 2. 7.1. Chemicals

- (3-Glycidyloxypropyl) trimethoxysilane (GPTMS, 98%) from ABCR,
- 1-methylimidazole (97%, Fluka),
- 2,2-Diphenyl-1-pikrylhydrazyl(DPPH, Aldrich, 98%),
- 2,3,5- triphenyltetrazolium chloride (TTC) Merck, Germany,
- 2-propanol 99.8% Fluka,
- Acetic acid 99.8% Baker,
- Catalase from bovin liver, activity ≥ 2000 units/mg from SIGMA-ALDRICH, GmbH, Germany,
- Chitosan samples of different molecular weights (coded as: S 85-60, He 85-250, He 85-500) were kindly supplied by Heppe GmbH, Queis, Germany,
- Ethanol 96%, Baker,
- fluorescein isothiocyanate FITC, Aldrich, 90%,
- Intracron red BF-3RM 150% YORKSHIRE FARBEN, GmbH, Germany,
- Lithium hydroxide monohydrate ($LiOH.H_2O$) 98% Merck,
- methanol, 99.8%, Baker,
- methylen blue (C.I. 52015) Merck,
- non-ionic detergent (Marlipal®) from Sasol AG, Germany;
- Standard I-nutrient agar (SI-agar) Roth, Standard I-nutrient broth medium Roth, Merck
- stearic acid,97% Merck, and
- zinc acetate dehydrate ($ZnAc.2H_2O$) 98% Merck.

## 2. 7.2. Test organism

In this study Escherichia coli (*E.coli*) DSMZ 498 and Micrococcus lutues (*M.lutues*) ATCC 9341 were used as non pathogenic substitutes for Gram-negative and Gram-positive bacteria.

## 2. 7.3. Preparation of microorganisms

One well-isolated colony was transferred aseptically, using a wire loop, to a 100 ml conical flask containing 50 ml SI-medium. The flask was incubated at 37 °C for 24 h and then the grown bacteria were diluted with sterile saline to a final working concentration of 1 x $10^5$ colony forming units (CFU)/ml

## 2. 7.4. Textile fabrics

As a test fabric, bleached cotton (100%) and cotton/polyester (65/35%) fabrics from WFK, Germany was used; the specific data of the material are summarized in Table 5.

**Table 5:** Specifications of the textiles used for all the experiments.

| No | substrate | weight ($g/m^2$) | threads/cm | | thickness (mm) |
|---|---|---|---|---|---|
| | | | warp | weft | |
| I | Bleached CO (100%) | 250 | 21 | 18 | 0.57 |
| II | Bleached CO/PET(65/35 %) | 162 | 27 | 25 | 0.33 |

Prior to application, the fabric was further purified by washing with warm water and methanol. For the washing, 1 g/l of non-ionic detergent (Marlipal® O 80/13); was added. After washing, the fabric was rinsed with warm water and dried, climatized for 24 h (22 °C, 65 % rel. humidity) and weighted before using.

# Chapter 3

# 3. Results and discussion

## 3.1. ZnO nanoparticles preparation and investigation

### 3.1.1. Preparation of ZnO nanoparticles and use for coating

The nanosized zinc oxide particles were synthesized and applied for the preparation of functional coating for inorganic organic hybrid materials. Some final coating solutions of ZnO nanoparticle of certain concentration and certain particle sizes were stable for several hours showing minimal precipitation which is sufficient for an industrial application. The synthesis of ZnO nanoparticles basically described by Spanhel [113] lead to the formation of colloidal ZnO particles with a comparably homogenous distribution as described in 2.1.1. Some of the ZnO sols show no precipitation for weeks. Table 6 shows the characterization of higher ZnO nanoparticle concentrations e.g. the theoretically weight, the experimental weight, the corresponding particle size and the stability of each concentration.

**Table 6:** Preparation and characterization of higher ZnO nanoparticle concentrations

| ZnO wt.% (theortically) | ZnO wt.% (experimentally) | Particle size (nm) | Stability (week or day) |
|---|---|---|---|
| 0.675 | 0.499 | 30 | ten weeks ± 3 days |
| 1.35 | 1.145 | 42 | seven weeks ± 3 days |
| 2.025 | 1.964 | 56 | four weeks ± 2 days |
| 2.7 | 2.497 | 115 | two weeks ± 3 days |
| 3.37 | 3.012 | 156 | eight days ± 2 days |

In this work five ZnO sols concentrations were prepared (0.675, 1.35, 2.025, 2.7 and 3.37 wt.%), for ZnO sol of 0.675 wt.% (30 nm), the solution was stable for ten weeks without any precipitations, for ZnO sol of 1.35 wt.% (42 nm), the solution was stable for seven weeks, for ZnO sol of 2.025 wt.% (56 nm), the solution was stable for four weeks, for ZnO sol of 2.7 wt.% (115 nm), the solution was stable for two weeks, and for ZnO sol of 3.37 wt.% (156 nm), the solution was stable for eight days.

The pictures shown in Figure 15 are for different ZnO sols concentrations, (a) shows a corresponding sol of ZnO in isopropanol (0.675 wt.%) of average particle size of 30 nm after ten weeks, (b) shows a sol of ZnO in isopropanol (2.7 wt.%) of average particle size of 115 nm after two weeks.

The absence of any precipitation proves the excellent stability of the colloidal solution. After the corresponding stability time of eachsolution, precipitation of the colloidal solution start to appears.

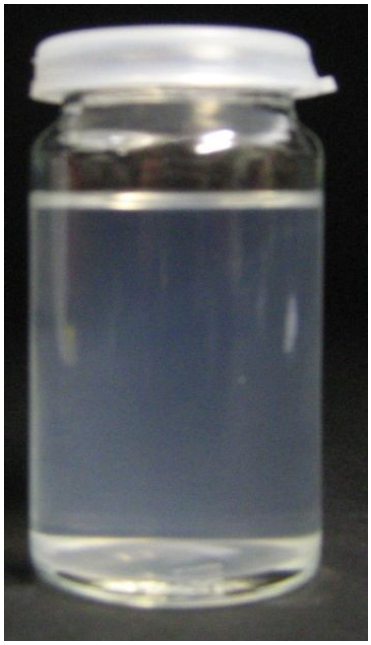

**(a)** ZnO nanoparticles 30 nm after ten weeks

**(b)** ZnO nanoparticles 115 nm after two weeks

**Figure 15:** Image of ZnO nanoparticle of different concentrations taken certain weeks after synthesis.

The particle sizes of the prepared solutions were determined using dynamic light scattering (DLS) measurements some examples are shown in Figure 16. Figure 16 shows DLS measurements of ZnO nanoparticle of different concentrations: (a) immediately prepared, and (b) after certain weeks.

**(1)** Immediately prepared ZnO nanoparticle DLS mesurments:

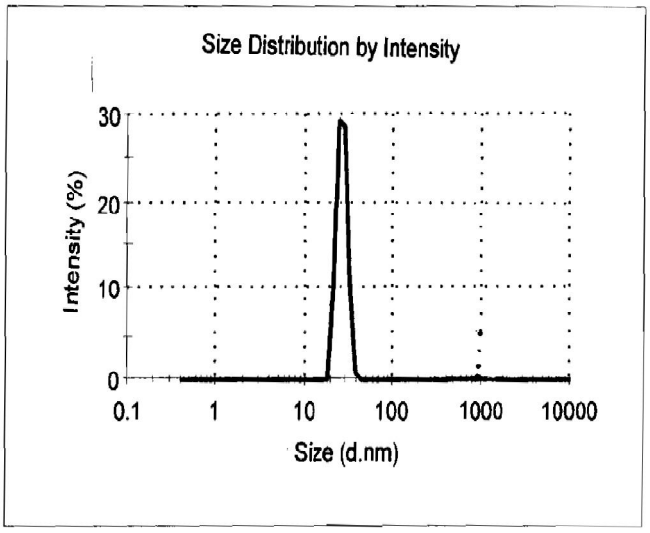


(a) Average particle diameter=30 nm

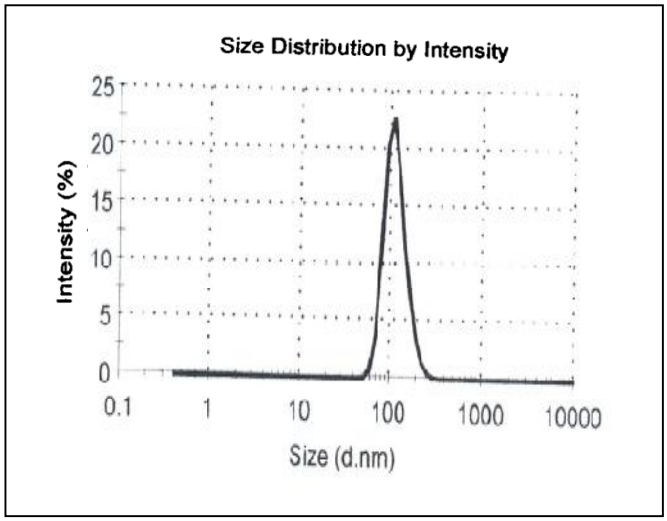


(b) Average particle diameter=115 nm

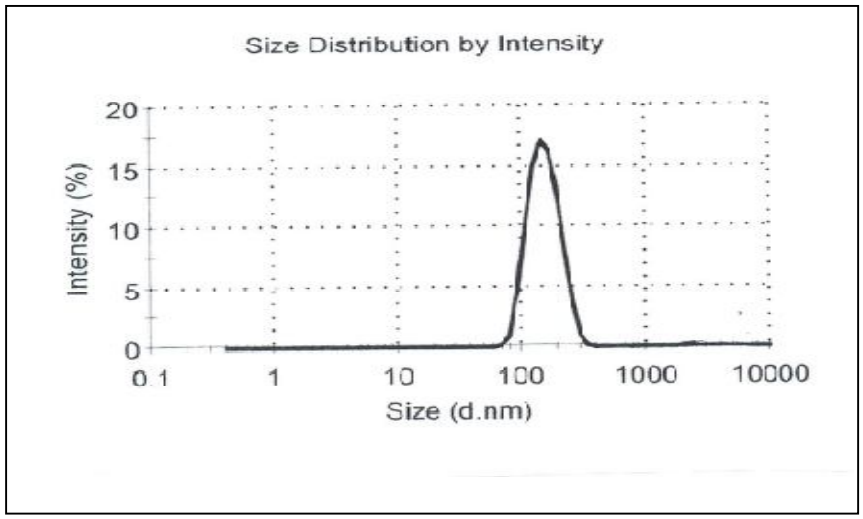


(c) Average particle diameter=156 nm

**(2)** ZnO nanoparticle DLS measurements for (b) and (c) after two weeks:

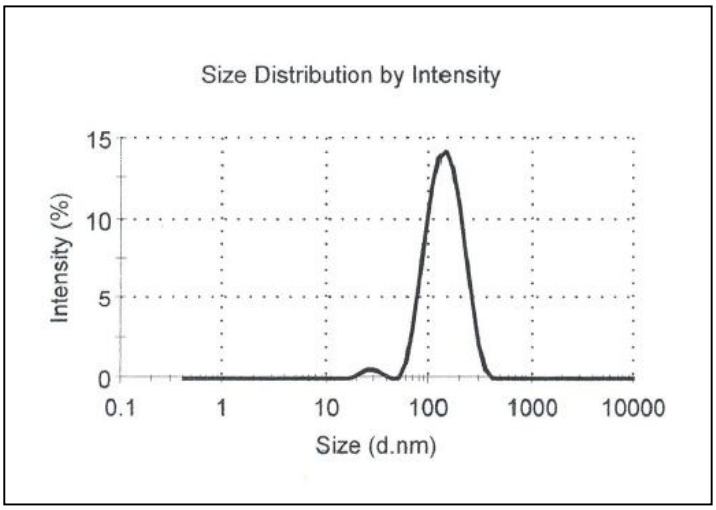


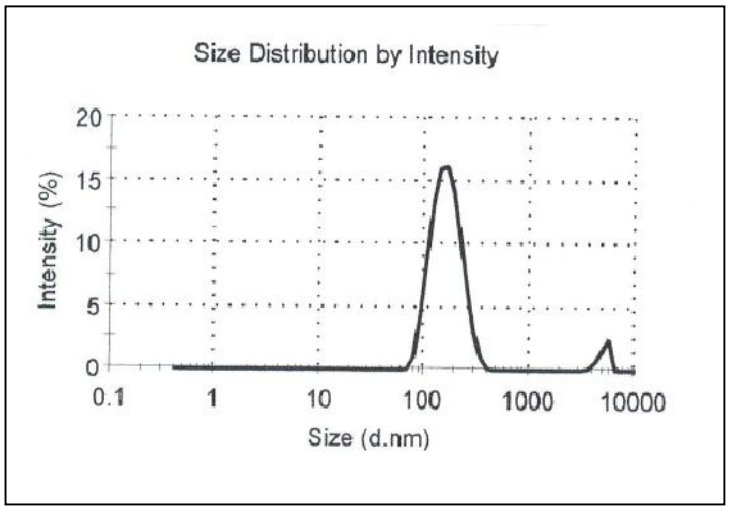


(b*) Average Particle diameter=146 nm (c*) Average particle diameter=171 nm

**Figure 16:** DLS measurements of different ZnO nanoparticle concentrations

DLS measurements for different ZnO nanoparticle concentrations after two week indicates that with time the some small ZnO nanoparticle can aggregate together resulting in change of the particle size of the solution within the time. Since, conversion of small particles into larger particles is enhanced by the agglomeration to form larger particles until equilibrium is reached.

Also ZnO sols of same concentration 0.675 wt. % but different particle sizes were also prepared, in the beginning some factors which may affect the preparation were changed to control the particle sizes, like refluxing time and temperature but no change for the size was obtained, then after several experiments it was found that by changing the solvent and the temperature, different particle sizes can be obtained.

The solvent has influences on the kinetics and the conformation of the precursor, some of the authors reported that the properties of the solvent e.g. saturated vapour pressure, viscosity [120], molecular structure [121] and the chain length of the solvent molecules (which lead to different physic-chemical properties of the solvent) [51], had been proposed to be one of the most important key parameters which could control the formation of the nanoparticles. But there is no general conclusion could be drawn on these solvent properties [51].

As shown in table 7 by changing the reaction solvent from isopropanol into ethanol or methanol bigger particles were obtained. The stability of the solution was noticed,

since the ZnO sol (245 nm) in ethanol is stable for 3 days and ZnO sol (625 nm) in methanol is stable for only 8 hours, and after that time precipitation of the colloidal solution appeared. Since larger particles generally deposit more rapidly than small particles.

**Table 7:** Zno nanoparticles prepared in different solvents

| Temperature | Reaction solvent | Particle size, DLS (nm) |
|---|---|---|
| 82 °C | Isopropanol | 30 |
| 78°C | Ethanol | 245 |
| 64°C | Methanol | 625 |

The DLS measurements for the different ZnO particle size were shown in Figure 17.

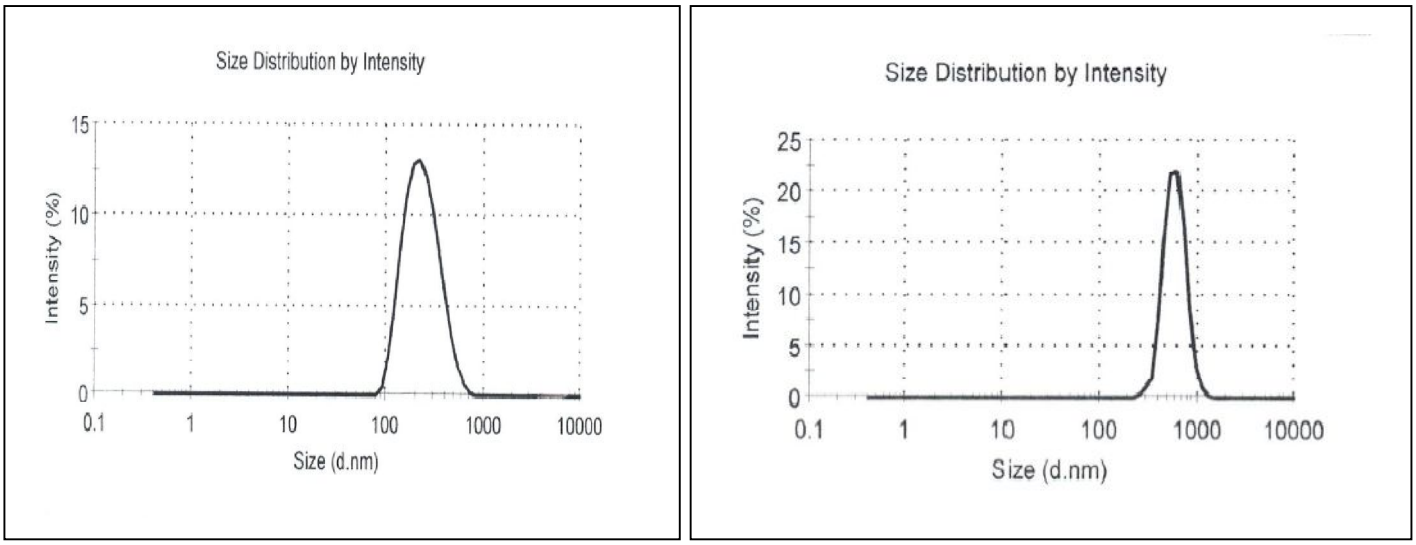


Average particle diameter=245 nm Average particle diameter=625 nm

**Figure 17:** DLS measurements of different ZnO particle sizes

After the preparation of both ZnO sol and GPTMS sol as described in the experiment part, ZnO/GPTMS sols were obtained by mixing these sols in different ratios.

The stability of different concentrations of complete finishing prepared ZnO/GPTMS sols was also measured. Figure 18 shows the stability of different concentrations of complete finishing prepared ZnO/GPTMS sols measured by turbidimetric

measurements (NTU...Normal-Turbidity-Unit). The relative amount of ZnO corresponds to the amount of GPTMS in the final sol (10% means 1g ZnO/10 g GPTMS).

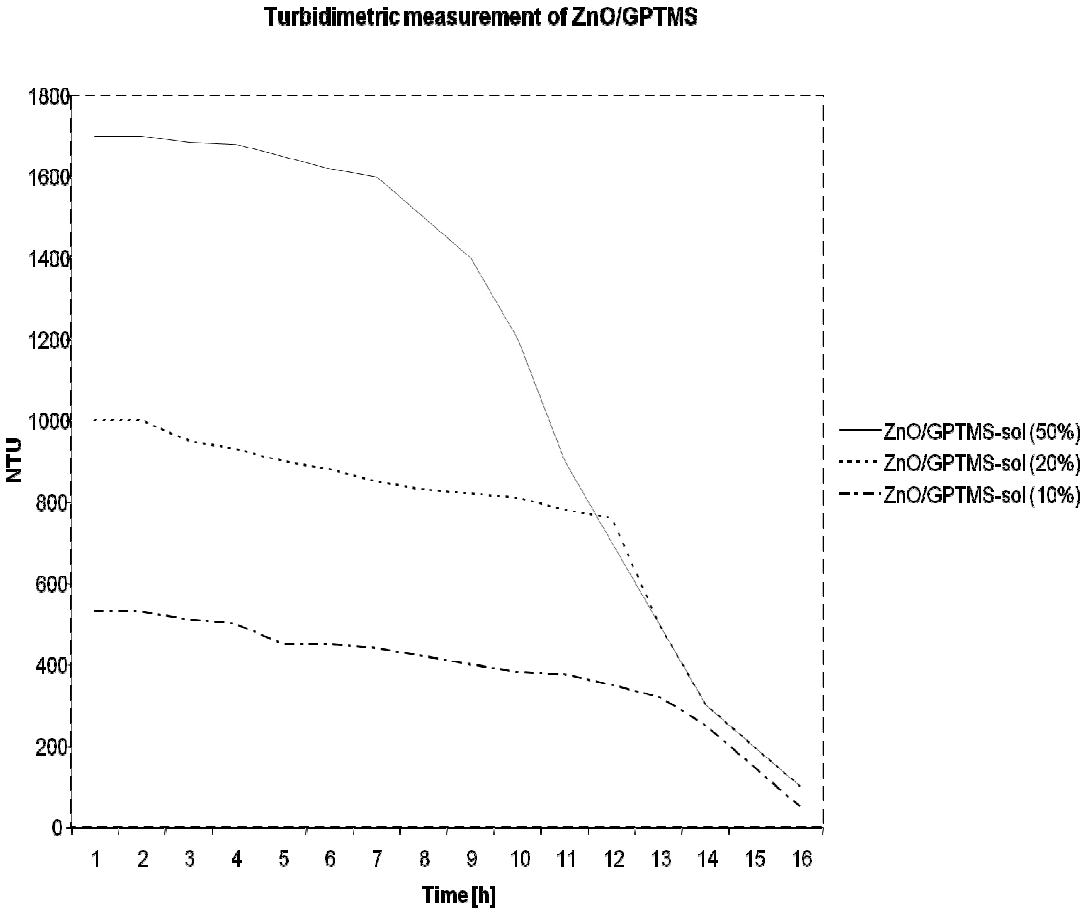


**Figure 18:** Stability of different ZnO /GPTMS sols according to turbidimetric measurements (NTU...Normal-Turbidity-Unit).

From the figure we can see that higher concentration of ZnO/GPTMS sol (50%) is more turbid and still stable till nearly 6 hours, but lower concentration of ZnO/GPTMS sol (10%) shows more stability nearly till 12-13 hours, and for ZnO/GPTMS sol (20%) it still stable till nearly 10-11 hours and this can be explained by the aggregation of the big particles in the solution which can finally lead to the precipitation and as we see from the figure the higher the concentration of ZnO in the sol, the higher the aggregation of the big particle in the final sol. Generally, if ZnO/GPTMS sol were stable for several hours showing minimal precipitation this is sufficient for an industrial application.

After the preparation of ZnO/GPTMS sol 1-methylimidazol (0.5 ml/10 ml GPTMS) was added as a catalyst for the cross-linking reaction of the epoxy group of the GPTMS. The final formulation was applied to the fabrics by a pad-cure-method at 130°C for 30 min. Figure 19 shows the assumed structure of fabric coated with ZnO /GPTMS sols. In this scheme and as a result of the hydrolysis and the condensation processes we can finally get the net work structure of the inorganic-organic hybrid polymers which were filled/modified with ZnO nanoparticles and fixed with the fabric surface through the interaction of the epoxy group with the cellulosic hydroxyl groups. The amount of $Zn^{2+}$ on the fabric treated with different ZnO nanoparticle concentrations was determined. As it was observed from Table 8, by increasing the concentration of ZnO nanoparticles within the coating layer, the amount of zinc on the treated fabric increases.

**Table 8:** ZnO nanoparticle content on fabric treated with different ZnO concentrations

| ZnO in GPTMS (%) | $Zn^{2+}$ ion (mg/l) | ZnO on the fabric (g/g) |
|---|---|---|
| 10 | 6.30 | 0.0078 |
| 20 | 11.20 | 0.014 |
| 30 | 14.45 | 0.018 |
| 40 | 18.31 | 0.023 |
| 50 | 21.69 | 0.028 |

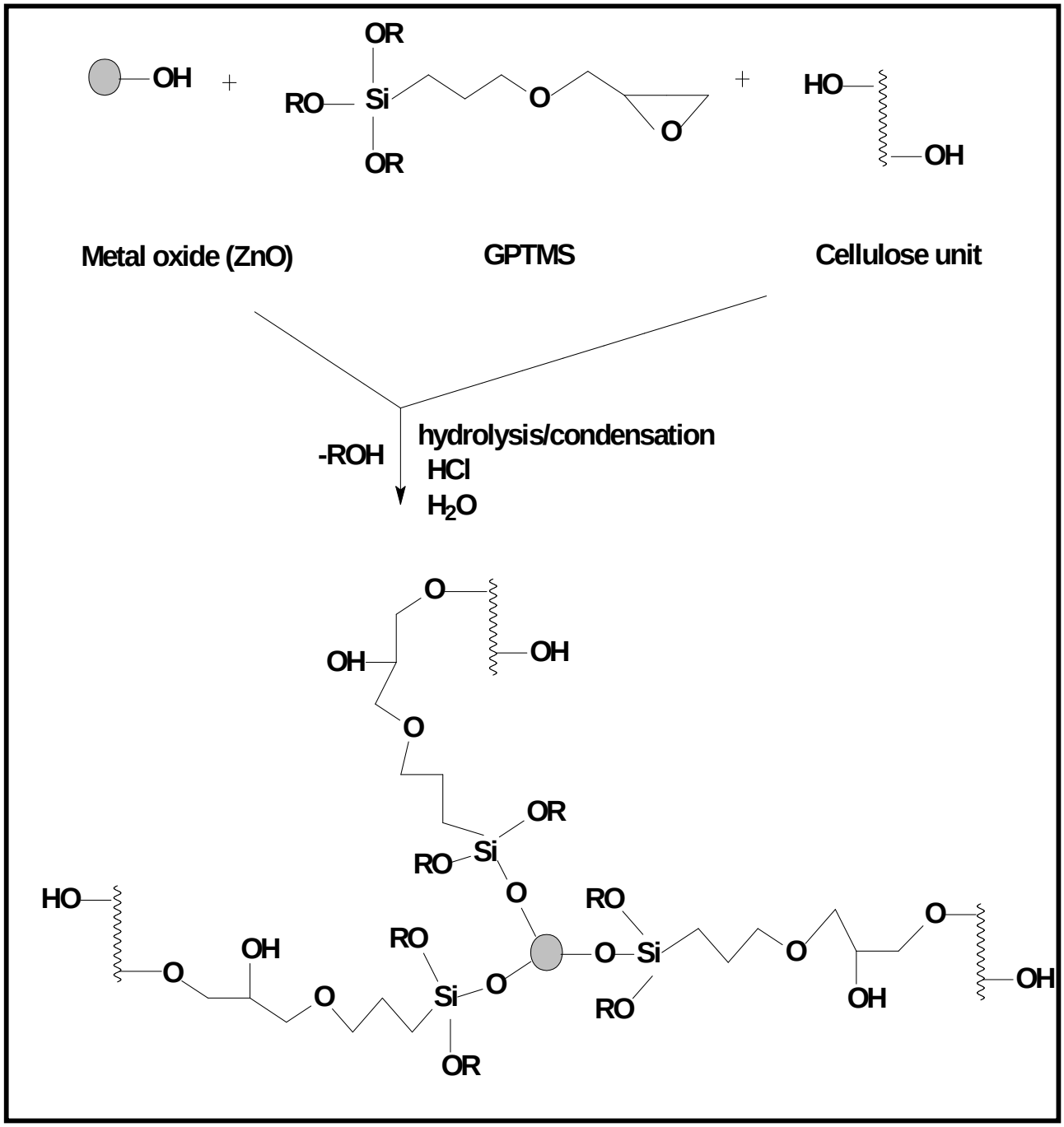


**Figure 19:** Assumed structure of fabric-finished with ZnO/GPTMS sol.

### 3.1.2. SEM investigation

SEM investigations were carried out to investigate changes in the topography. The corresponding SEM micrographs are shown in Figure 20. The surface of the untreated fibres is comparably rough, the surface of the treated fibres appear much smoother, because the coatings obviously lead to a flattening of the fibre surface.

**(1) Cotton 100%**

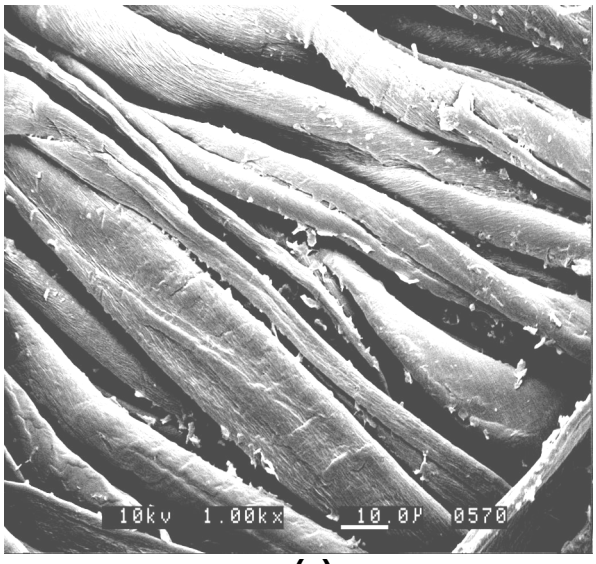


**(a)**

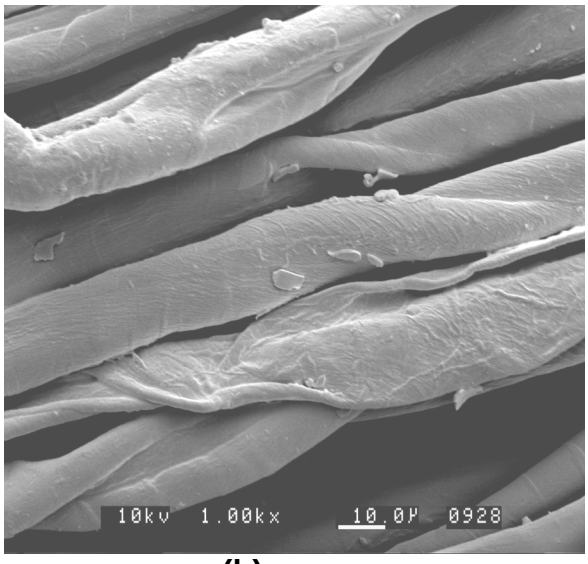


**(b)**

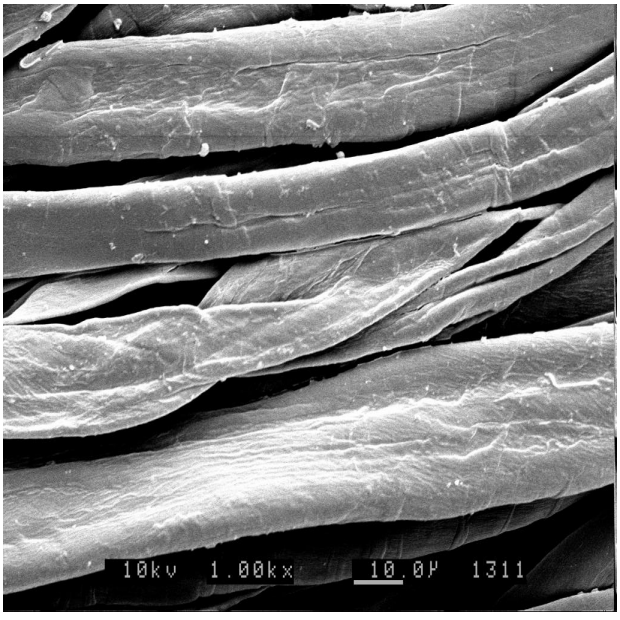


**(c)**


**(d)**

**(2) CO/PET blend**

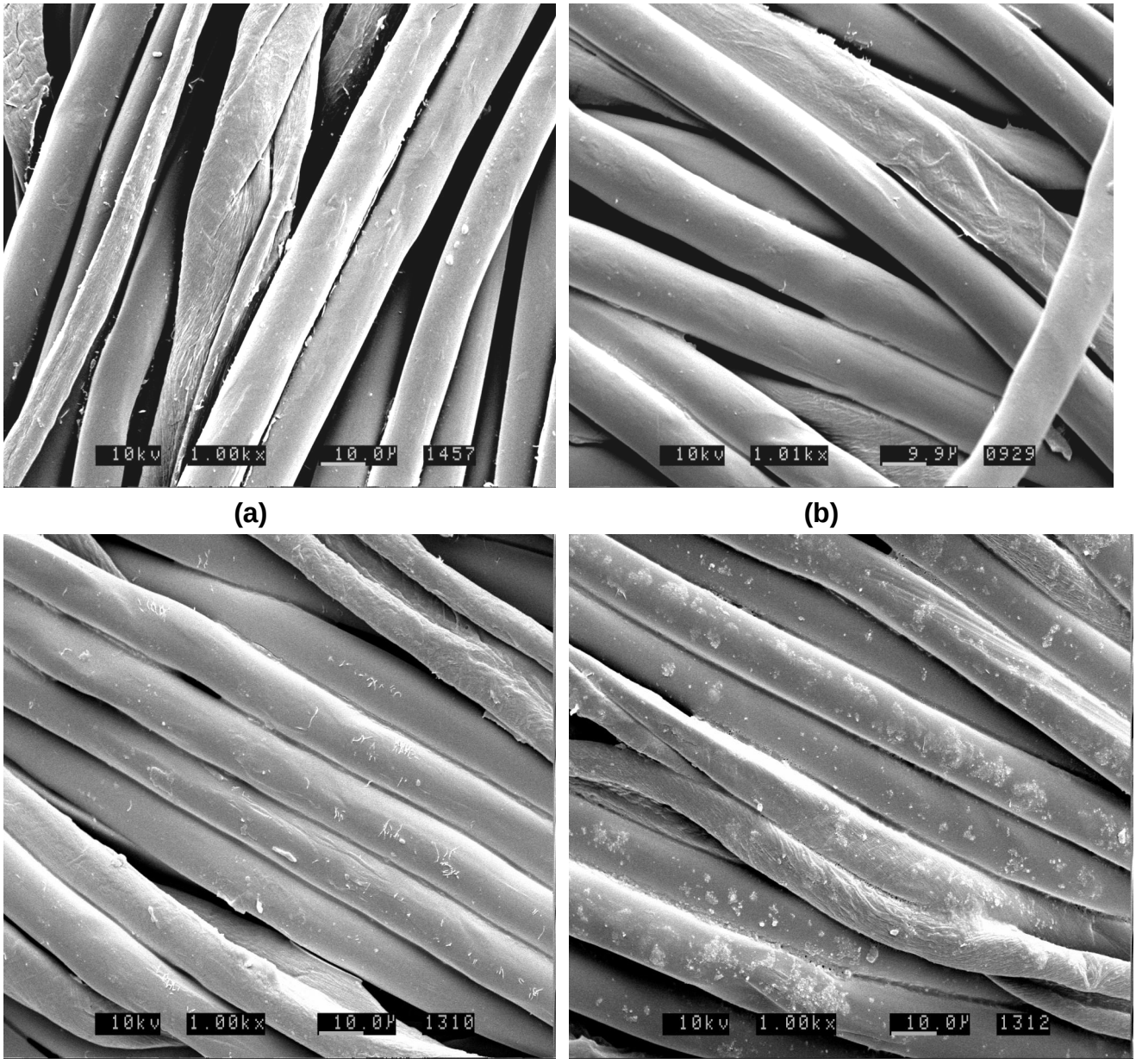


**(a)** **(b)**

**(c)** **(d)**

**Figure 20:** SEM micrographs of (1) cotton fabrics and, (2) CO/PET blend treated with different ZnO nanoparticle concentrations, (a) blank fabrics, (b) fabrics treated with ZnO in GPTMS-sol (20%), (c) fabrics treated with ZnO in GPTMS-sol (30%), (d) fabrics treated with ZnO in GPTMS-sol (50%). [20% means 2g ZnO/10 g GPTMS].

In the micrograph in case of fabrics treated with ZnO in GPTMS-sol (20%) or (30%), no agglomerated particles are visible on the surface which indicates a homogeneous distribution of the ZnO in the coating layer and the absence of unwanted

agglomeration during formation of the resulting coatings, but in case of fabrics treated with ZnO in GPTMS-sol (50%), the coating surface layer seem to be thicker.

SEM investigations were also carried out to investigate changes in the topography after coating with different ZnO particle sizes. The corresponding SEM micrographs are shown in Figure 21. In the micrograph 21a there is no agglomeration, therefore a homogenous distribution of the ZnO in the coating layer is expected, but in figure 21b there is little agglomerations appear, and in figure 21c with increasing the particle size, the bigger particles cause observed agglomeration on the fabrics surfaces.

**Cotton 100%**

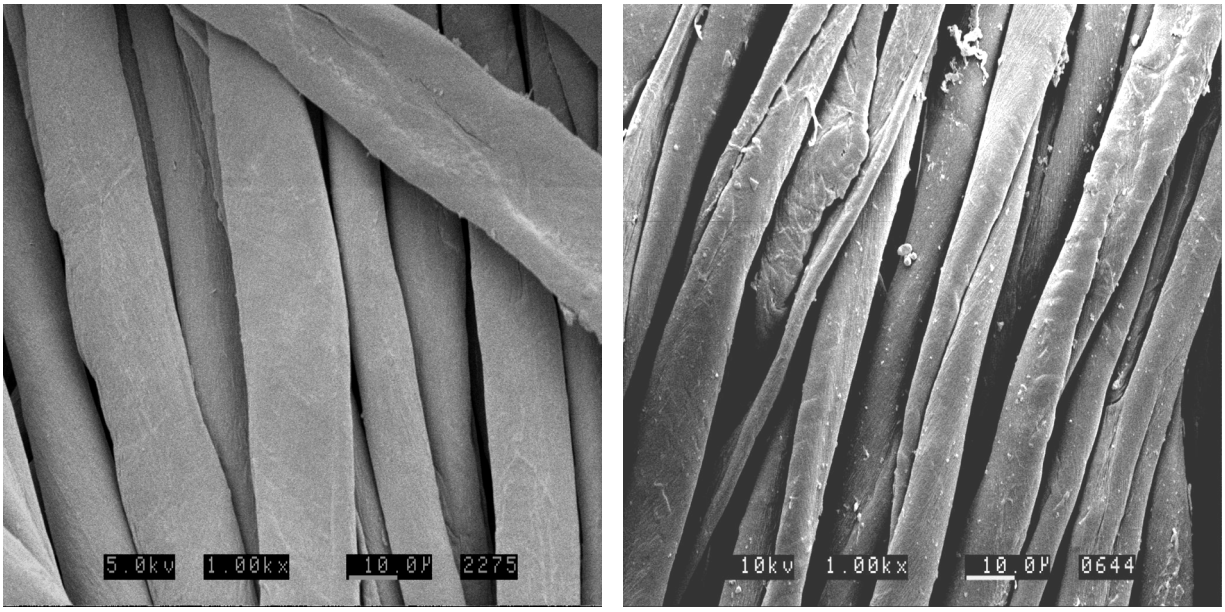


**(a)** **(b)**

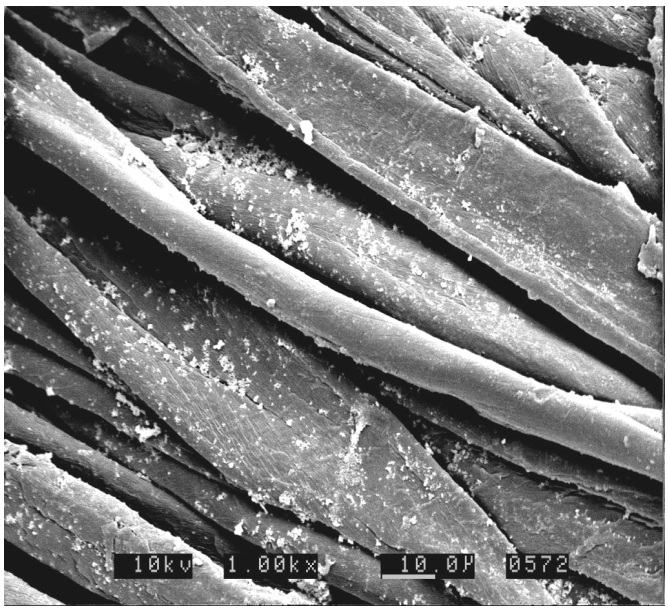


**(c)**

**(1) CO/PET blend**

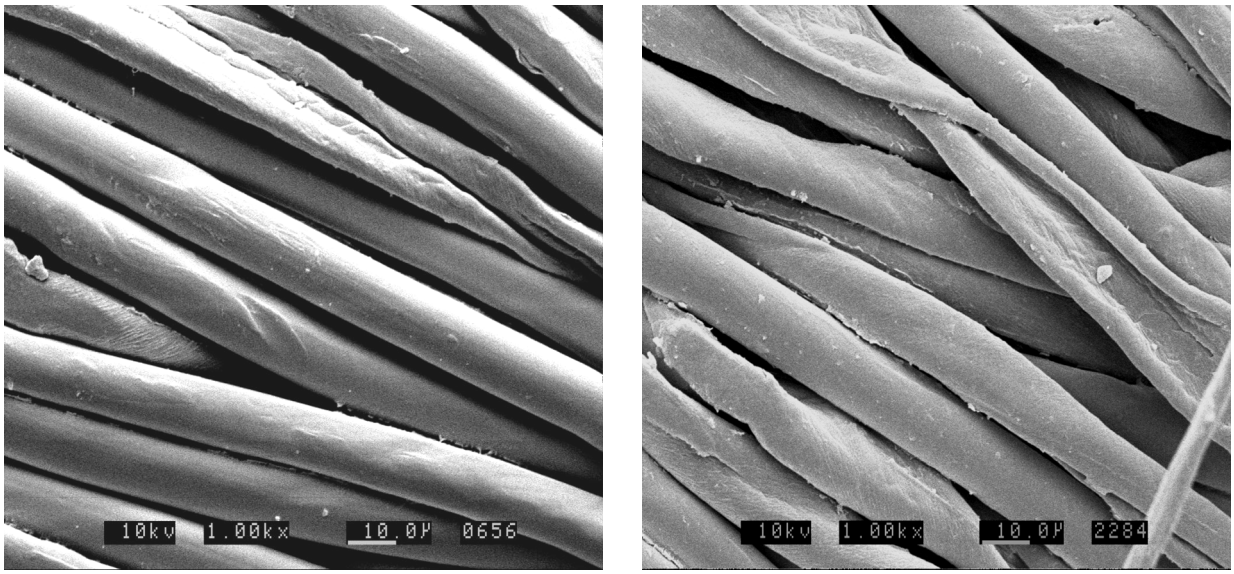


**(a)** **(b)**

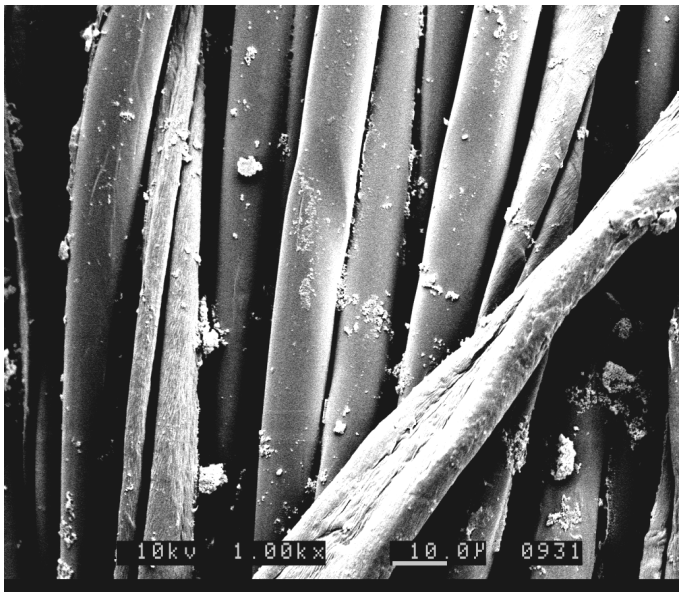


**(c)**

**Figure 21:** SEM micrographs of: (1) cotton fabrics and, (2) CO/PET blend treated with different ZnO particle sizes, (a) fabrics treated with ZnO particles 30 nm, (b) fabrics treated with ZnO particles 245 nm, and (c) fabrics treated with ZnO particles 625 nm

## 3.2. ZnO nanoparticles as UV-protection finish for textile

Sol-el finishing of cellulosic fabrics (Cotton 100% and CO/PET blend) decreases the transmission of UV radiation compared to the untreated cellulosic fabrics markedly which leads to an increase in the automatically calculated UPF (ultraviolet protection factor) value, this value shows how much longer a person wearing the particular clothing can stay out in the sun before the skin starts reddening compared to an unprotected person [12,13]. Table 8 shows the transmitted UV radiation in both UVA (280-320 nm) and UVB (320-400 nm) regions (which were expressed as TUVA and TUVB) of cotton and CO/PET blend fabric before and after treatment with the hybrid polymer based on GPTMS and nano-sized ZnO, since the use of suitable fabrics that block UV-B as well as UV-A radiation has been recommended. Different amounts of ZnO are showed. The table shows significantly decreased transmission values which were accompanied by an increasing in the UPF values in case of cotton and CO/PET blend coated with different concentration of ZnO in GPTMS-sol, since by increasing the ZnO nanoparticles concentration the transmission of UV radiation decreases and the UPF value increases. Figure 20 shows the UPF value of cotton and CO/PET blend coated with different ZnO nanoparticles concentrations. Based on its aromatic backbone polyester fibre should absorb certain amounts of UV radiation. Nevertheless, from Table 8 and Figure 22 it can be seen that blended with cotton the grey fabric yields only good UV protection as well as untreated cotton fabric, this may be explained by changing in some other factors which affect the transmission value of a given fabrics such as, structural characteristics of the fabrics (weave, yarn number, thread count, etc.) have a major influence on the porosity, weight and thickness of fabrics and therefore on the transmission of UV radiation through them. Light fabrics with open structures provide lower protection than more compacted fabrics. All these factors can affect finally on the UPF value after the coating process. Treatment with GPTMS results in equally good UV protection. Results presented in Table 9 as well as in Figure 22, show the increment of UV protection ability with the increment of concentration of ZnO-sol on the both treated fabrics – cotton and cotton/polyester. All cotton fabrics give off excellent UV protection, as well as the most of cotton/polyester fabrics. The only exception is Cotton/Polyester fabric treated with 10 % ZnO nanoparticles in GPTMS-sol that gives off very good protection.

**Table 9:** Effect of increasing the concentration of ZnO-sol on the UV-protection properties of cotton and cotton blend fabric samples after treatment.

| Substrate | | UPF value | $\tau_{UVA}$ | $\tau_{UVB}$ | UV Protection | |
|---|---|---|---|---|---|---|
| Untreated | Cotton | 21 | 7.355 | 3.629 | 20 | good |
| | CO/PET | 19 | 14.758 | 3.206 | 15 | good |
| Treated with GPTMS | Cotton | 19 | 15.846 | 2.643 | 15 | good |
| | CO/PET | 16 | 12.659 | 1.877 | 15 | good |
| Treated with ZnO in GPTMS-sol (10%) | Cotton | 78 | 3.429 | 0.744 | 50+ | excellent |
| | CO/PET | 37 | 10.704 | 1.227 | 35 | very good |
| Treated with ZnO in GPTMS-sol (15%) | Cotton | 147 | 2.201 | 0.451 | 50+ | excellent |
| | CO/PET | 47 | 7.662 | 1.199 | 45 | excellent |
| Treated with ZnO in GPTMS-sol (20%) | Cotton | 150 | 1.606 | 0.416 | 50+ | excellent |
| | CO/PET | 49 | 6.988 | 1.153 | 45 | excellent |
| Treated with ZnO in GPTMS-sol (30%) | Cotton | 163 | 1.574 | 0.331 | 50+ | excellent |
| | CO/PET | 45 | 8.583 | 1.187 | 45 | excellent |
| Treated with ZnO in GPTMS-sol (50%) | Cotton | 177 | 0.795 | 0.293 | 50+ | excellent |
| | CO/PET | 48 | 7.677 | 1.168 | 45 | excellent |

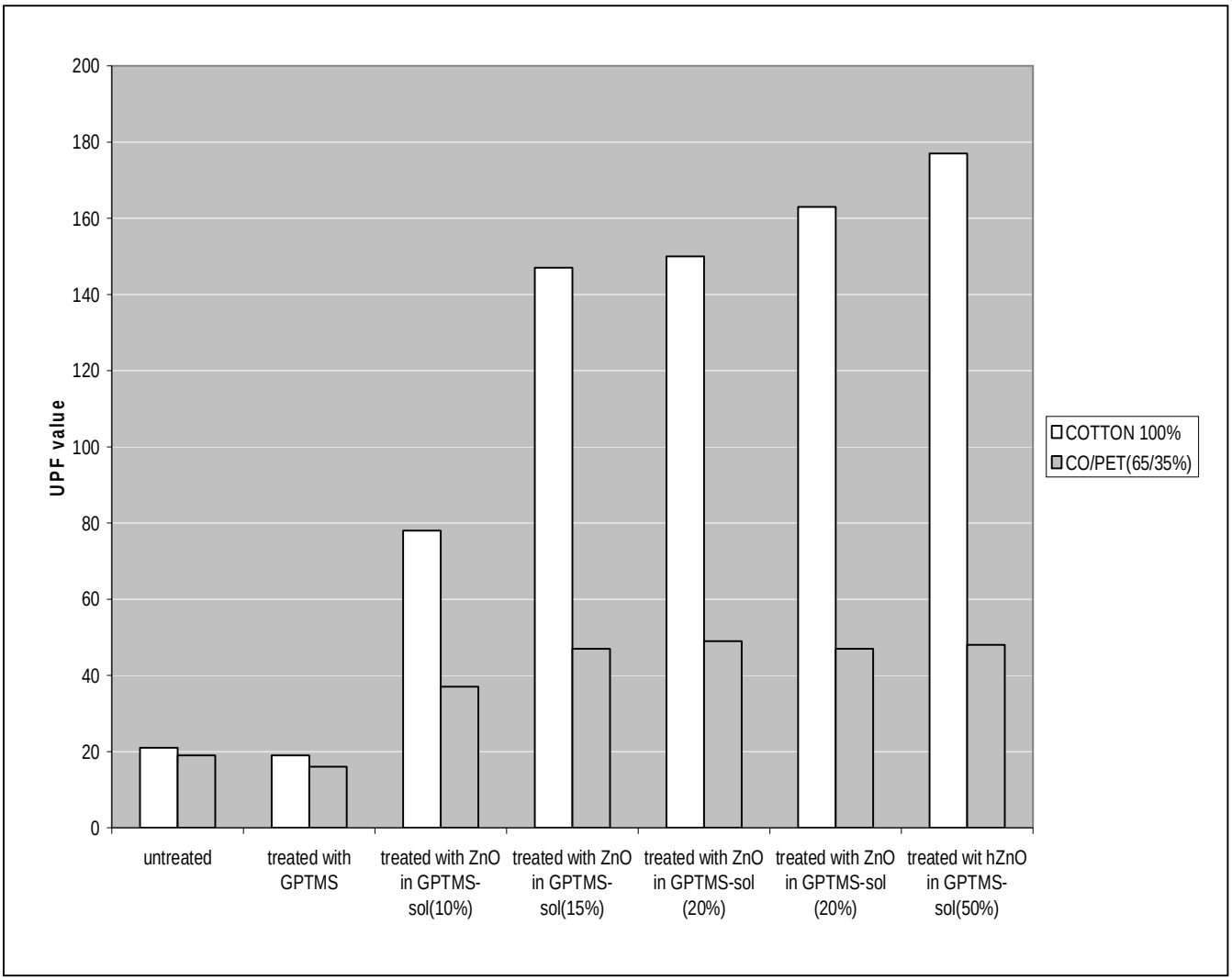


**Figure 22:** UPF value of Cotton and CO/PET substrates treated with different conditions.

To investigate the durability of the treatments laundry test were carried out. All samples were exposed to five washing cycles (40°C, 20 min, washing agent 1 g/l) before the UV transmission was investigated again. The corresponding data for selected fabrics are summarized in Table 10 indicating only slight changes in the absorption characteristics which were expressed as UPF values. These slight changes could be explained by an important factor which affect the transmission of UV radiation through the finished fabrics, this factor is the Laundering conditions of the garments: Shrinkage, pilling, the use of optical brightening agents in detergent formulation, temperature, time etc…) are factors that influence the UV radiation transmission of textile products.

From tables 10 it can be seen that sol-gel treatment have high durability since the 5 washing cycles have no effect on the UPF value of the fabric. Therefore, UV protection level of the treated fabrics is excellent even after laundering, except for Cotton/Polyester treated with ZnO in GPTMS-sol (10%), which remains very good.

**Table 10:** Effect of increasing the concentration of ZnO-sol on the UV-protection properties of cotton and cotton blend fabric samples after treatment and 5 laundering cycles.

| Substrate | | UPF value | $\tau_{UVA}$ | $\tau_{UVB}$ | UV Protection | |
|---|---|---|---|---|---|---|
| Untreated | Cotton | 22 | 7.957 | 3.119 | 20 | good |
| | CO/PET | 18 | 7.365 | 3.614 | 15 | good |
| Treated with GPTMS | Cotton | 20 | 8.577 | 3.881 | 15 | good |
| | CO/PET | 17 | 13.980 | 3.469 | 15 | good |
| Treated with ZnO in GPTMS-sol (10%) | Cotton | 76 | 7.563 | 0.409 | 50+ | excellent |
| | CO/PET | 38 | 10.398 | 1.121 | 35 | very good |
| Treated with ZnO in GPTMS-sol (15%) | Cotton | 146 | 1.723 | 0.373 | 50+ | excellent |
| | CO/PET | 48 | 7.982 | 1.244 | 45 | excellent |
| Treated with ZnO in GPTMS-sol (20%) | Cotton | 152 | 6.035 | 0.321 | 50+ | excellent |
| | CO/PET | 48 | 5.395 | 1.014 | 45 | excellent |
| Treated with ZnO in GPTMS-sol (30%) | Cotton | 162 | 4.336 | 1.021 | 50+ | excellent |
| | CO/PET | 47 | 7.342 | 1.321 | 45 | excellent |
| Treated with ZnO in GPTMS-sol (50%) | Cotton | 179 | 1.255 | 0.397 | 50+ | excellent |
| | CO/PET | 49 | 4.010 | 1.362 | 45 | excellent |

### 3.2.1. Effect of ZnO-sol on the performance properties of the fabrics

It is very important thing to study the effect of the finishing treatment on the performance properties of the fabrics compared to the untreated fabrics. These performance properties can be known by following the effect of some tests, e.g. tensile strength, elongation at break, air permeability, degree of whiteness, martindale test and the bending stiffness of the treated fabrics. In tensile strength and elongation tests we affect by certain tension test on the fabric then we can determine the strength and the elongation of the fabric, in air permeability test the fabric was exposed to high air pressure then the rate of air flow through the fabric was determined, in degree of whiteness test we determine the change of the degree of whiteness after the treatment compared to the blank sample, from Martindale test we can determine the degree of fabric resistance to the abrasion after subject to straight line rubbing motion using the effect of certain weight, and from the bending stiffness test measurements we can get information about the degree of rigidity/stiffness of the fabric after the coating process.

The mechanical data of the treated and untreated samples and the influence of the sol treatment for the degree of whiteness and for the air permeability were investigated and the corresponding data are given in Table 11. It can be determined that tensile strength of the coated cotton as well as the coated cotton blend fabrics is slightly decrease as a result of the finishing process. Also the whiteness of the fabrics is slightly decreased, but in a tolerable degree. The decrease for cotton is between 3.8 to 6.4 % the decrease for CO/PET between 3.2 and 6.6 % only. Air permeability is an important factor in the performance of textile materials used to provide an indication of the breathability of coated fabrics, within the investigation summarized in Table 11 it can be seen that there is no worsening of the air permeability but at least a slight improvement of maximum 6 %. The mentioned increase of the bending stiffness values recorded by increasing the concentrations of nano ZnO could be explained by a higher up take of the inorganic-organic hybrids polymers on cellulosic fabric surface, due to an increasing solid content for sol with higher amount of ZnO.

**Table 11:** Effect of increasing the concentration of ZnO–sol on some performance properties of cotton and cotton blend fabric samples.

| Substrate | | Tensile strength (daN) | Elongation at break (%) | Air permeability l/dm$^2$*min. | Degree of Whiteness (Berger) | Bending Stiffness (cNcm$^2$) |
|---|---|---|---|---|---|---|
| Untreated | Cotton | 101.5 ±2.07 | 21.6 ±1.02 | 250.5 | 66.0 | 12.12 ±.028 |
| | CO/PET | 87.4 ±1.48 | 30.7 ±1.42 | 334.0 | 70.9 | 3.88 ±.023 |
| Treated with ZnO in GPTMS-sol (10%) | Cotton | 97.5 ±2.18 | 22.8 ±1.11 | 258.8 | 56.1 | 13.46 ±.018 |
| | CO/PET | 86.6 ±1.41 | 32.3 ±1.02 | 350.7 | 68.3 | 5.23 ±.013 |
| Treated with ZnO in GPTMS-sol (15%) | Cotton | 96.5 ±1.02 | 22.3 ±1.12 | 256.0 | 56.7 | 13.83 ±.025 |
| | CO/PET | 84.2 ±1.028 | 33.0 ±1.01 | 350.7 | 68.9 | 8.38 ±.014 |
| Treated with ZnO in GPTMS-sol (20%) | Cotton | 98.2 ±1.028 | 20.8 ±1.08 | 254.6 | 56.9 | 15.21 ±.018 |
| | CO/PET | 84.4 ±1.92 | 32.6 ±1.48 | 355.2 | 69.2 | 9.65 ± .022 |
| Treated with ZnO in GPTMS-sol (30%) | Cotton | 95.4 ±1. 28 | 20.6 ±1. 28 | 256.0 | 61.6 | 18.54 ±.017 |
| | CO/PET | 82.9 ±1.01 | 32.7 ±1.52 | 350.1 | 70.2 | 13.83 ±.026 |
| Treated with ZnO in GPTMS-sol (50%) | Cotton | 96.2±1.10 | 21.3 ±1.38 | 258.8 | 62.2 | 20.81 ± .012 |
| | CO/PET | 83.9 ±1.028 | 31.6±1.16 | 352.2 | 70.6 | 15.19 ±.024 |

It has been reported that comparable hybrid polymers modified with alumina particles will improve the wear-resistance of the treated fabrics [122]. Against this background Martindale tests were carried out. An exemplarily chosen pair of samples is shown in Figure 23. The picture shows an untreated and a treated sample both after 20.000 scrubbing cycles in case of both cotton 100% and Cotton/polyester (65/35%) fabrics. As can be clearly seen the ZnO in GPTMS-sol (10%) treated sample is still intact showing no destruction while the untreated one is already destroyed.

**Cotton fabric 100%**

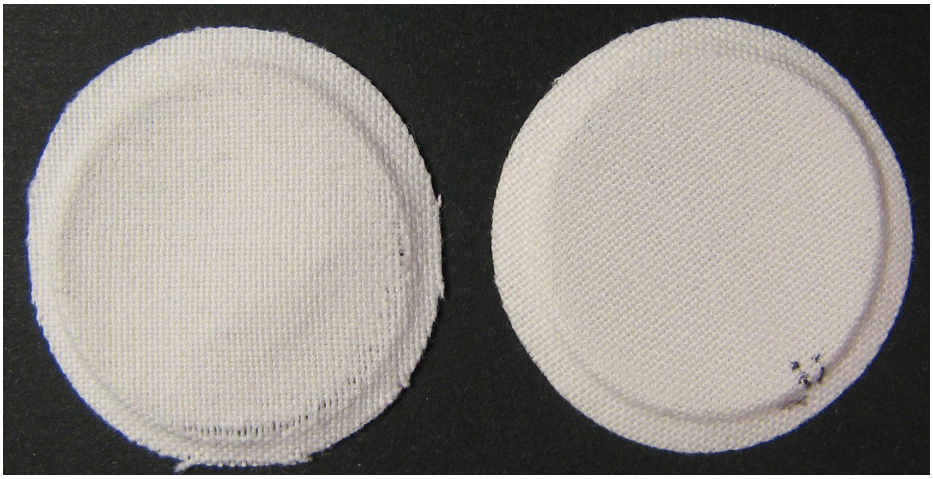

(a) Untreated (b) treated

**CO/PET blend**

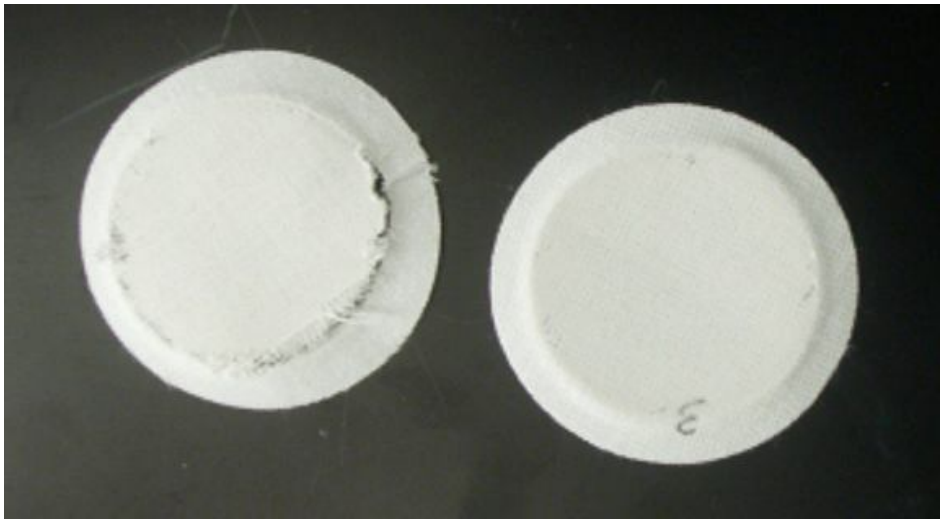

(c) Untreated (d) treated

**Figure 23:** Results of a Martindale test investigating the wear resistance of the ZnO in GPTMS-sol (10%) treated samples after 20.000 scrubbing cycles compared to the untreated sample in case of cotton 100% and CO/PET blend fabrics.

Martindale tests were carried out also for cotton and CO/PET fabrics treated with ZnO in GPTMS-sol (20% and 30%), the same results were obtained, since the untreated fabrics were destroyed while the treated samples have no destruction.
SEM investigations were also carried out to investigate changes in the topography of the treated and untreated fabrics after 20.000 scrubbing cycles. Figure 24 shows that compared to the treated fabric surface, the untreated one is already destroyed.

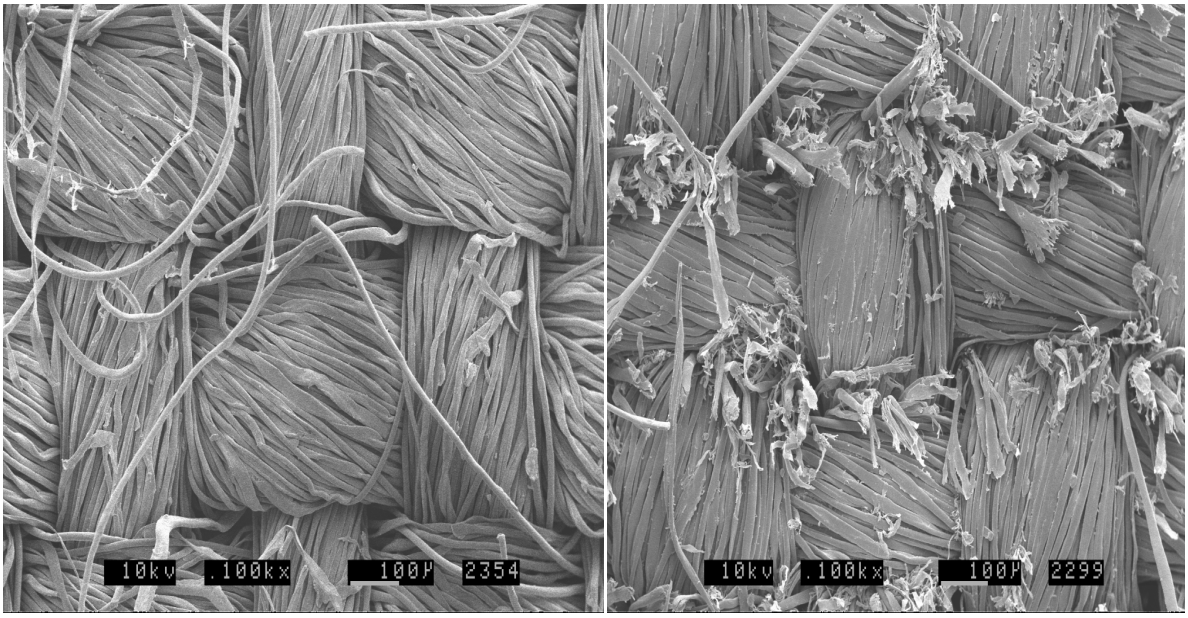


(a) treated (b) untreated

**Figure 24:** Results of a Martindale test investigating the wear resistance of the ZnO in GPTMS-sol (10%) treated samples after 20.000 scrubbing cycles compared to the untreated sample

## 3.3. ZnO nanoparticles as antibacterial finish for textile

### 3.3.1. Introduction

Fabrics are excellent media for the growth of microorganisms when the basic needs such as, moisture, oxygen, nutrients and suitable temperature are available. Natural fibres like cotton are more subject to the attack of microbs than synthetic fibres. In this study, cotton and cotton/polyester fabrics coated with hybrid polymers containing ZnO nanoparticles were evaluated for antibacterial activity to assess the effectiveness of ZnO nanoparticle coating. The activity is qualitatively and quantitatively evaluated.

The antibacterial action of ZnO is reported by several authors. The hybrid materials prepared are applied to cellulosic cotton (100%) and cotton/polyester (65/35%) fabrics. The antibacterial performance of these sol-gel derived hybrid materials is exemplarily investigated against Gram-negative bacterium *E.coli* DSMZ 498 and Gram–positive *Micrococcus lutues* ATCC 9341. The effect of particle size and concentration on the antibacterial performance is examined. This study shows an enhanced antibacterial activity against the Gram-negative and Gram–positive bacterium in repeated experiments as well for increasing concentrations of ZnO nanoparticles as for decreasing particle sizes. Literature discusses various (active) species and processes responsible for the antibacterial action of ZnO. Therefore a particular attention is paid to investigate active species available in the described systems as well as to observe possible interaction between the nanoparticles and bacteria, first results will also be presented.

## 3.3.2. Evaluation of ZnO-nano treated fabrics for antibacterial activity

### 3.2.3.1. Disc diffusion method

In this study, the cellulosic fabrics were selected for the evaluation of the relative antibacterial activity of ZnO sol of various concentrations of the particle sizes of 30-157 nm, and different particle sizes of the same concentration toward *E.coli* and *Micrococcus lutues* was studied qualitatively in agar plate media by halo method (zone of inhibition). Antibacterial effect of treated cotton fabric in the form of inhibition zones, evaluated by the disc diffusion assay, is shown in Figure 25. The bactericidal activity against *E.coli* and *M.lutues* shows a clear zone of inhibition within and around the samples finished with the hybrid polymers modified with different concentrations of ZnO nanoparticles.

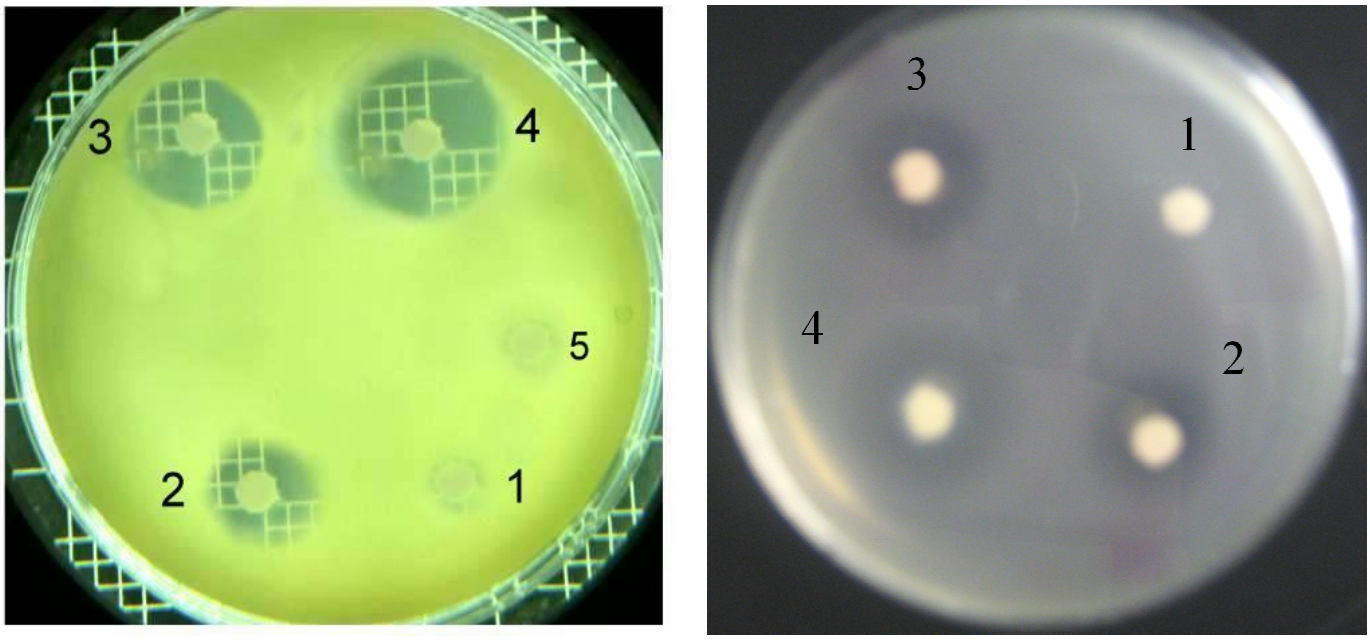


**(a)** ) ***M.lutues*** **(b)** ***E.coli***

**Figure 25:** The disc diffusion test of different concentrations of ZnO nanoparticles for the growth inhibition. (a) *M.lutues* and (b) *E.coli.* Both photographs show the clear zone of inhibition around the samples impregnated with different concentrations of ZnO nanoparticles compared with untreated fabrics and treated with only GPTMS. In Figure (1) untreated, (2) treated with ZnO in GPTMS-sol (10%), (3) treated with ZnO in GPTMS-sol (30%), (4) treated with ZnO in GPTMS-sol (50%), and (5) treated with GPTMS.

From Figure 25 it can observed that, compared to the untreated fabrics or the fabric treated only with GPTMS, the fabrics treated with different ZnO concentrations have more antibacterial activity represented by the presence of halo around the fabric. Since the zone of inhibition is simply the area on the agar plate that remains free from bacterial growth, therefore, the size of the halo is usually related to the level of antibacterial activity of the used finishes - a larger zone of inhibition usually means that the antibacterial is more effective. So, from the figure we can see that, the higher the ZnO concentrations within the coating layer, the higher the antibacterial activity of the finished fabrics.

In additional experiments we tested the antibacterial activity of cotton 100% samples that were treated with hybrid coatings filled with a constant amount of ZnO but with

varying ZnO particle sizes (30, 245, and 625 nm). Corresponding results are shown in Figure 26.

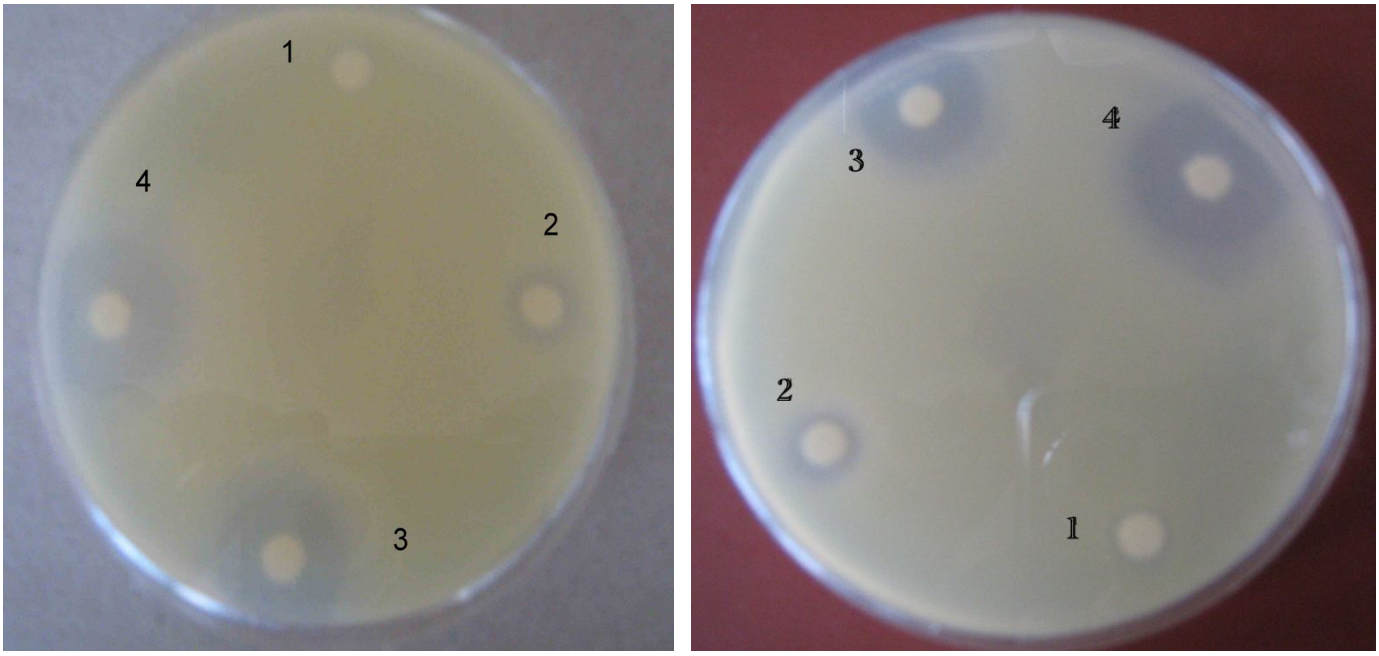


**(a)** ) ***M.lutues*** **(b)** ***E.coli***

**Figure 26:** The disc diffusion test of different ZnO particle sizes for the growth inhibition of: (a) *M.lutues* and (b) *E.coli.* (1) untreated fabric, (2) fabric treated with ZnO (10%) in GPTMS-sol (625 nm), (3) fabric treated with ZnO (10%) in GPTMS-sol (245 nm), and (4) fabric treated with ZnO (10%) in GPTMS-sol (30 nm).

Experiments were carried out with *E.coli* and *M.lutues*. The image shows a clear zone of inhibition around the samples modified with different particle size of ZnO nanoparticles compared with untreated fabrics. As can be observed, for a constant amount of ZnO the antibacterial activity increased with decreasing size of ZnO particles employed.

Generally, from Figure 25 and 26 it can be concluded that the untreated fabrics and the fabrics treated with only GPTMS had no antibacterial ability. An antibacterial activity can be observed when fabrics are treated with the hybrid polymer modified with ZnO nanoparticles. The antibacterial activity of ZnO nanoparticles increases as well with increasing nanoparticle concentration as with decreasing particle size. Since by increasing the ZnO nanoparticles concentration, the ZnO amount within the coating layer increase and this increase the possibility of the inhibition growth of the

bacteria as a result of the interaction between the ZnO particles and the bacteria. Also the smaller the particle sizes of the same weight, the higher the specific surface area which also increase the possibility of the interaction between the ZnO particles and the bacteria. Since the smaller particles improved the antibacterial activity of the treated textiles.

### 3.2.3.2. The AATTC Test Method 100-2004

The antibacterial activity of the coated fabrics was estimated for the *E.coli* and *M. lutues* according to the AATTC100-2004 standard method. Following a modified AATCC Test Method 100-2004 [115], the antibacterial effect of treated fabrics was determined in several test series.

Results for the antibacterial activity of cellulosic coated fabrics are presented in figure 26 and 27. Figure 27 shows the bacterial reduction rate of cotton 100% fabric treated with ZnO (30nm) in GPTMS-sol (10%) against both *E.coli* and *M. Lutues.* As expected, no reduction of the bacteria *E.coli* and *M. lutues* was found in case of the untreated fabrics. On the contrary, there was an increase in the reduction of bacteria after 5 h of incubation in comparison to 0 h contact time. As shown in Figure 27 cotton treated fabric leads to nearly 100% reduction of *E.coli* after 5h while to nearly 97% reduction of *M. Lutues*, since after 1h 43% of *E.coli* and 36% of *M. Lutues* bacteria are killed, after 2 h 71% of *E.coli* and 69% of *M. Lutues* bacteria are killed, and the longer the experiment is carried out the more bacteria are killed and finally after 5h 99.5% of *E.coli* and 96.5% of *M. Lutues* bacteria are killed.

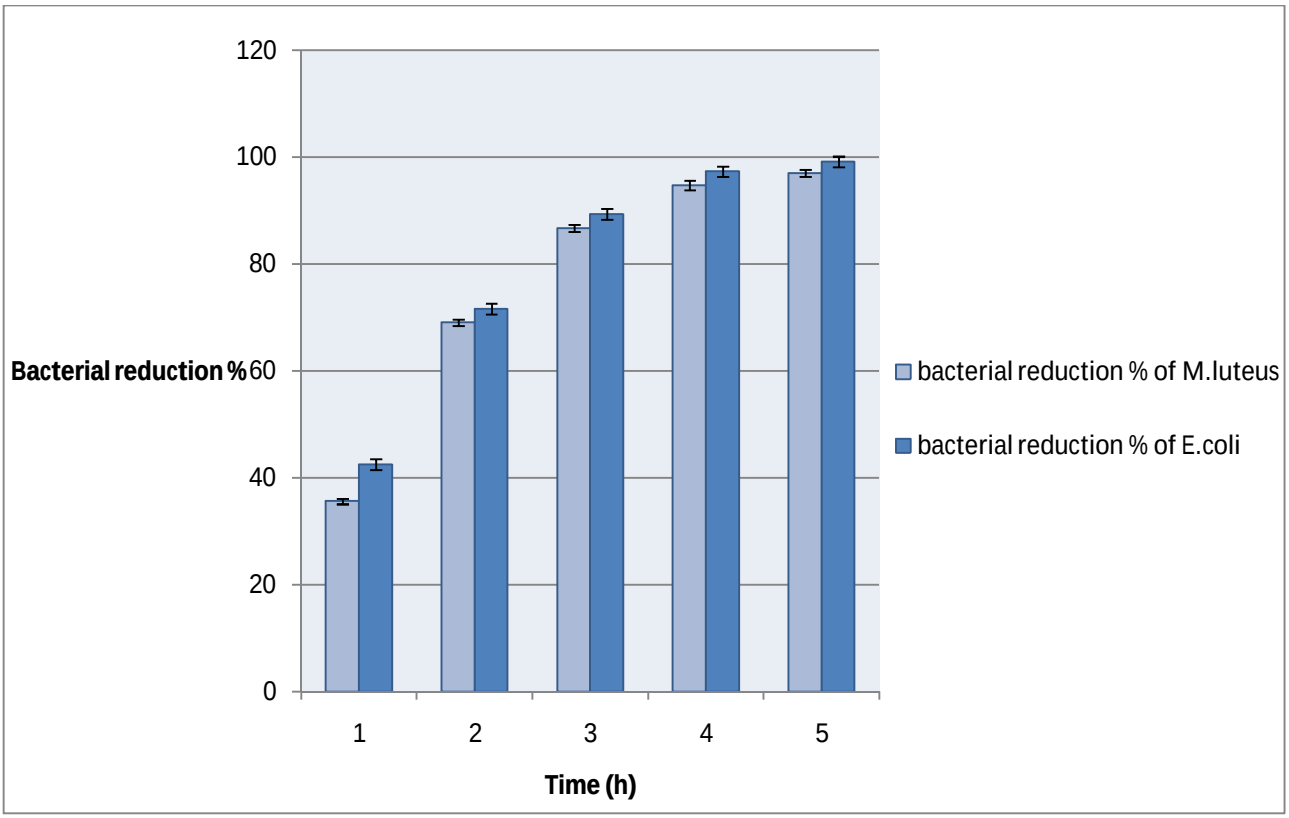


**Figure 27:** Reduction rate of the cotton 100% fabric treated with ZnO (10%, 30 nm) in GPTMS sol against *E.coli & M.lutues*

From the previous repeated experiments it can be concluded that in case of ZnO (10%, 30 nm) /GPTMS-sol cotton coated fabric and after 5h nearly 100% reduction rate of the bacteria can be obtained.

The antibacterial activity of cotton/polyester blend fabrics coated with a hybrid polymer modified with a constant amount of ZnO of different particle sizes was also determined using *E. coli* and *M. lutues*. In this test, ZnO of three different particle sizes (30, 245, 625 nm) were used. Figure 28 shows the bacterial reduction rate of cotton/polyester blend fabrics coated with different ZnO particle sizes (same concentration) in GPTMS-sol. As shown in Figure 28, after 5 h the cotton/polyester blend fabrics coated with smaller particle size of ZnO (30 nm) leads to the complete inhibition of *E. coli* and *M.luteus* growth (99% and 99.8%) respectively, while in case of fabrics coated with ZnO of particle size (245 nm) bacterial reduction rate of 95.8% and 97.7% of *E. coli* and *M.luteus* growth respectively were obtained. In case of fabrics coated with bigger ZnO particle of (622 nm) bacterial reduction rate of 93.6% and 94.3% of *E. coli* and *M.luteus* growth respectively were obtained.

From the previous repeated experiments it can be concluded that for cotton/polyester blend fabrics coated with different ZnO particles of same concentration, the smaller the particle sizes of ZnO, the higher the antibacterial activity of the coated fabrics, since the smaller particles are more active and has great effect due to the higher specific surface area of the smaller particles.

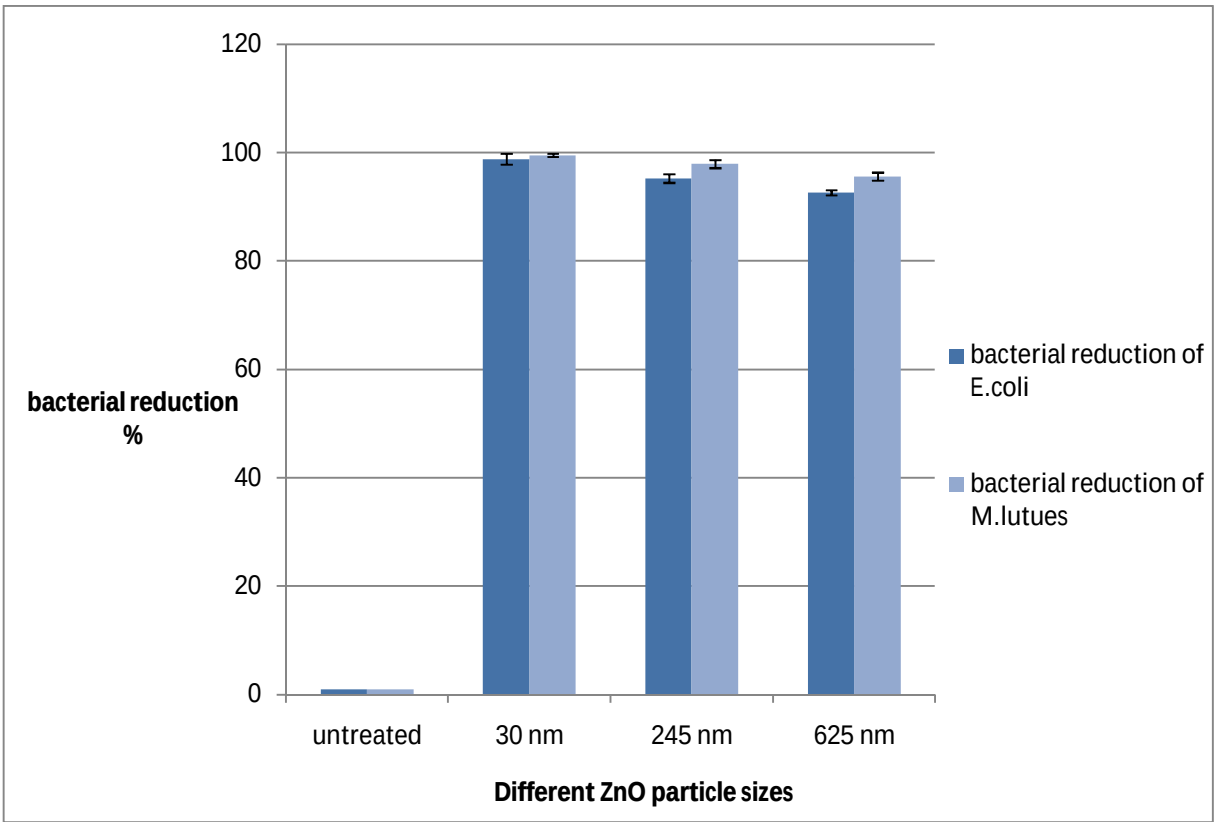


**Figure 28:** Reduction rate of the CO/PET (65/35%) fabric treated with different particle sizes of ZnO-sol against *E.coli & M.lutues* after 5h

### 3.2.3.3. Tetrazolium/formazan-test method TTC

The antibacterial activities of the cotton 100% treated fabric samples were evaluated against *E.coli* and *M. lutues* using the TTC test method.

This test serves as indicating system for the determination of the viability of bacterial cell, since absorbance of formazane is directly proportional to the amount of living bacteria. Figure 29 shows the antibacterial activity (which was expressed by formazan absorbance values) for cotton fabrics treated with different ZnO nanoparticle concentrations (10%, 20%, 30% and 40%) in GPTMS-sol. The results shown in Figure 29 are in good agreement with the results shown before. We observe a strong reduction of the vital cells due to the presence of ZnO-modified

textiles. Increasing the amount of the ZnO within the hybrid polymer increases the resulting antibacterial activity. A concentration of 10% ZnO in GPTMS-sol in the hybrid polymer yields a reduction of 91%, an increase of this concentration to 50% ZnO in GPTMS-sol improve this value to 97%, since the higher the ZnO concentration the lower the formazan absorption value (i.e. more bacteria are killed) which indicates the higher antibacterial activity.

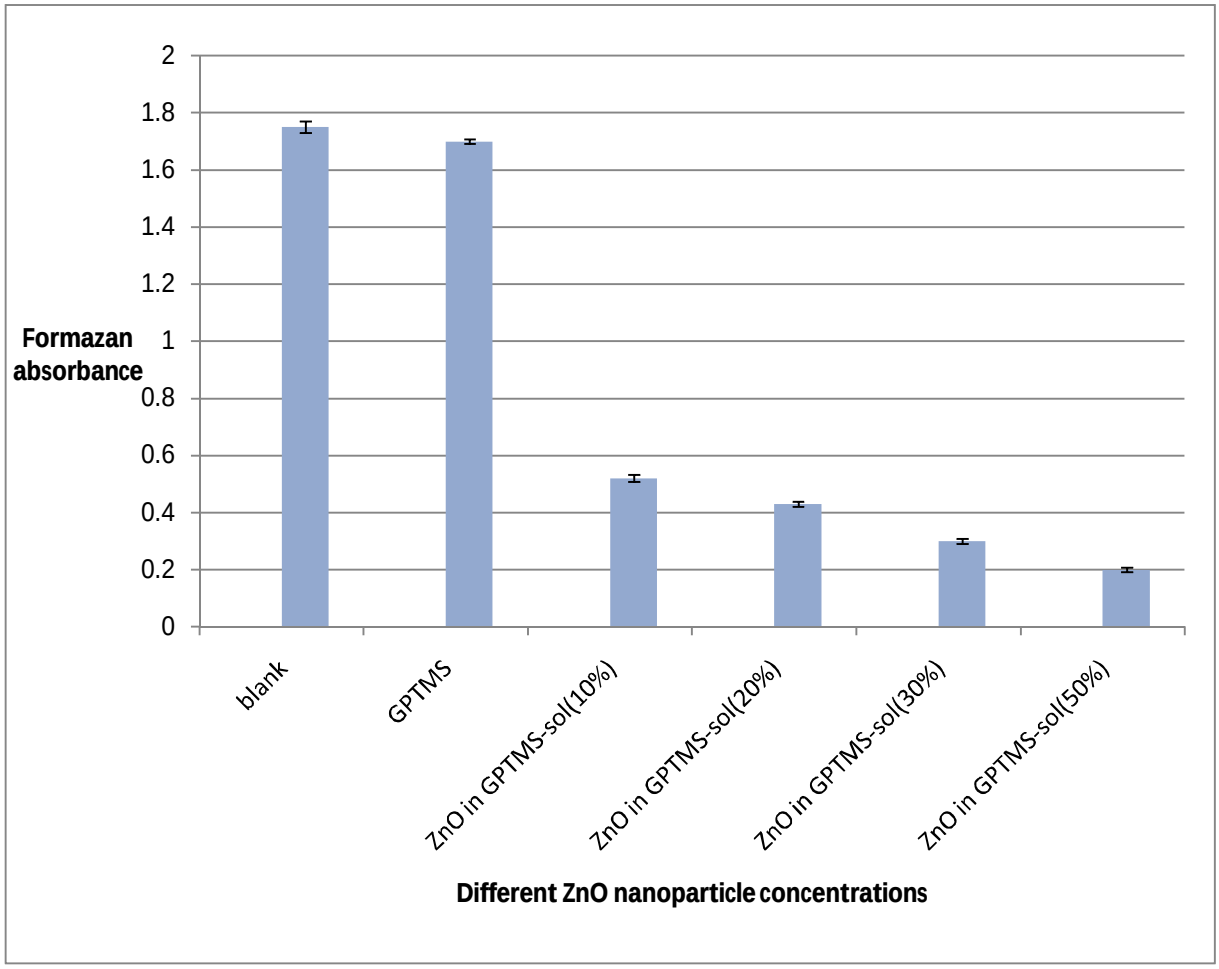


**Figure 29:** Absorbance of formazan for cotton 100% fabrics coated with different ZnO nanoparticle concentrations in GPTMS-sol.

### 3.3.3. ZnO sol labeled with FITC

In this test, ZnO nanoparticle in the range of (30 nm), FITC (Fluorescein isothiocyanate) and *E.coli* bacterial cell are used for this test using the microscope (KEYENCE all-in-one- Type Fluorescence Microscope, BZ-Analyzer 8100E, Japan). ZnO nanoparticles and FITC were chemically linked, then ZnO nanoparticles can be worked as a fluorescent agent for bacterial cell labelling through the green

florescence observed after using ZnO/FITC solution together with the bacteria; since as shown in Figure 30 both only bacteria and bacteria/FITC have no green florescence observed under the Fluorescence Microscope.

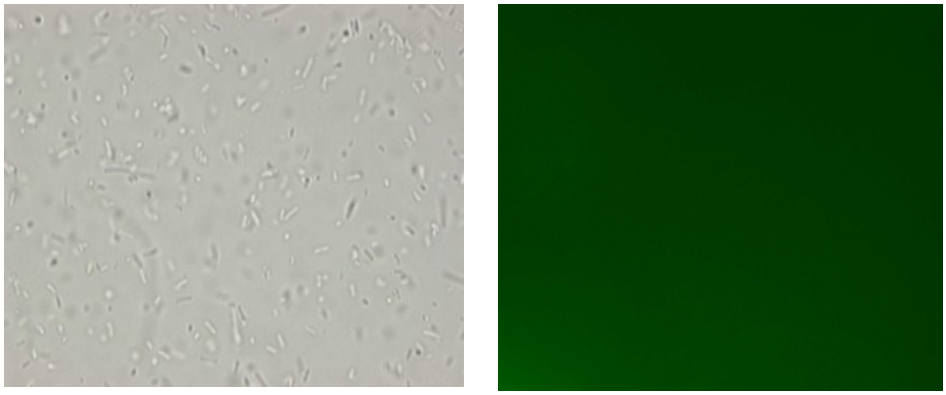

**(Only bacteria)**

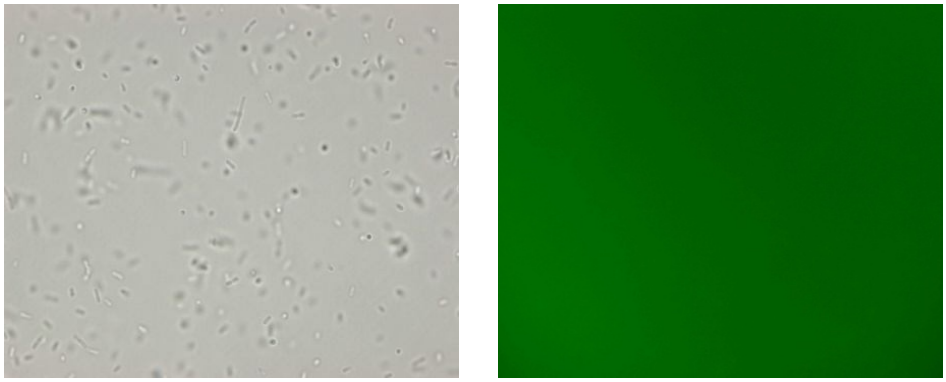

**(Bacteria and FITC)**

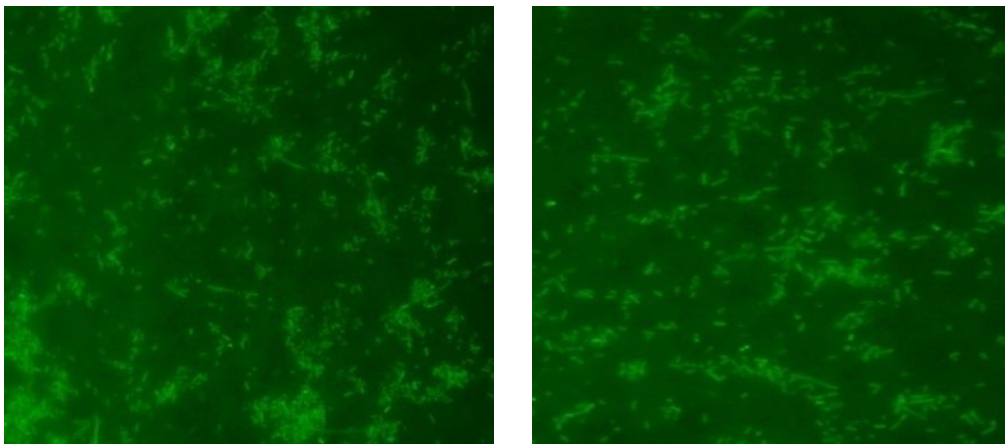

**(a: zero time)** **(b: 1h)**

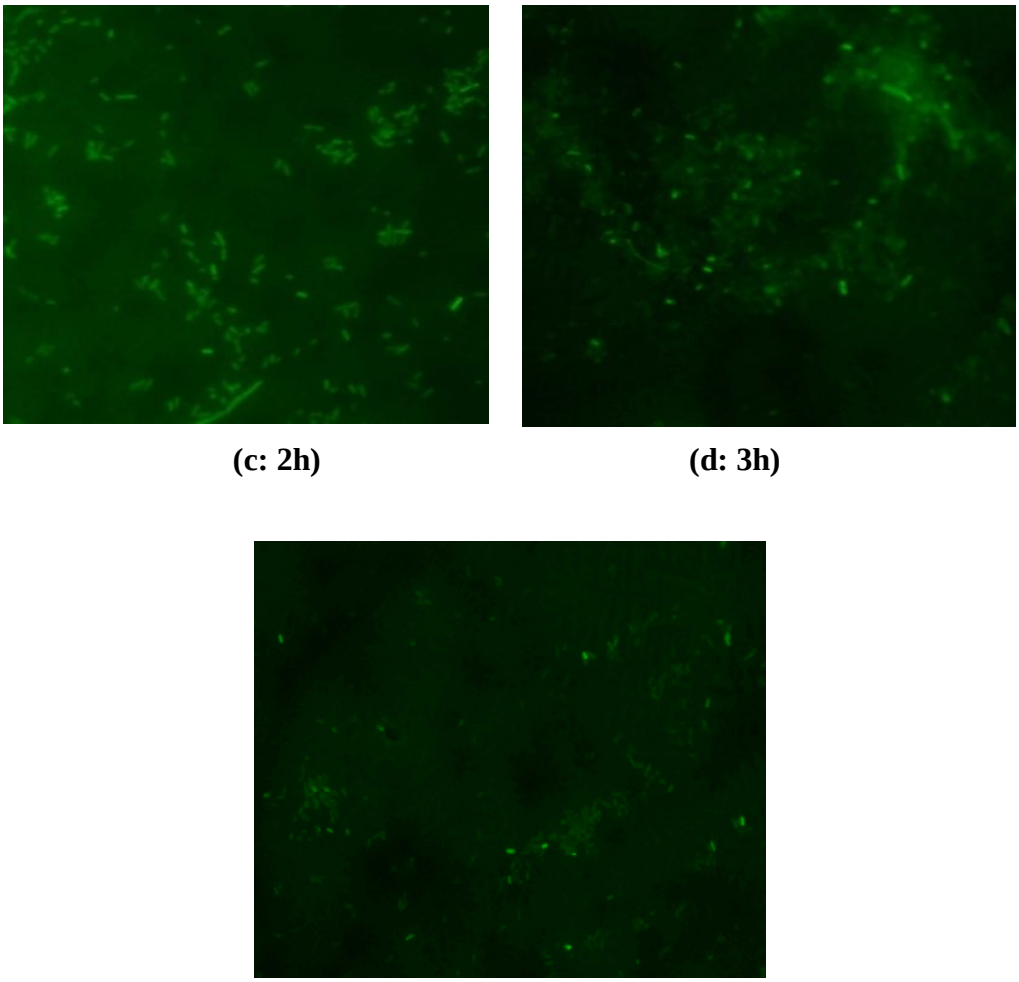

**(c: 2h)** **(d: 3h)**

**(e: 4h)**

**Figure 30:** Cell imaging with FITC-ZnO nanoparticles

These images in Figure 30 (a-e) are fluorescence microscopic image of *E.coli* cells treated with FITC (fluorescein isothiocyanate)-labeld ZnO nanoparticles. The first image (a) indicates that many of the FITC-ZnO associated *E.coli* cells are still viable (the number of fluorescing particles is very high), but this is because of the short incubation time (zero time) which used to prepare the cell for imaging.

We can observe that after two hours the number of fluorescing labeled particles goes down indicating that more and more cells are decomposed. Other authors [123] describe a “green granular appearance” of the *E.coli* as a result of the particulate nature of the nanoparticles adhering to the surface of the cell. The reduction of the bacteria was nearly complete after 4h. Visualization of the FITC-ZnO signal alone indicates that the FITC-ZnO particles were associated with the bacterial cells and emitting very clear green fluorescence and this prove the direct interaction between

ZnO nanoparticles and the membrane surface of the cell. If ZnO nanoparticles migrate to the cell, then the cell can be breaked up and the local concentration of ZnO particles decreased result in lower intensity of the FITC. FITC only and dead (non viable) cell is on empty image. To be sure that the bacteria is dead, counting test was done after 4h to sample from the FITC-ZnO/bacteria solution and no bacterial colonies were grown in the agar plate, this mean that the bacteria was completely dead.

To complete test for the action of ZnO nanoparticles and the bacteria SEM analyses were carried out. SEM analyses were performed to investigate the morphological changes of the *M.lutues*, 100 µl of ZnO nanoparticles resuspended in isopropanol (0.1 g/100 ml) as described in 2.1.1 was added to 50 ml of 100 µl - $10^8$ CFU/ml of the *M.lutues* culture in LB broth medium with shaking. Cultures were grown at 37°C under an agitation condition while shaking. Then 10 µl from ZnO/bacteria (treated) or from only bacterial culture solution (control) was investigated under the SEM. Figure 31 (a) shows the cultures of bacteria (blank), (b) shows that direct interaction between ZnO nanoparticles and the external bacterial membrane surface could be one of the possible causes for antibacterial activity of ZnO nanoparticle. By the time, the longer the experiment the higher the reduction of the bacterial culture number can be observed as shown in figure 31 (c) and (d). ZnO nanoparticles used in this test are in the average size of (30nm) and the bacteria has cell diameter of [~840 nm] as shown in Figure 31 (a)], single ZnO particles cannot be observed since they are too small.

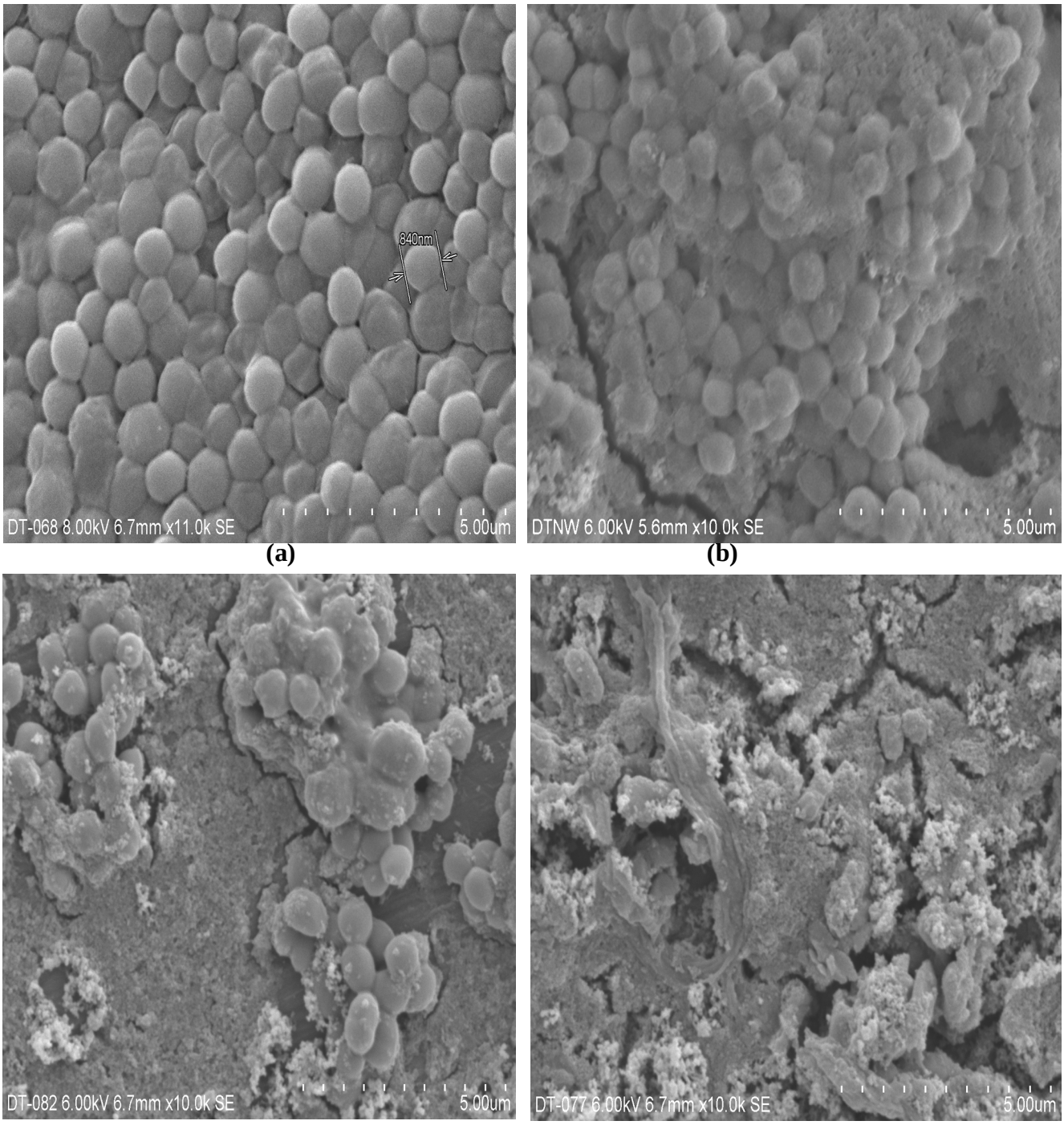


**Figure 31:** SEM micrographs of ZnO and *M.lutues.*

Since: (a) blank *M.lutues* culture, (b) bacterial *M.lutues* culture treated with ZnO nanoparticles after 1h, (c) bacterial *M.lutues* culture treated with ZnO nanoparticles after 2h, (d) bacterial *M.lutues* culture treated with ZnO nanoparticles after 3h.

The same experiments were done using *E.coli* culture. Figure 32 (a-d) shows the SEM investigations which indicate the morphological changes of the *M.lutues* as a result of the direct interaction between the bacterial cell membrane and ZnO nanoparticles. In figure 31a, many bacterial colonies were observed but this is due to the short incubation time (1h), but in figure 31b the reduction of the bacteria was nearly complete.

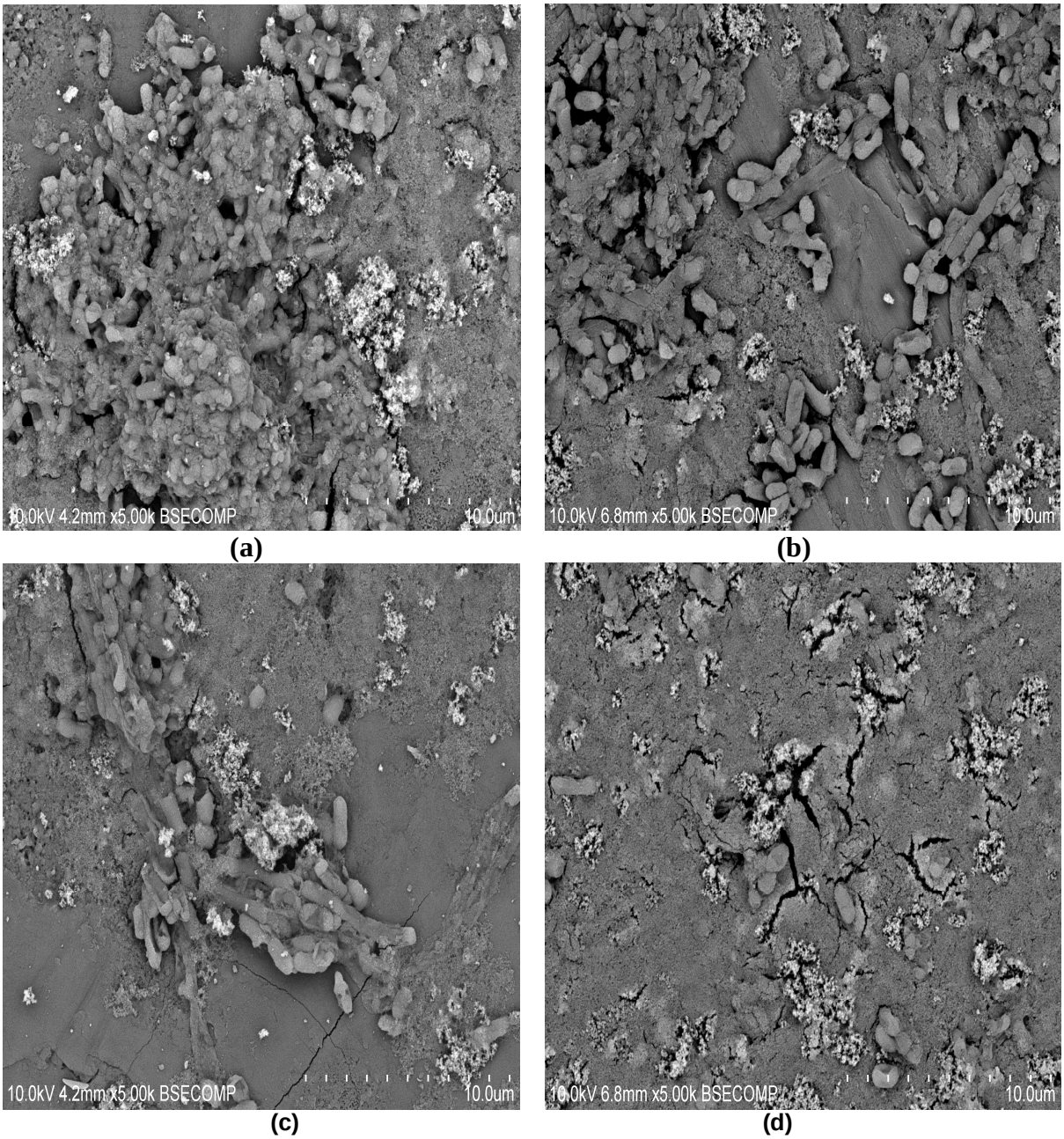


**Figure 32:** SEM micrographs of ZnO with *E.coli*.

Since: (a) bacterial *E.coli* culture treated with ZnO nanoparticles after 1h, (b) bacterial *E.coli* culture treated with ZnO nanoparticles after 2h, (c) bacterial *E.coli* culture

treated with ZnO nanoparticles after 3h, (d) bacterial *E.coli* culture treated with ZnO nanoparticles after 4h.

SEM micrographs of two cross sections of *E.coli* culture treated with ZnO nanoparticles after 1h and 3h respectively are shown in Figure 33a and 33b.The reduction of the *E.coli* culture numbers with the time is clearly observed also the change in the topography of *E.coli* cell due to the decomposition as a result of the direct interaction with ZnO nanoparticles due to the coverage of the cell with the nanoparticles.

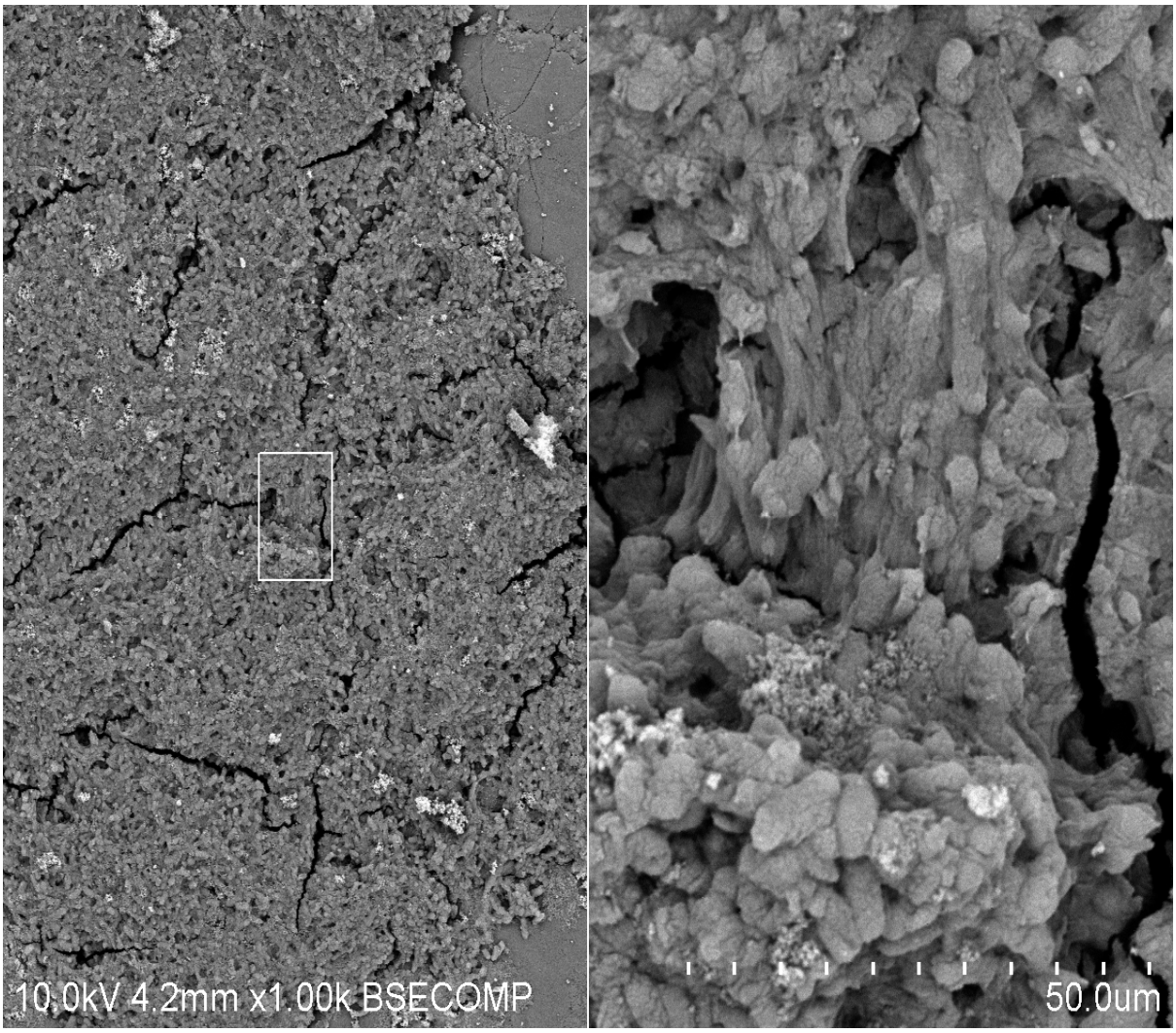


(a) bacterial *E.coli* culture treated with ZnO nanoparticles during the 1h

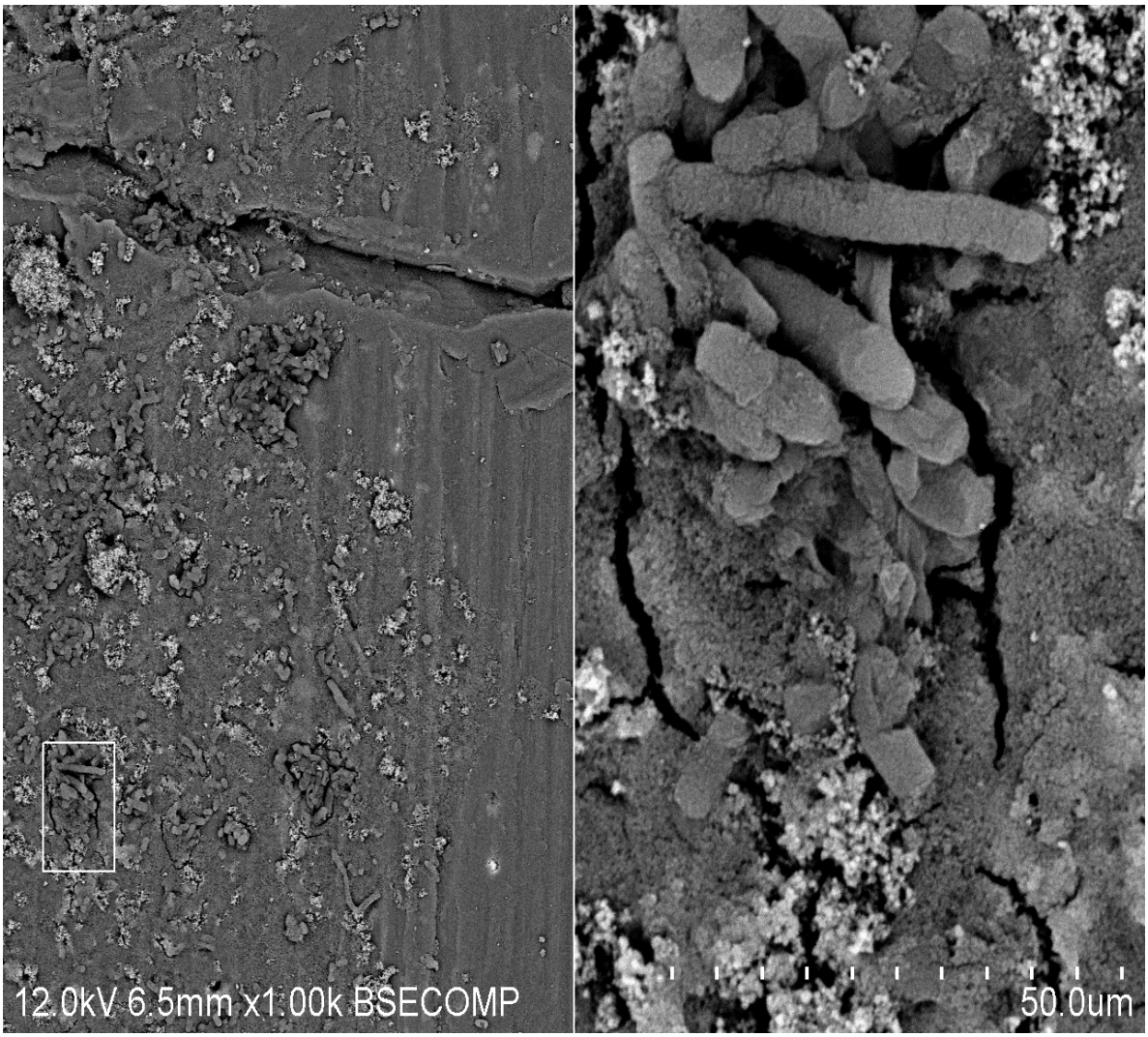


(b) bacterial *E.coli* culture treated with ZnO nanoparticles during the 3h

**Figure 33:** SEM micrographs of: (a) bacterial *E.coli* culture treated with ZnO nanoparticles after 1h, and (b) bacterial *E.coli* culture treated with ZnO nanoparticles during the 3h

### 3.3.4. Mechanism of the antibacterial activity of ZnO nanoparticles:

There are many studies investigating the antibacterial effect of ZnO nanoparticles. All observations reported by the researchers were explained by a number of mechanisms, these mechanisms include production of active oxygen species due to the existence of the nanoparticles [96,124], damage of membrane cell wall because of the binding of the particles on the bacteria surface due to the electrostatic forces [104], penetration through the cell membrane [124], interaction between the active oxygen species and the cell [105], and cellular internalization of ZnO nanoparticles, another study suggests that small particle are able to penetrate and accumulate in the bacterial membrane and cytoplasm region of the cell [125].

But most of these studies are not able to give exact or clear mechanism for the easy understanding of the behaviour of ZnO nanoparticles as antibacterial material.

In this study various tests were carried out focusing on a better understanding of the antibacterial mechanisms of ZnO nanoparticles.

It should be noted that the preparation of ZnO nanoparticles for this study were done under dark condition and the antibacterial activity tests of ZnO in this work has been studied in normal laboratory environment and without special UV-irradiation source, which might be important since ZnO might show a photo-catalytic activity.

In the beginning, it should be known if the release of Zinc (II) ions is responsible for the antibacterial activity of ZnO nanoparticles or not?

- To exclude the possibility that zinc ions existing in the ZnO aqueous suspension were responsible for the antibacterial activity, zone of inhibition test for special control experiment was done by dissolving the precursor salt $Zn(Ac)_2 \cdot 2H_2O$ in water (0.045 M) and test the antibacterial activity against *E.coli*, since 10 µl from (0.045 M) $Zn(Ac)_2 \cdot 2H_2O$ was added to the agar plate containing *E.coli*. Finally, no zone on inhibition was observed around the tested solution, so it was found that under the condition of this study, Zinc (II) ions are not responsible for the antibacterial activity of ZnO. Figure 34 shows the zone of inhibition test for $Zn(Ac)_2 \cdot 2H_2O$ salt, from the figure we can observed that there is no inhibition for the bacteria within or around the solution.

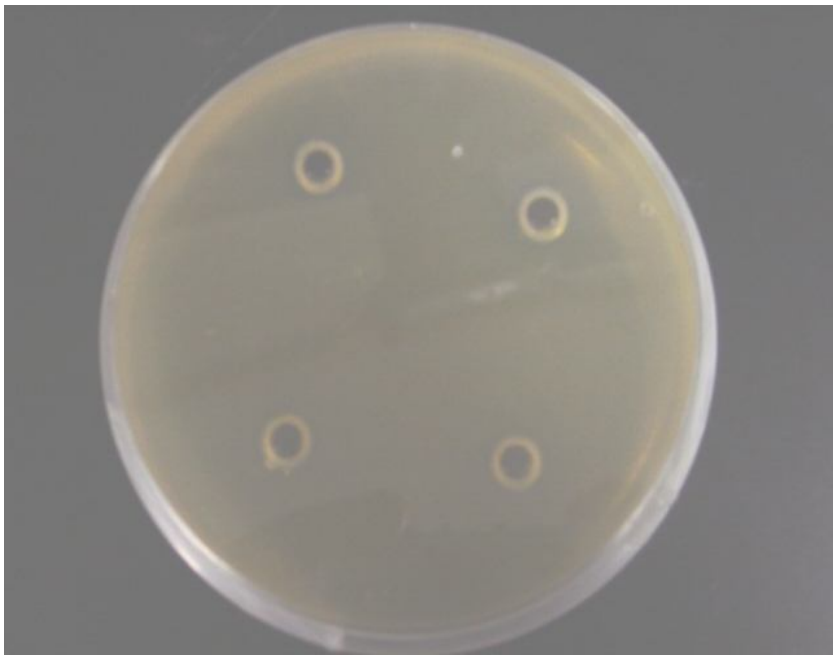

**Figure 34:** The disc diffusion test of Zinc acetate salt against *E.coli* for the growth inhibition

After that, it should be known if the generation of $H_2O_2$ due to the presence of ZnO nanoparticles contributes in the mechanism of the antibacterial activity or not?

- For proving that $H_2O_2$ is involved in the antibacterial activity, the release of $H_2O_2$ from ZnO was tested using HPAEC-PAD system, in this test different concentration of aqueous resuspended ZnO nanoparticles (30 nm)(0.5, 0.8, and 1 g/l) were prepared as described in 2.1.1 and then were injected in the HPAEC-PAD system to be able to get information about the unknown amount of $H_2O_2$ generated due to the presence of ZnO nanoparticles. After the calculation it was found that the amount of released $H_2O_2$ is depending on the concentration of ZnO nanoparticles, it increased with increasing the ZnO concentration as calculated from the $H_2O_2$ calibration curve in Figure 14 and as shown in Table 11. So chemical reaction between the cell envelope components and chemical species such as hydrogen peroxide, generated due to the presence of ZnO particles could contribute to the antibacterial behaviour of ZnO-sol. In spite of these results may be far from the safe results since in this curve the expected amount of $H_2O_2$ is in the end of accuracy point, but it can give hint to the expected $H_2O_2$ amounts.

Table 12 shows the amounts of $H_2O_2$ generated as a result of the injection of different ZnO nanoparticles concentrations

**Table 12:** Amount of $H_2O_2$ generated from ZnO nanoparticles (30 nm)

| ZnO nanoparticle concentration | $H_2O_2$ concentration |
|---|---|
| 0.5 g/l | 0.00015 g/l |
| 0.8 g/l | 0.00029 g/l |
| 1 g/l | 0.00038 g/l |

- Also for proving that $H_2O_2$ is involved in the antibacterial activity, antibacterial activity of ZnO/catalase enzyme solution was tested. The idea of this test is that catalase enzyme can make decomposition to $H_2O_2$, so if $H_2O_2$ generated due to the presence of ZnO nanoparticle is involved in the antibacterial activity this mean that the antibacterial activity of ZnO/catalase enzyme should be decreased compared to the antibacterial activity of only ZnO nanoparticle. Finally it was found that the antibacterial activity ZnO/catalase enzyme decreased compared to only ZnO nanoparticle most probably due to the decomposition of $H_2O_2$ in the presence of catalase enzyme. This means that $H_2O_2$ is involved in the antibacterial activity. Figure 35 shows the Zone of inhibition test for both only ZnO nanoparticle solution and ZnO/catalase enzyme solutions. From the figure we observed that the presence of catalase enzyme together with ZnO nanoparticle reduce the zone of inhibition around the tested solution which mean that the generation of $H_2O_2$ is not only the reason for the antibacterial action of ZnO nanoparticle but should be other things involved in the antibacterial activity.

**Figure 35:** The disc diffusion test of ZnO/catalase enzyme.

Since: (1) ZnO/catalase enzyme solutions, and (2) ZnO nanoparticle solution against *E.coli* for the growth inhibition.

Table 13 shows the effect of ZnO nanoparticle solution on the antibacterial activity against both *E.coli* and *M.luteus* compared to ZnO /Catalase enzyme solution.

**Table 13:** Effect of different ZnO solutions on the antibacterial activity.

| Bacteria | ZnO | ZnO /Catalase |
|---|---|---|
| *E.coli* | + | - |
| *M.luteus* | + | - |

(+): mean that the solution has antibacterial activity and, (-): mean that the solution reduces the effect of the antibacterial activity.

From the previous results we can see that the generation of $H_2O_2$ is not only the antibacterial action of ZnO nanoparticle, so another active species may be contributed to the antibacterial action of ZnO nanoparticle.

- It was found that another suggested mechanism responsible for the antibacterial activity of ZnO nanoparticles is the generation of oxyradicals or hydroxyl radicals. For proving that, 2,2-Diphenyl-1-pikrylhydrazyl (DPPH• ) stable free radical was used. DPPH was used as scavenger for any radicals (hydroxyl radical, superoxide anion radical,…), and as a result of this process the violet colour of DPPH convert to colourless after the scavenging of radicals present in the solution. From the result we found that there is a clear relation between the decreased particle size and increased amount of the radical species. As shown in Figure 36 the maximum absorption of DPPH is 514 nm. By the time and as a result of the reaction of DPPH and the radical species, discoloration of DPPH takes place.

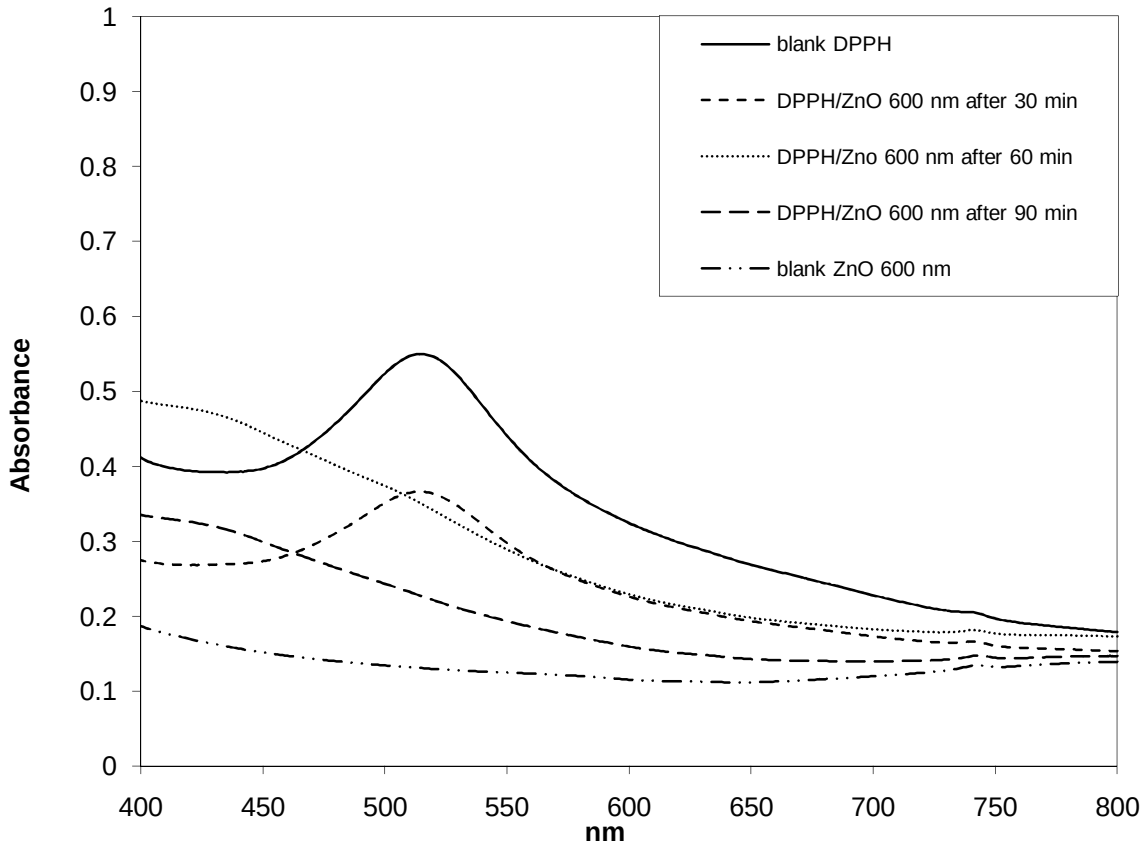


**Figure 36:** UV-Vis Spectra of (20 mg/l) DPPH /ZnO (600 nm) nanoparticles.

Also from the result it was found that the particle size can influence the decomposition of DPPH. As shown in figure 37, the decomposition rate of the dye increased with decreased particle sizes.

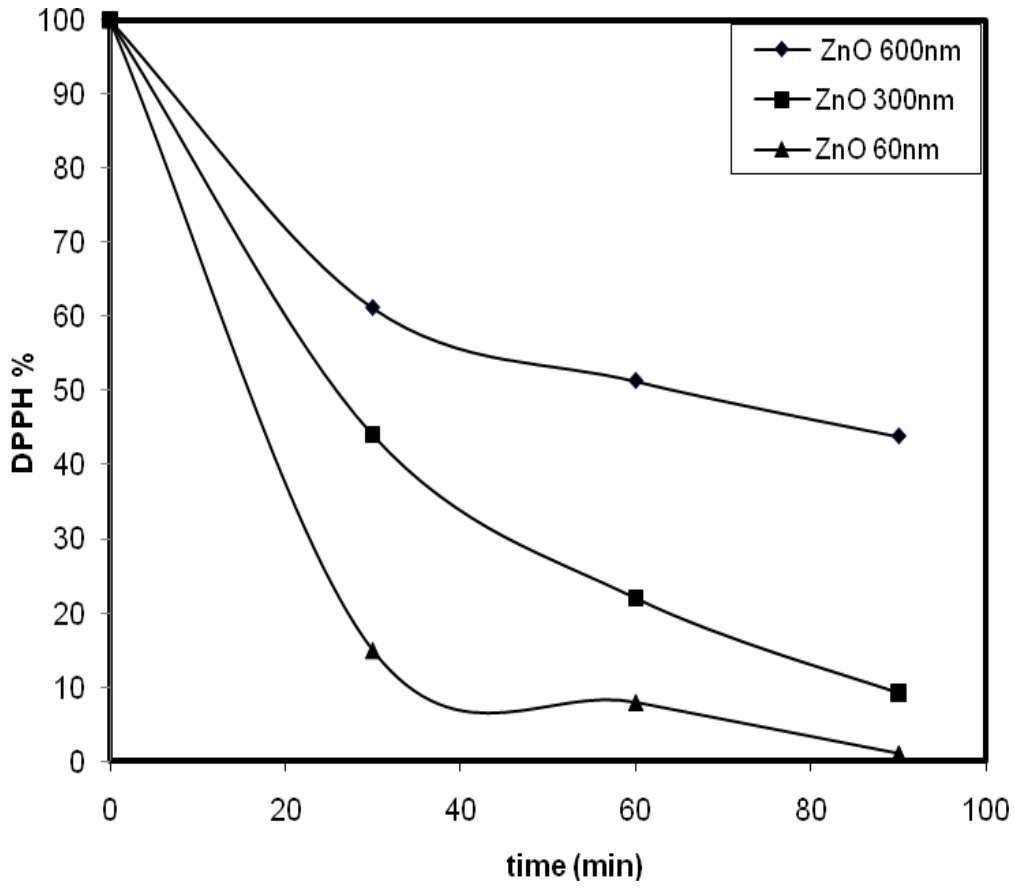


**Figure 37:** relation between the decomposition of the dye with time for different ZnO particle sizes

- Also, electrostatic interaction between the surface charge of ZnO particles and the membrane charge surface of bacteria could contribute to the antibacterial behaviour of ZnO-sol. Since, it is known that the pH of zero-point charge for ZnO is 9.0 [126], and the pH of the solutions is 7.0, this means that there are positive charges on the ZnO particles surface which can interact with the negative charges of the surface of bacteria as discused before in Figure 30.

# 3.4. ZnO nanoparticles-chitosan composite as antibacterial finish for textile

## 3.4.1. Introduction

After the preparation of sol-gel derived inorganic-organic hybrid polymers which was based on 3-glycidyloxypropyltrimethoxysilane (GPTMS) and filled with ZnO nanoparticles of different concentrations and/or different particle sizes and after its application to the textiles as antibacterial activity, then we get the idea to search for suitable additive which has also antibacterial activity, may the antibacterial activity increased as a result of using this additive under certain conditions. Finally the addition of chitosan as additive was studied. Chitosan is an important biopolymer, the advantage of chitosan include availability, medium cost, high biocompatibility, biodegradability, many chemical sources and ease chemical modification [127].

Chitosan/ZnO nanoparticle (CS/nano-ZnO) composite membranes were recently prepared [128] and this study concluded that the antibacterial activities of CS membranes for *Bacillus subtilis*, *Escherichia coli*, and *Staphylococcus aureus* were enhanced by the incorporation of ZnO. Also preparation, characterization and dye adsorption properties of biocompatible composite (Chitosan-zinc oxide nanoparticle) were recently reported [129] since it was conclude that the CS/n-ZnO being a biocompatible, eco-friendly and low-cost adsorbent might be a suitable alternative for elimination of dyes from colored aqueous solutions.

The antibacterial performance of sol-gel derived inorganic-organic hybrid polymers based on GPTMS and filled with ZnO nanoparticles - chitosan against *E.coli* and *M. lutues* has been investigated. Three different molecular weights (MW) of chitosan (CTS) $1.36*10^5$, $2.2*10^5$and $3.0*10^5$Da with equal degree of deacetylation (DD, 85%) (Coded as: S 85-60, He 85-250, He 85-500) were tested. ZnO was prepared as described in 2.1.1. Preparation and application of GPTMS-ZnO-chitosan composite was described in 2.1.4.

Bacteriological tests were performed in nutrient agar media on solid agar plates and in liquid broth systems using ZnO nanoparticles with average particle size of (30nm). This study showed the enhanced antibacterial activity of ZnO nanoparticles-chitosan (different MW) composite against *E. coli* and *M.lutues* in repeated experiments. The antibacterial activity of textile treated with ZnO nanoparticles-chitosan increases with

decreasing the molecular weight of chitosan. In this study, ZnO nanoparticles (10%-30 nm) in GPTMS and different chitosan concentrations 0.1, 0.5 and 1 % (wt/v) were used.

Figure 38 shows the proposed scheme for the preparation of ZnO sol /chitosan and its application to cellulosic fabrics.

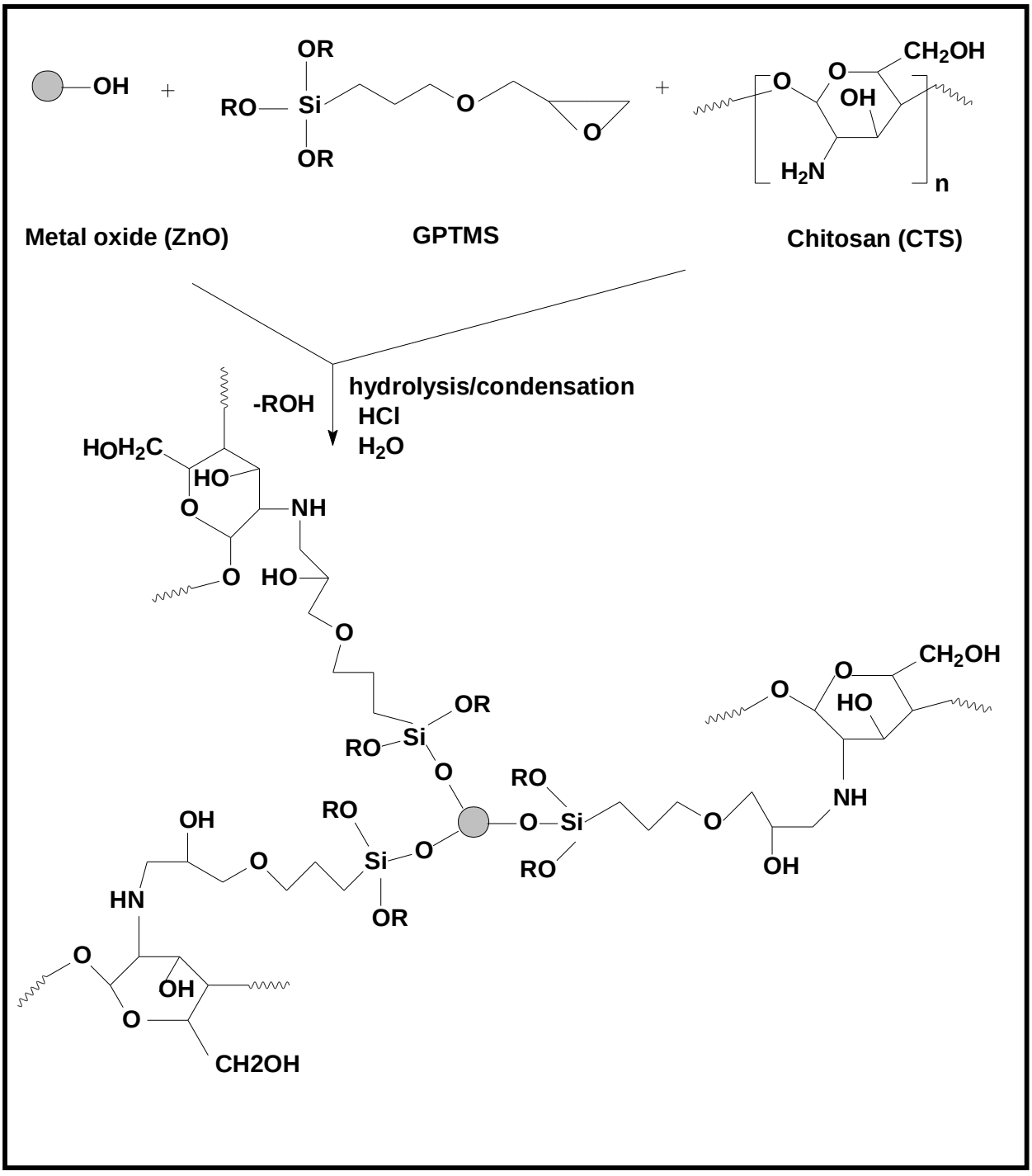


**Figure 38:** Proposed scheme for the preparation of GPTMS-ZnO /chitosan Composite

### 3.4.2. ATR-FTIR-spectroscopic analysis

The ATR-FTIR measurement for blank cotton compared with cotton coated with only CTS, GPTMS/CTS, ZnO/GPTMS, and ZnO-GPTMS/CTS composite was investigated. As observed from Figure 39, compared with the blank cotton, all the fabric coated with GPTMS has absorption peak of C-H bond of three member ring appears at 2999-3045 $cm^{-1}$. The difference between the different cotton fabrics treatments appear in the collection Figure. The broad absorption peak at 3336 $cm^{-1}$ can be attributed to the characteristic absorption of hydroxyls. It is found that the infrared spectrum of the ZnO/GPTMS treated fabrics contain characteristic peaks of –Si-OH- stretching vibration at 1169 $cm^{-1}$ , Zn-O-Si- stretching vibration at 940 $cm^{-1}$ and Si-O-Si- stretching vibration at 818 $cm^{-1}$.

Figure 39 shows ATR-FTIR- Spectroscopy of (a) cotton blank, (b) cotton treated with CTS, (c) cotton treated with GPTMS/CTS, (d) cotton treated with GPTMS/ZnO, and (e) cotton treated with GPTMS/ZnO/CTS composite.

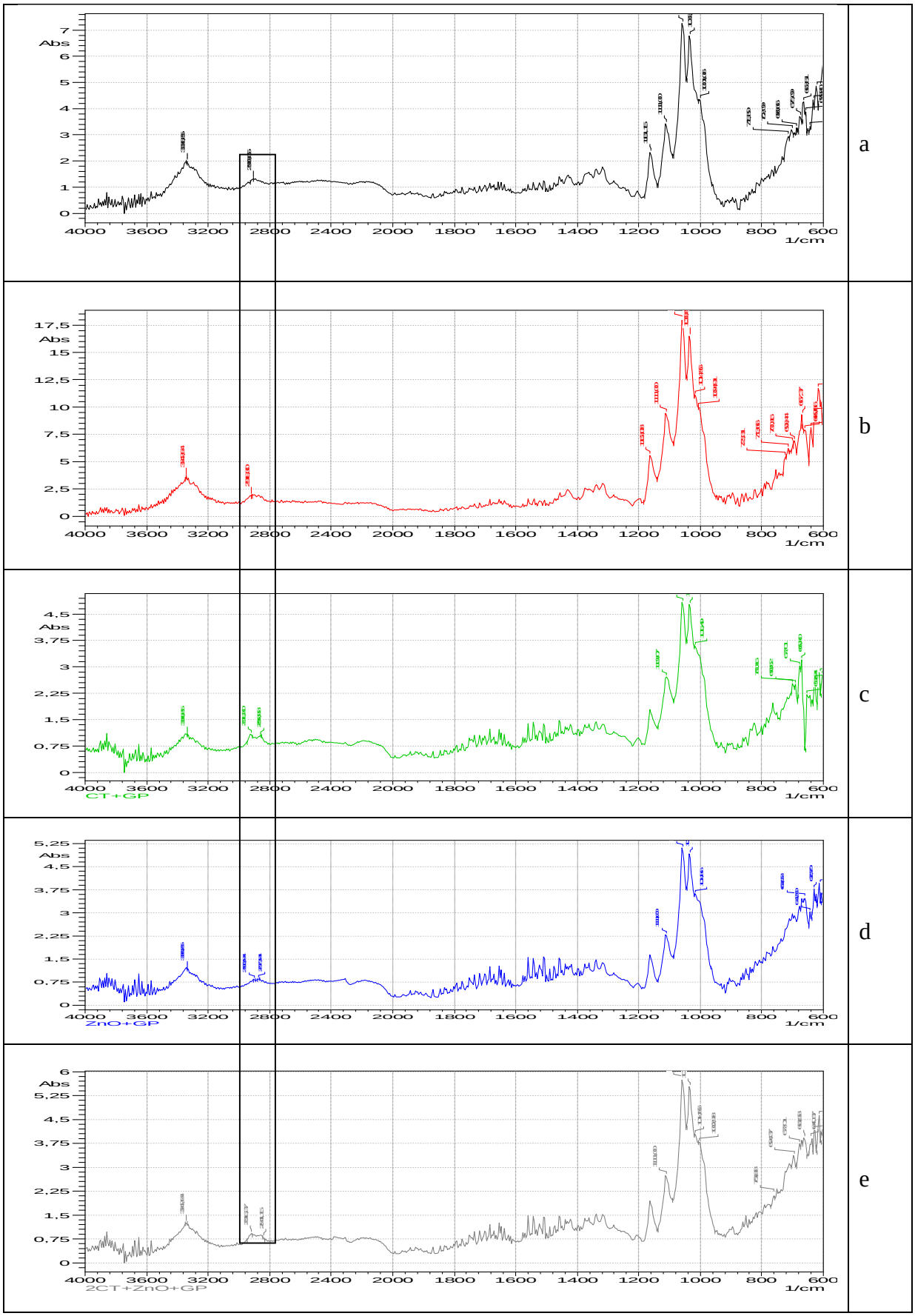


**Figure 39:** ATR-FTIR- Spectroscopy of cotton treated with different condition

### 3.4.3. SEM Investigation

SEM investigations were carried out to examine changes in the topography after treatment process compared to the blank sample. The corresponding SEM micrographs are shown in Figure 40. As shown from the figure, after GPTMS-ZnO (30 nm) nanoparticles/chitosan composite the surface of the treated fabric became smoother compared with the untreated fabrics or fabric treated with only CTS due to the homogenious distribution of ZnO-CTS composite within the coating layer.

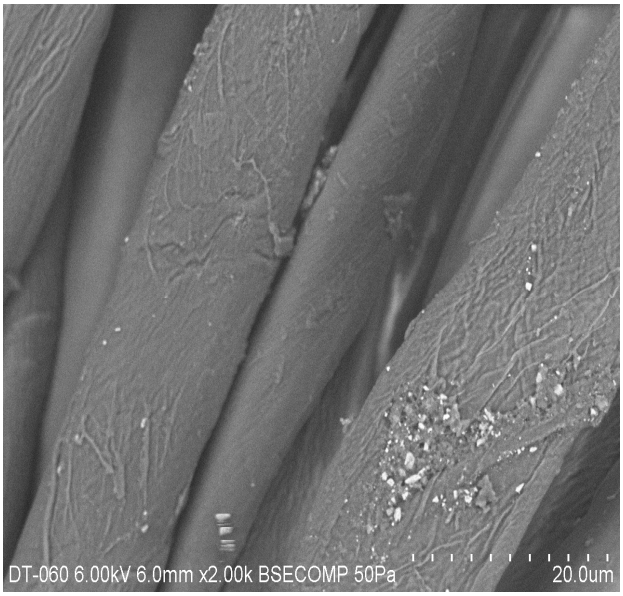


**(a)**

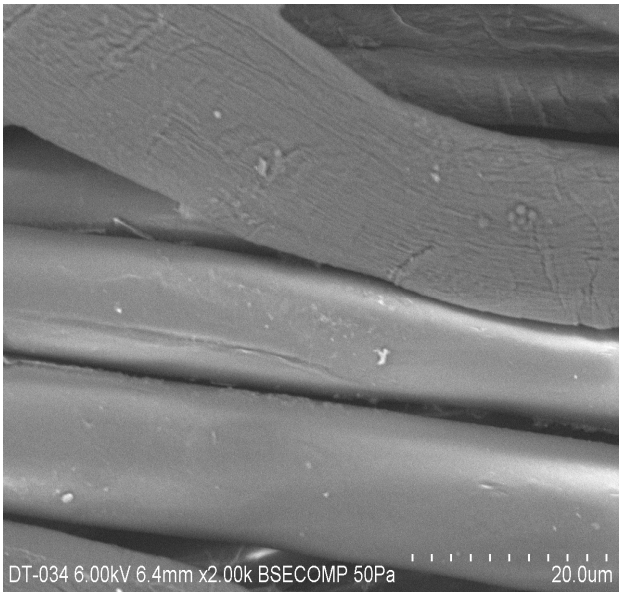


**(b)**

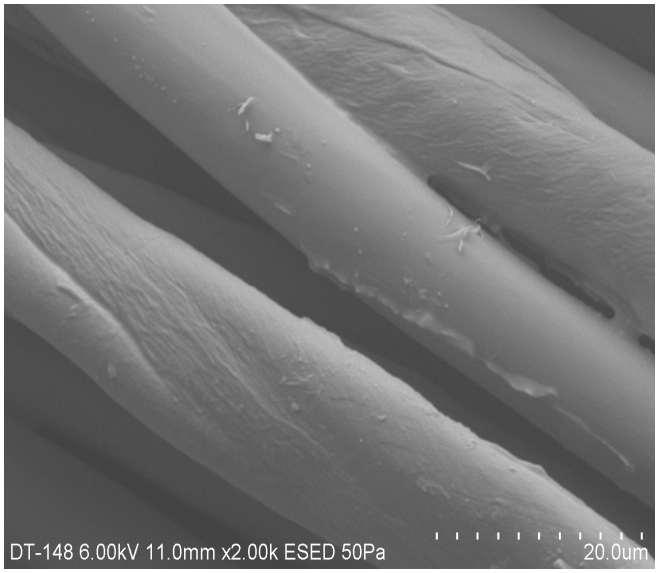


**(c)**

**Figure 40:** SEM photograph of the (a) untreated cotton/polester (65/35%) fabric, (b) 0.5% chitosan treated fabric, and (c) GPTMS-ZnO (30 nm)/chitosan composite.

### 3.4.4. Characterization of the amino groups by dropping colour:

After the application of GPTMS-ZnO–CTS composite to the textile surface using the pad-dry-cure method, ninhydrin test as colouring test was done to determine of the present degree of the -$NH_2$ group of the Chitosan molecule on textile surface, since -$NH_2$ group serves as basis for the test of Chitosan. This test is used mainly in order to discover the immobilized amino groups which are at the surface of finished fabrics which considered most important factor for the antibacterial activity of chitosan. Figure 41 is dropping test for identification of immobilized amino groups on treated cotton surface before and after washing. The figure shows that this test was positive for all finished chitosan containing fabrics since the brownish colour of ninhydrin converts to violet as a result of the reaction with the chitosan amino groups (Ninhydrin reacts with the free amino group of chitosan and develops a violet colour). The respective blank test showed no effect as shown.

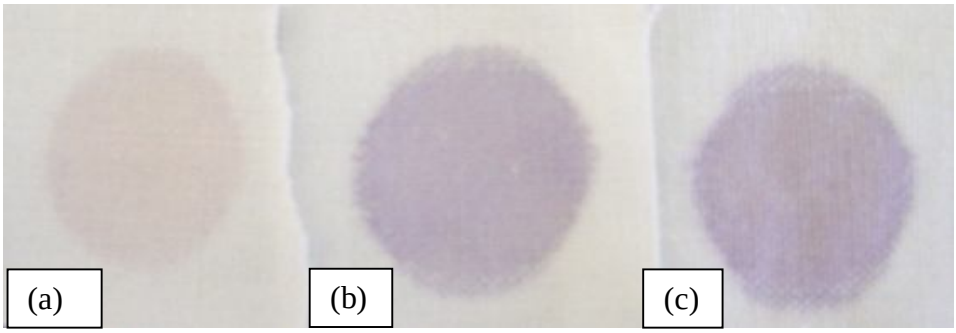


**Figure 41:** Dropping test for identification of immobilized amino groups on treated cotton surface. (a) Cotton blank, (b) cotton treated with ZnO sol/chitosan (0.5%)(low MW) composite and (c) cotton treated with ZnO sol/chitosan (0.5%)(low MW) composite after washing.

### 3.4.5. Polyelectrolyte titration and nitrogen content of the treated fabrics

Polyelectrolyte titration was carried out in order to determine the amount of charged immobilized amino groups on cotton and cotton/polyester chitosan treated surfaces. To get more information about degree of crosslinking or the mobility of biopolymer on the fibre, Polyelectrolyte titration measurements can be used [116]. A polyelectrolyte titration measurement and the nitrogen content of chitosan treated fabrics were described in 2.6.1 and 2.6.3 respectively. Table 14 shows polyelectrolyte titration and nitrogen content results of the treated cotton fabrics.

**Table 14:** polyelectrolyte titration and nitrogen content results

| Treated cotton with | Amount of nitrogen [mmol/g fibre] | Amount of cationic charges [meq/g fibre] |
|---|---|---|
| 0.5% Chitosan (lower MW) | 0.32 | 0.040 |
| 0.5% Chitosan(lower MW)/GPTMS | 0.53 | 0.057 |
| GPTMS-ZnO(10%, 30 nm) | - | 0.032 |
| GPTMS-ZnO(10%, 30 nm) /0.5% chitosan composite | 0.55 | 0.065 |

As It was observed from table 13 that the amount of nitrogen and the amount of cationic charges of only chitosan treated fabric is weak compared to fabric treated with 0.5% Chitosan (lower MW)/GPTMS which were explained by effect of GPTMS which work as crosslinking agent for the chitosan into the cotton fabric surface. Also the Amount of cationic charges increased in case of cotton treated with GPTMS-ZnO(10%, 30 nm) /0.5% chitosan composite due to the presence of cationic charge from both chitosan as well as ZnO nanoparticles surface.

In case of nitrogen content measurements all the amount of nitrogen can be detected, but in case of polyelectrolyte titration the amount of cationic charges which was detected are lower than the expected value. This is because of that not all nitrogen charges are available for the polyelectrolyte titration, since the cationic charges which were detected are only the charges on the surface.

### 3.4.6. Antibacterial activity measurement of ZnO nanoparticles solution containing chitosan of different MW

#### 3.4.6.1. Disc diffusion method

In this test, cotton 100% and cotton/polyester blend fabrics were selected for the evaluation of the relative antibacterial activity of chitosan/GPTMS, ZnO/GPTMS sol and GPTMS-ZnO/chitosan composite against *E.coli* and *M.lutues*.

In the beginning the antibacterial activity of three different MW (with equal degree of deacetylation) (85%) (0.1%) chitosan in GPTMS cotton coated fabric was tested as shown in Figure 42. From the figure we can see that, the strongest growth inhibition was observed with the low MW chitosan and the weakest was observed with the high MW chitosan. This could explain by the difficulty of the high MW chitosan to diffuse into the agar gel which contains the bacteria due to its high viscosity.

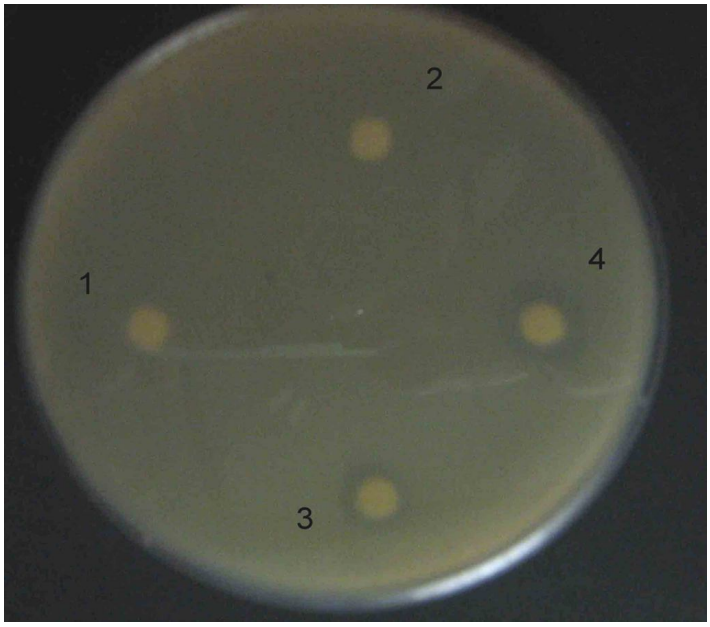


**Figure 42:** The qualitative disc diffusion test of cotton treated with GPTMS/ different MW of chitosan agaist *E.coli*. (1) untreated fabric, (2) GPTMS/0.1% high MW chitosan treated fabric, (3) GPTMS/0.1% medium MW chitosan treated fabric, (4) GPTMS/0.1% low MW chitosan treated fabric.

Then three different concentrations 0.1, 0.5 and 1 %( wt/v) of low MW chitosan /GPTMS were used for fabrics coating to test the antibacterial activity due to the presence of chitosan on fabrics. Zone of inhibition test was done. Figure 43 shows the zone of inhibition test for 0.1, 0.5 and 1 % (wt/v) low MW chitosan/GPTMS coated cotton fabrics against *E.coli*. From the figure we can observe that by increasing the chitosan concentration from 0.1 to 1%, the antibacterial activity of the coated fabric increased.

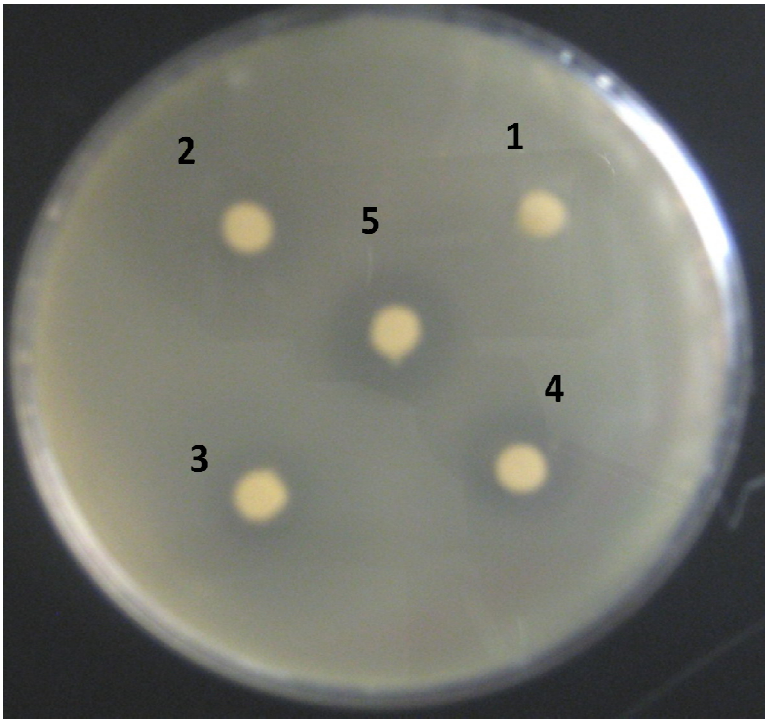


**Figure 43:** The qualitative disc diffusion test of cotton treated with GPTMS/ different chitosan concentrations agaist *E.coli.* (1) untreated fabric, (2) GPTMS treated fabric, (3) GPTMS/0.1% chitosan, (4) GPTMS/0.5% chitosan treated fabric, and (5) GPTMS/1% chitosan treated fabric.

After testing the antibacterial activity of different CTS concentration, it was observed that the antibacterial activity of low CTS concentration (0.1%) is weak, so only other two concentrations of (0.5 and 1%) were studied together with ZnO nanoparticles to prepare the GPTMS/ZnO-chitosan composite, but under the preparation condition which previously described in 2.1.4, the highest concentration 1% of CTS together with GPTMS/ZnO form unstable and not homogenous solution since the CTS tend to

collect together and finally it precipitate.

So the optimum condition for this study is ZnO (10%, 30 nm)/GPTMS and 0.5% CTS with different MW and same degree of deacetylation (85%). Figure 44 shows the zone of inhibition test for cotton fabric treated with (0.5%) CTS/GPTMS compared with samples treated with only GPTMS or with only CTS; since the samples treated with (0.5%) CTS/GPTMS composite has the higher antibacterial activity and this could be explained by the slow release of CTS from the fabric surfaces. May be other experiments should be carried out in the future to be able to understand the wash fastness or durability of the effect against several washing cycles of the treated fabrics.

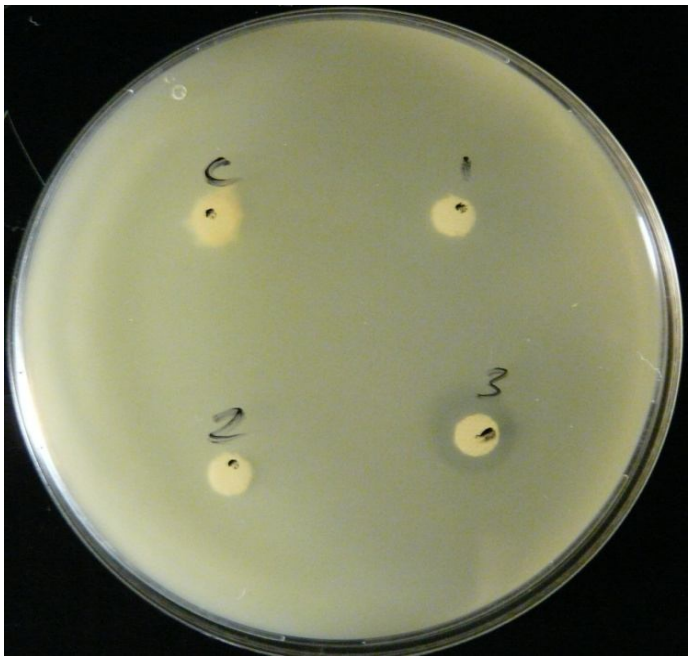


***(a) E.coli***

**Figure 44:** The disc diffusion test of cotton fabrics treated with CTS for the growth inhibition of *E.coli.* Since: (c) untreated, (1) treated with GPTMS, (2) treated with (0.5%) CTS and (3) treated with (0.5%) CTS/GPTMS.

After that the antibacterial activity of GPTMS-ZnO (10%-30 nm)-CTS (0.5%, different MW, same DD) composite was tested.

As shown from figure 45, the antibacterial activity of finished CO/PET fabric treated with ZnO sol/chitosan against *E.coli* and *M.lutues* improved compared to fabric treated with only ZnO sol, since the antibacterial activity increased with chitosan MW decreased, this phenomenon was explained as decrease of the MW of chitosan

improves its solubility and improves the movement of polymer chains in the solution by decrease the viscosity.

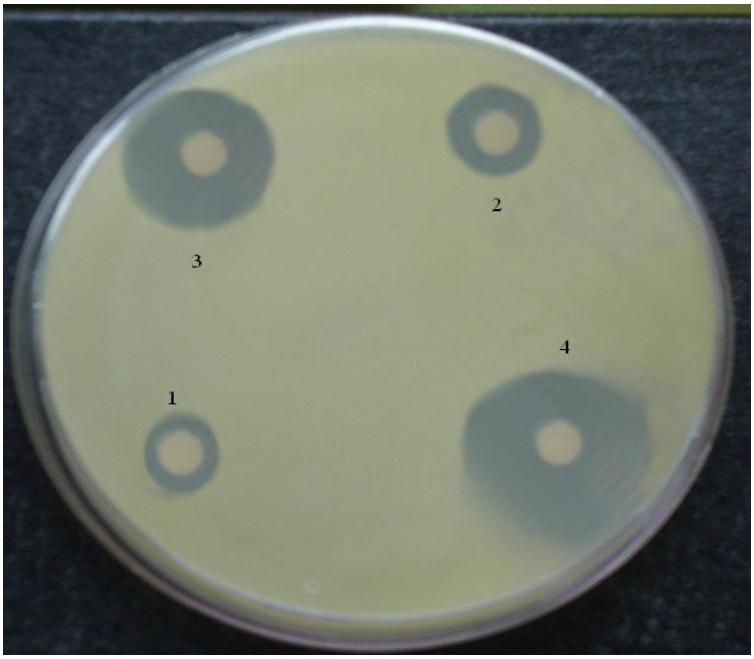


***(a) E.coli***

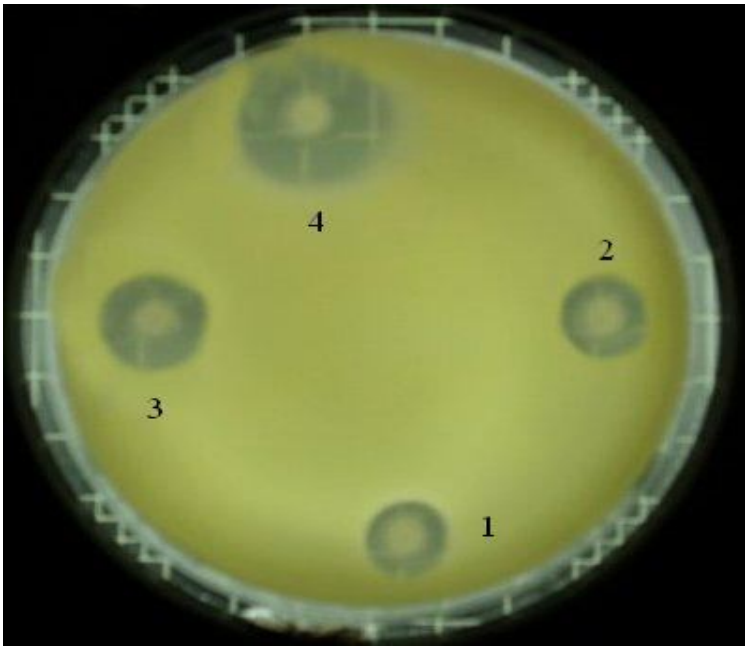


***(b) M.lutues***

**Figure 45:** The qualitative disc diffusion test of cotton treated with ZnO sol/chitosan composite for the growth inhibition of: (a) *E.coli* and (b*) M.lutues*.

In the figure, the antibacterial activity against *E.coli* and *M.lutues* showes a clear zone of inhibition within and around the sample treated with (1) ZnO sol, (2) ZnO

sol/chitosan (higher MW) composite, (3) ZnO sol/chitosan (medium MW), (4) ZnO sol/chitosan (lower MW).

The lower the molecular weight of chitosan in GPTMS-ZnO-chitosan composite within the coating material the more the antibacterial properties (clear zone of inhibition around the samples indicates areas with no growth of bacteria).

### 3.4.6.2. Quantitative Evaluation (The AATTC Test Method 100-2004)

The antibacterial activity of the coated fabrics was estimated for the *E.coli* and *M. lutues* according to the AATTC100-2004 standard method. Figure 46 shows *E.coli* and *M.lutues* bacterial growth with the time for GPTMS-ZnO nanoparticles / chitosan (0.5%) (low MW) composite treated fabrics, (a) *E.coli* bacterial growth, and (b) *M. Lutues* bacterial growth.

From figure 46, it was observed that in case of both *E.coli* and *M.lutues*, that there is nearly 100% reduction of the number of colonies after 3h in case of cotton 100% treated fabrics against *E.coli* and *M.lutues* bacteria. In case of cotton 100% fabrics treated with GPTMS-CTS and GPTMS-ZnO the complete reduction of the number of colonies was observed after 4h and 5h respectively.

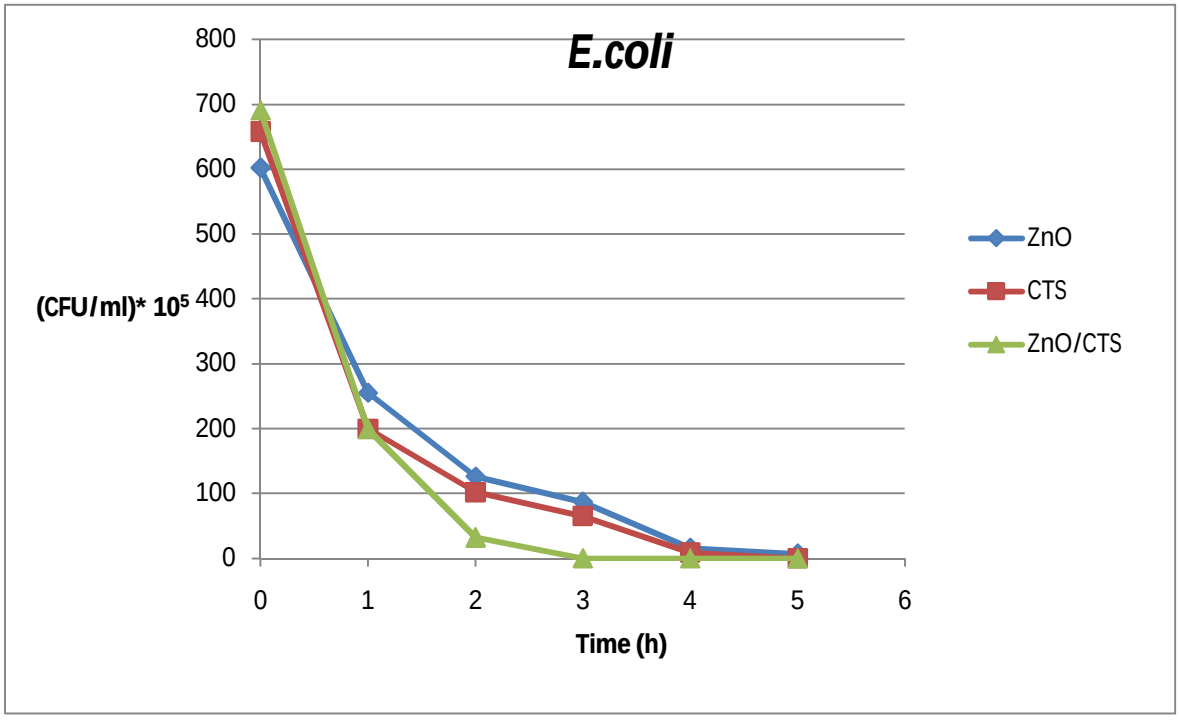


**(a)**

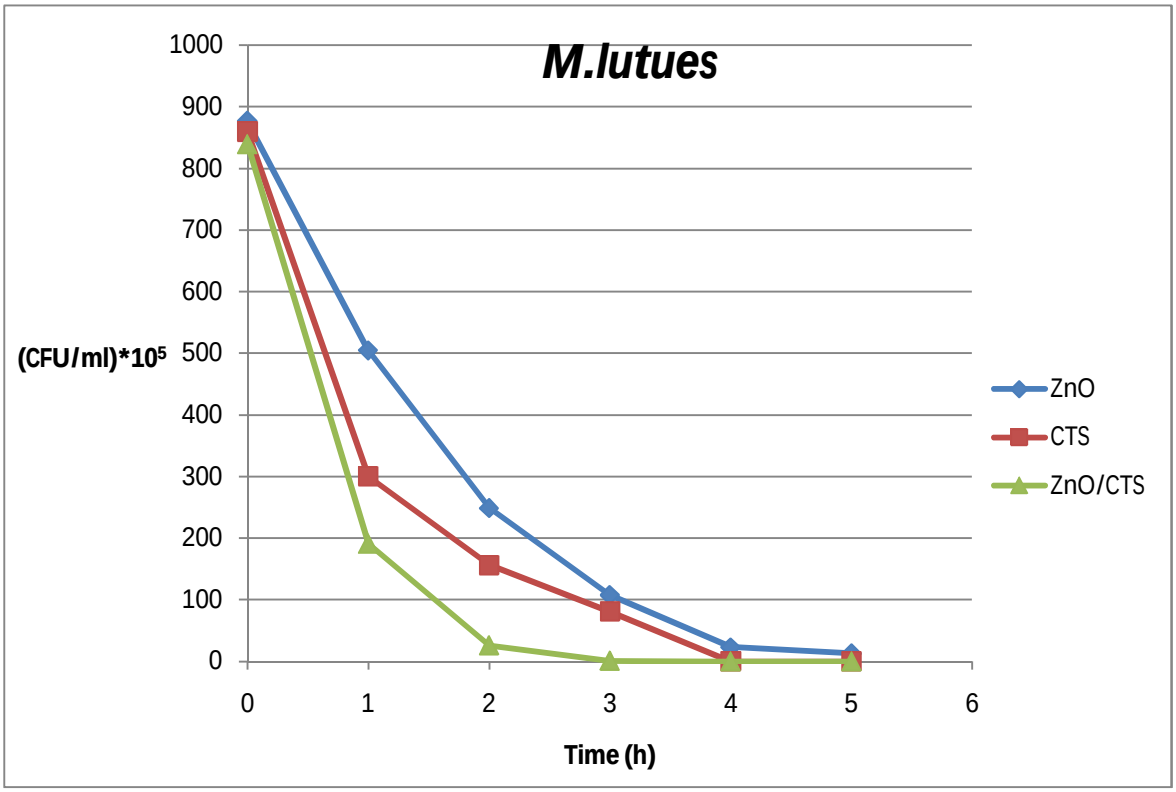


**(b)**

**Figur 46:** *E.coli* and *M.lutues* bacterial growth for ZnO nanoparticles sol/ chitosan (low MW) composite treated fabrics, (a) cotton 100% treated fabric and (b) cotton/polyester (65/35%) treated fabric.

### 3.4.6.3. Tetrazolium/formazan-test method TTC

The antibacterial activity of the treated fabric samples was evaluated against *E.coli* and *M. lutues* using the TTC test method. As it was mentioned before, this test serves as indicating system for the determination of the viability of micro organisms, since absorbance of formazane is directly proportional to the amount of living bacteria. Figure 47 shows the absorbance values of formazan for different cotton/polyester fabric treatment against *E.coli* bacterial cultures.

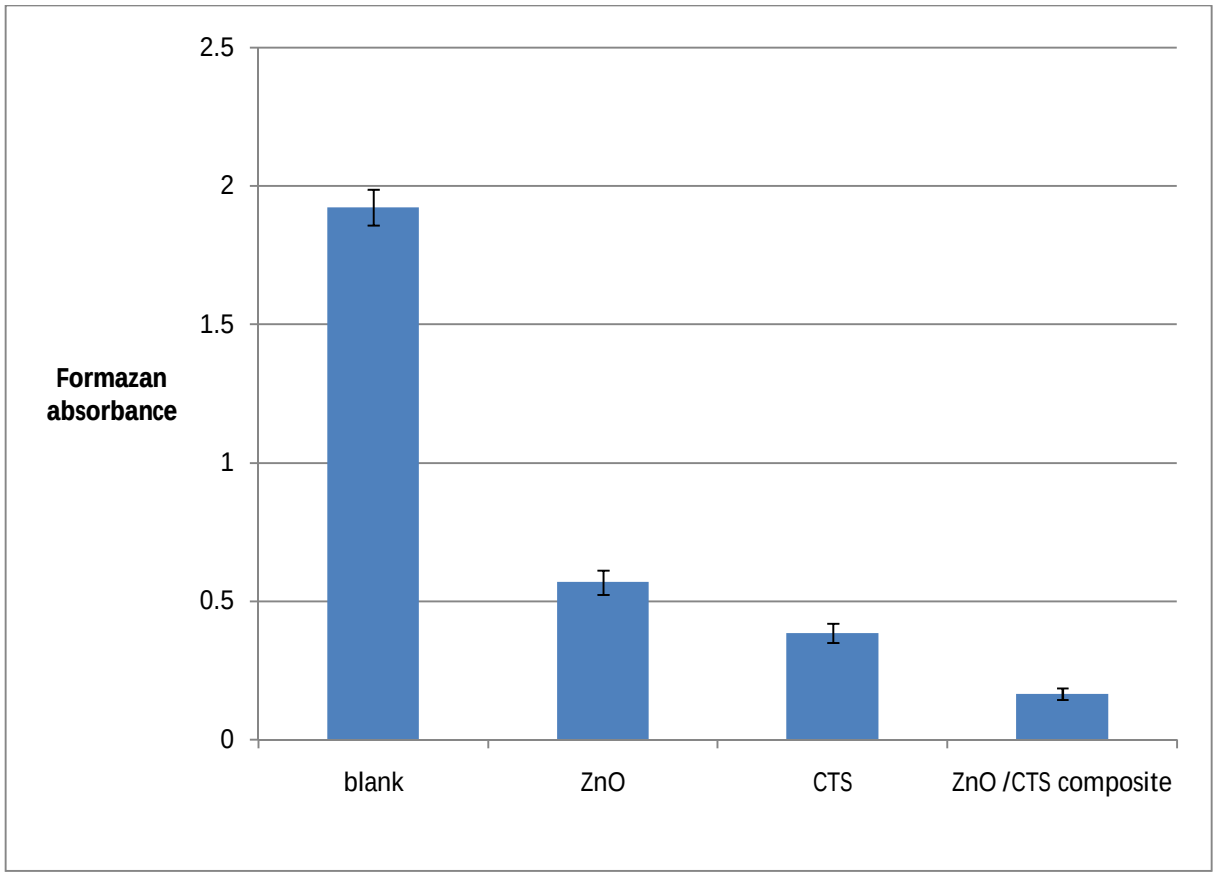


**Figure 47:** Absorbance of formazan for different cotton/polyester fabric treatment

As we observed from the formazan absorbance value in Figure 47, cotton fabric treated with ZnO nanoparticles sol/ chitosan (low MW) composite has the lower absorbance value of formazan, indicating the higher antibacterial activity, compared to the formazan absorbance value of cotton treated with GPTMS-ZnO sol or cotton treated with GPTMS-CTS, we can see also that the antibacterial activity of cotton treated with GPTMS-CTS composite is more higher than that treated with GPTMS-ZnO sol. The antibacterial activity is in this order:

GPTMS-ZnO –CTS composite **>** GPTMS-CTS composite **>** GPTMS-ZnO sol.

### 3.4.7. Effect of ZnO-sol-chitosan on some performance properties of the fabrics

The mechanical data of the treated and untreated samples and the influence of the ZnO sol /chitosan composite treatment for the degree of whiteness, the air permeability, stiffness, tensile strength and crease recovery (CRA) angle were investigated and the corresponding data are given in Table 15.

**Table 15:** Effect of ZnO sol – chitosan composite on some performance properties of cotton and cotton blend fabric samples.

| Substrate | | Tensile strength (daN) | Elongation (%) | Air permeability ($l/dm^2*min.$) | Degree of Whiteness (Berger) | Bending Stiffness ($cNcm^2$) | CRA (W+F)° |
|---|---|---|---|---|---|---|---|
| Untreated | Cotton | 102.1 ±0.75 | 21.9 ±1.06 | 250.5 | 66.0 | 12.19 ±.025 | 143° |
| | CO/PET | 87.4 ±1.02 | 31.7 ±1.04 | 334.0 | 70.9 | 3.23 ±.029 | 175° |
| Treated with ZnO in GPTMS-sol (10%) | Cotton | 96.5 ±1. 25 | 22.9 ±1.15 | 258.8 | 56.1 | 13.64 ±.014 | 150° |
| | CO/PET | 86.6 ±1.35 | 33.3 ±1.45 | 350.7 | 68.3 | 5.47 ±.017 | 181° |
| Treated with chitosan/ GPTMS | Cotton | 107.7 ±1.47 | 23.8 ±0.95 | 245.3 | 53.7 | 15.88±.014 | 180. ° |
| | CO/PET | 94.2 ±1.025 | 33.7 ±1.02 | 328.4 | 64.9 | 7.38±.022 | 196° |
| Treated with chitosan of low MW | Cotton | 104.8 ±1.04 | 21.9 ±1.14 | 247.0 | 54.8 | 15.12±.024 | 178° |
| | CO/PET | 91.3 ±1.14 | 31.9 ±0.85 | 330.5 | 65.6 | 6.65±.041 | 187° |
| Treated with ZnO sol /chitosan | Cotton | 107.2 ±1.03 | 23.5 ±1.12 | 243.2 | 53.1 | 16.93±.017 | 181° |
| | CO/PET | 92.7 ±0.98 | 33.0 ±1.07 | 326.1 | 64.3 | 8.81±.026 | 197° |
| Treated with GPTMS | Cotton | 99.8 ±1.01 | 21.5 ±1. 22 | 257.6 | 56.9 | 13.11±.028 | 151° |
| | CO/PET | 86.3 ±1.41 | 31.4±1.31 | 350.0 | 69.4 | 4.83±.025 | 181° |

- As it was expected, the tensile strength of fabric samples treated with chitosan, chitosan/GPTMS and ZnO sol /chitosan slightly increased. The increase can be explained by the penetration of low MW chitosan molecules into the fibres and enhance the tensile strength.
- The crease recovery angle (CRA) enhancement of the chitosan finished fabrics suggest that chitosan undergoes cross linking with GPTMS on the fabric to form network hybrid matrix.
- Also the whiteness of the fabrics is slightly decreased, but in a tolerable degree as a result of the finishing process.
- Air permeability is an important factor in the performance of textile materials used to give an indication to the breathability of the coated fabrics, within the investigation summarized in Table 15 it can be seen that there is no reduction of the air permeability values in case of fabrics treated with GPTMS as well as ZnO/GPTMS-sol but at least slight decreased in case of fabrics treated with chitosan a slight decrease could be due to closing of open interstices caused by the coating layer of the finish [130].
- Bending stiffness of the fabrics increasing could be due to the expected higher uptake of the inorganic-organic hybrids polymers containing chitosan molecules on cellulosic fabric surface which made the structure more rigid.

# 3.5. Superhydrophobic cellulosic fabrics prepared by sol-gel coating of ZnO

## 3.5.1. Introduction

Sol-gel based inorganic-organic hybrid polymers based on 3-glycidyloxypropyltrimethoxysilane (GPTMS) were modified with ZnO particles and then applied to cotton (100%) and cotton/polyester (65/35%) fabrics, followed by hydrophobization with stearic acid, hydrophilic cellulosic fabrics were made superhydrophobic. In this study hydrophobicity were measured by two tests TEGAWA and contact angle measurements, more details about these measurements was described in 4.2. Topology of cellulosic fabrics was studied by scanning electron microscopy. For the cellulosic fabrics treated with stearic acid only, the water contact angle on the fabric surface remained lower than 50°, treatment with ZnO nanoparticle only did not change the hydrophilic surface of cellulosic fabrics used. However, for the fabrics treated with both inorganic-organic hybrid polymer filled with ZnO nanoparticle and stearic acid, a contact angle higher than 150° can be obtained, since stearic acid impart the hydrophobic property to the hydrophilic fabrics previously applied with ZnO nanoparticle as shown in Figure 48.

Figure 48 shows suggested schematic diagram of ZnO in GPTMS-sol preparation and coating process to get hydrophobic cellulosic fabric surface.

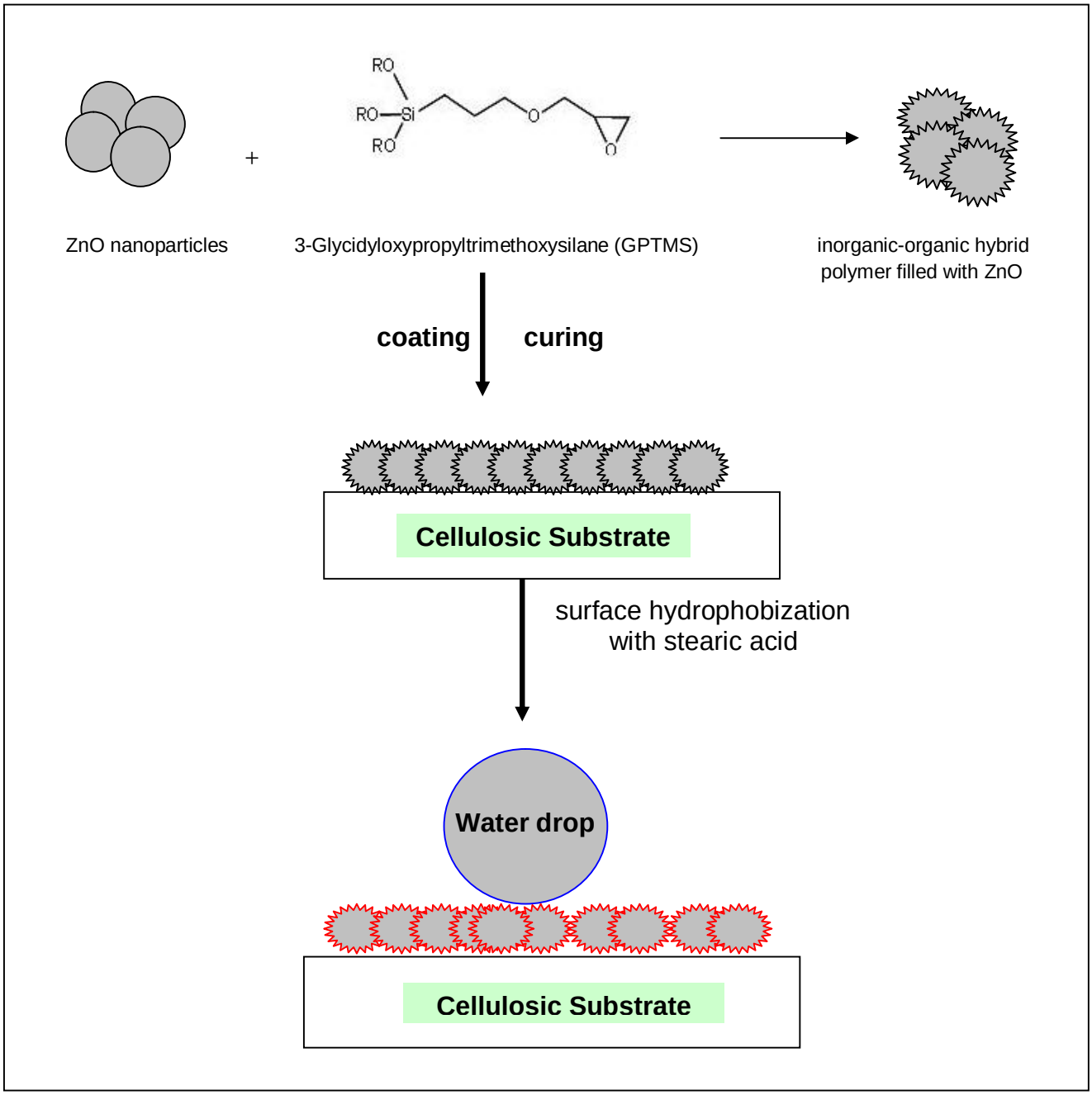


**Figure 48:** Schematic diagram of ZnO in GPTMS-sol preparation and coating process to get hydrophobic cellulosic fabric surface.

### 3.5.2. Surface topography of cellulosic fabrics

SEM investigations were carried out to investigate changes in the topography. The corresponding SEM micrographs are shown in Figure 49. From the figure we can see that the surface of the untreated fabric is comparably rough, the surface of the fabric treated with coating containing GPTMS-ZnO nanoparticle (30nm)-stearic acid appear much smoother, but the surface of the fabric treated with coating containing GPTMS-ZnO nanoparticle (625 nm)-stearic acid contain some

agglomerations due to the bigger particles coating which cause roughness to the surface and this could contribute to the hydrophobic property of the surface.

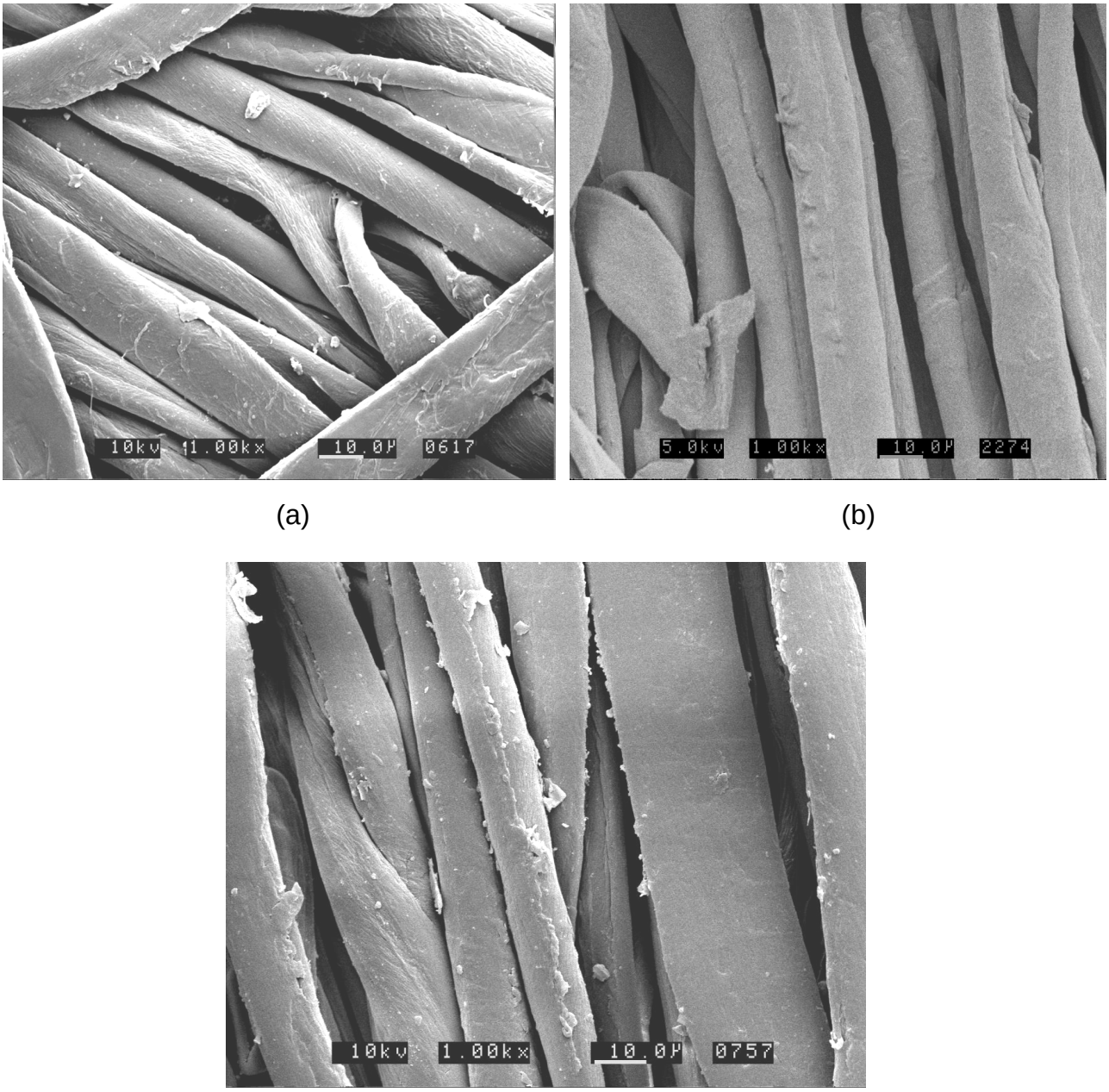


(a) (b)

(c)

**Figure 49:** SEM micrographs of: (a) blank cotton fabric, (b) cotton fabric treated with ZnO/GPTMS (30nm) and stearic acid, (c) cotton fabric treated with ZnO/GPTMS (625 nm) and stearic acid.

### 3.5.3. Hydrophobic coatings

A superhydrophobic coating for cellulosic fabrics based on (GPTMS) filled with nanosized zinc oxide particles was prepared through a sol-gel procees using cotton 100% and cotton/polyester (65/35%) as substrate. Stearic acid on the top layer of the surface lowers the surface free energy. Textiles coated with this coating showed good hydrophobic property. Since stearic acid impart the hydrophobic property to the hydrophilic fabrics previously applied with ZnO nanoparticle.

Surface wettability was examined by TEGAWA and contact angle measurements. The results are shown in Table 16. Table 16 shows drop penetration time (TEGEWA test) and contact angle for cellulosic fabrics before and after treatment with stearic acid as hydrophobic additive [after 2 washing cycles].

Untreated fabrics can be completely wetted by water, due to the high hydrophilic property of cellulosic textiles. After that samples modified by stearic acid and washed for 2 washing cycles were turned hydrophobic, with a water CA over 140°. From the figure we observed that the blank fabric has hydrophilic property, compared to the treated samples. Also as shown in the table the contact angle of the treated fabrics increases slightly with increasing the particle sizes, and this could be due to the structure of the textile not due to the surface structure. Since the roughness of the surface which comes from the aggregation of the bigger particles of ZnO nanoparticlse on the surface has no observed change in the contact angle, it was changed from 150° in case of fabric treated with 30 nm particle size into 155° in case of fabric treated with 650 nm particle sizes.

**Table 16:** Drop penetration time (TEGEWA test) and contact angle for cellulosic fabrics befor and after treatment with stearic acid as hydrophobic additive [after 2 washing cycles].

| Substrate | | Drop penetration time [s] before treatment with stearic acid [1.0 wt.%] | Drop penetration time [s] after treatment with stearic acid [1.0 wt.%] | CA (°) after treatment with stearic acid/after washing [1.0 wt.%] |
|---|---|---|---|---|
| Untreated | Cotton | 0 | 20 |  - |
| | Cotton-Polyester | 0 | 50 | - |
| Treated with GPTMS | Cotton | 5s | >3600s |  141°±1 |
| | Cotton-Polyester | 10s | >3600s | 142°±0.86 |
| Treated with ZnO -sol | Cotton | 20s | 200s | 95°±1 |
| | Cotton/Polyester | 30s | 300s | 100°±1 |
| Treated with ZnO in GPTMS-sol (10%) (≈30nm) | Cotton | 100s | >3600s |  150°±1.5 |
| | Cotton/Polyester | 150s | >3600s | 152°±1 |
| Treated with ZnO in GPTMS-sol (20%) (≈42nm) | Cotton | 170s | >3600s |  151°±1 |
| | Cotton/Polyester | 200s | >3600s | 153°±1 |
| Treated with ZnO in GPTMS-sol (10%) (≈250 nm) | Cotton | 300s | >3600s |  154°±1 |
| | Cotton-Polyester | 340s | >3600s | 155°±1 |
| Treated with ZnO in GPTMS-sol (10%) (≈650nm) | Cotton | 350s | >3600s | 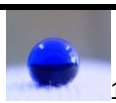 155°±1 |
| | Cotton-Polyester | 365s | >3600s | 156°±1 |

### 3.5.4. Non-wetting coatings

The mechanical stability was characterized using Martindale test. An exemplarily chosen pair of samples is shown in Figure 50. The picture shows cotton and cotton/polyester samples treated with GPTMS-ZnO (10%-30 nm)-stearic acid both after 20,000 scrubbing cycles. Mechanical stable, permanent coated surfaces were obtained. Figure 50 shows the results of a Martindale test which investigate the durable non-wetting coating of the treated cotton and cotton/polyester samples after 20.000 scrubbing cycles. Before the Martindale test, the contact angles of the treated cotton and cotton/polyester are 150° and 152° respectively, but after 20,000 scrubbing cycles the contact angles are slightly changed into 145° and 149° respectively.

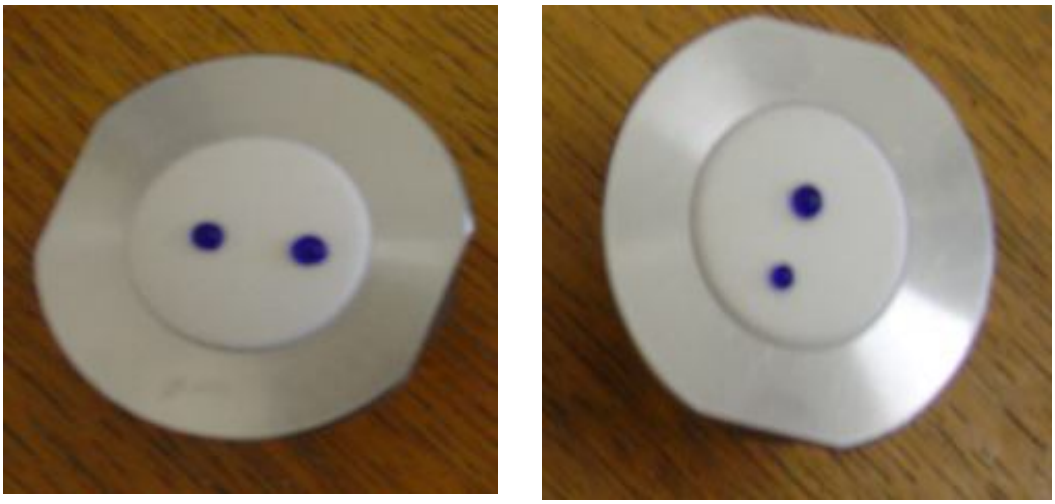

(a) (b)

**Figure 50:** Results of a Martindale test investigating the durable non-wetting coating of the treated (a) cotton treated with GPTMS-ZnO (10%-30 nm)-stearic acid and (b) cotton/polyester treated with GPTMS-ZnO (10%-30 nm)-stearic acid samples after 20.000 scrubbing cycles.

### 3.5.5. SEM investigation

SEM investigations were carried out to investigate changes in the topography after 20.000 scrubbing cycles. The corresponding SEM micrographs are shown in Figure 51. Treated cotton fabric with GPTMS-ZnO (10%-30 nm)-stearic acid has a tightly woven fibrous structure and there is no significant observed change after the Martindale test, since there is no weakness or damage in the fibrous.

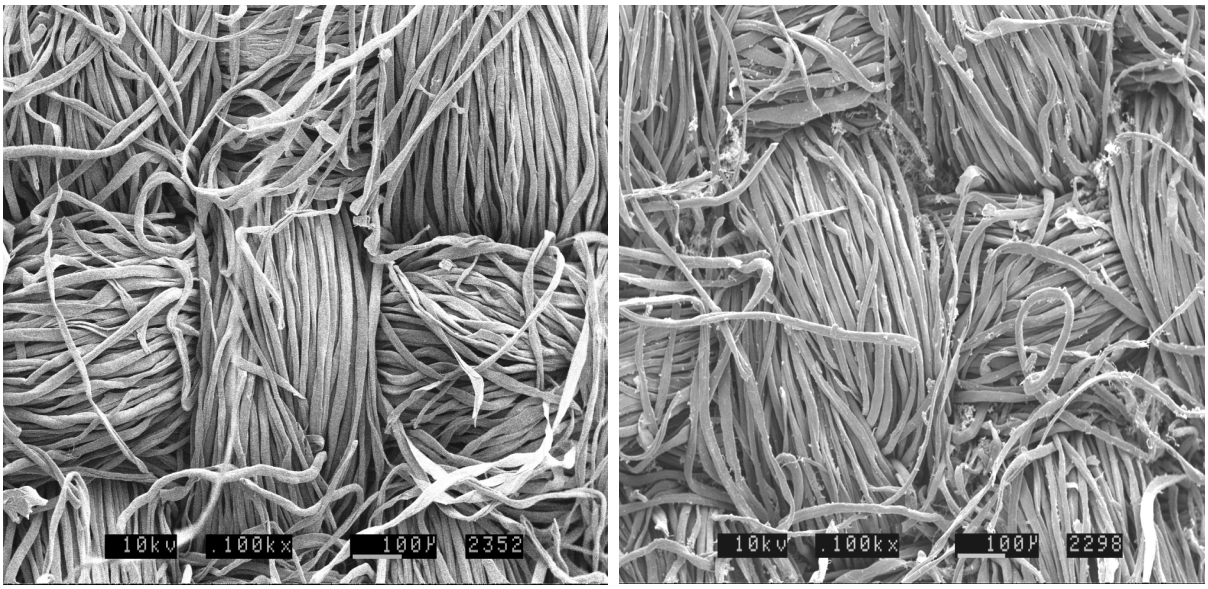


**Figure 51:** SEM micrographs of: (a) cotton fabric treated with GPTMS-ZnO (10%-30 nm)-stearic acid before Martindale test, and (b) cotton fabric treated with GPTMS-ZnO (10%-30 nm)-stearic acid after 20.000 scrubbing cycles.

# 3.6. Photocatalytic degradation of methylene blue by ZnO nanoparticles.

## 3.6.1. Photocatalytic activity of ZnO nanoparticles

Zinc oxide (ZnO) is semiconductor material with band-gap energy of approximately 3.2 eV. (≈ 370 nm). Therefore, ZnO absorbs ultraviolet (UV) light during an electronic excitation process between the valence band and conduction band and this is connected with the photocatalysis phenomenon. Irradiation with UV light results in the promotion of electrons (e-) from the valence band to the conduction band and the resulting formation of holes (h+) in the valence band. Excited state conduction band electrons and valence band holes can recombine and thereby release the incident energy as heat or react with electron donors and electron acceptors adsorbed on the semiconductor surface and this is idea of using ZnO nanoparticles in this study to follow the degree of methylene blue degradation on ZnO nanoparticles surface.

Photocatalytic degradation of organic dyes with manganes-doped ZnO nanoparticles reported [131], the photocatalytic degradation of reactive brilliant blue X-BR using ZnO particles was also studied [132].

In this study, photocatalytic activity of ZnO nanoparticles (30 nm) resuspended solution with different concentrations (0,1 g/l, 0,5 g/l and 1 g/l) was evaluated under dark condition, in normal laboratory environment and after UV-irradiation as shown in Figure 52.

Figure 52 shows the photocatalytic degradation degree of methylene blue by using ZnO nanoparticles under certain conditions and within certain time. As observed in figure 52a there is no change in the colour of MB dye in the ZnO nanoparticles solution but this is due to the short incubation time (zero time), under dark condition there is only slightly change in cuvette number 2 and 3 with the higher ZnO nanoparticles concentrations but after 1h in the normal laboratory environment as shown in Figure 52c, the colour of the MB dye is completely disappeared in case of methylene blue with 0.5 g/l ZnO nanoparticles (cuvette 2) and methylene blue with 1 g/l ZnO nanoparticles (cuvette 3) compared to methylene blue with only 0.1 g/l ZnO nanoparticles or methylene blue with 0.5 g/l ZnO nanoparticles in GPTMS. On the other hand, in figure 5d and after UV-irradiation using photochemical reactor (normal operating temperature is approximately 35ºC with fan in operation), the colour of the

MB dye is completely disappeared after 20 min in case of using all ZnO nanoparticles concentrations (0,1 g/l, 0,5 g/l and 1 g/l) as well as in 0.5 g/l ZnO nanoparticles in GPTMS.

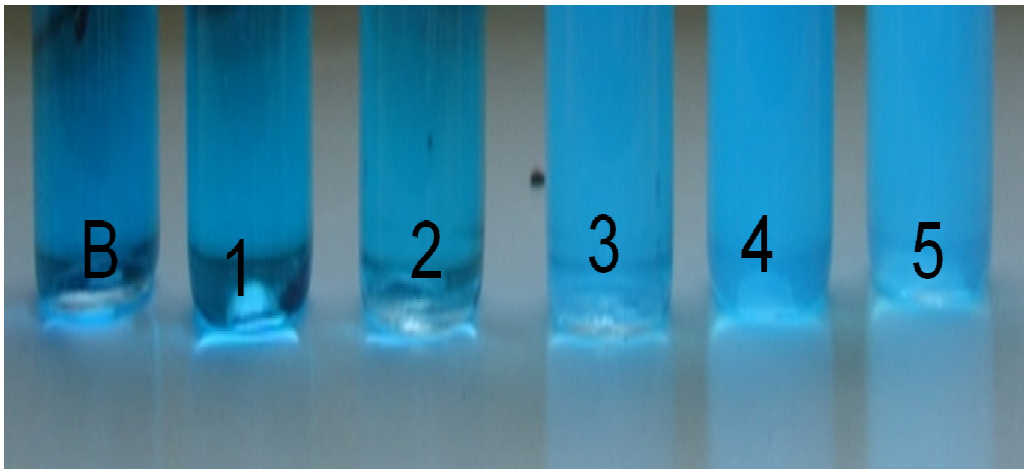


(a) Before UV-irradiation.

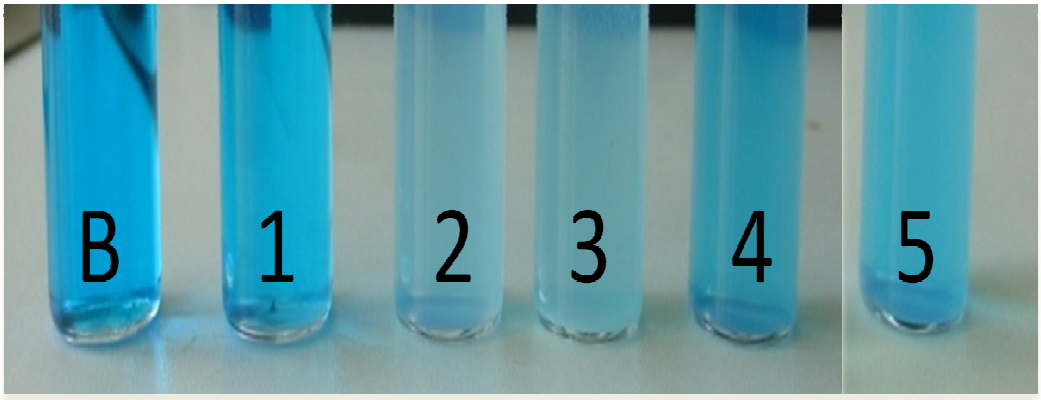


(b) After 1h under dark condition.

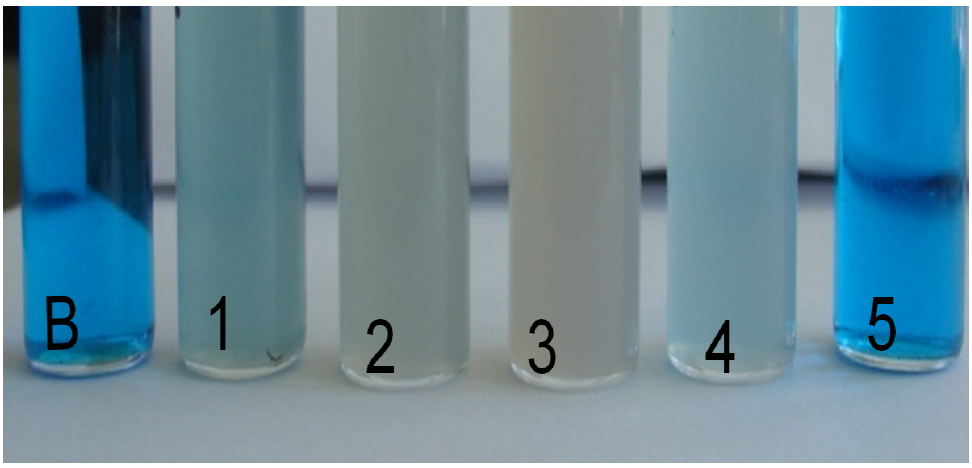


(c) After 1h in normal laboratory environment.

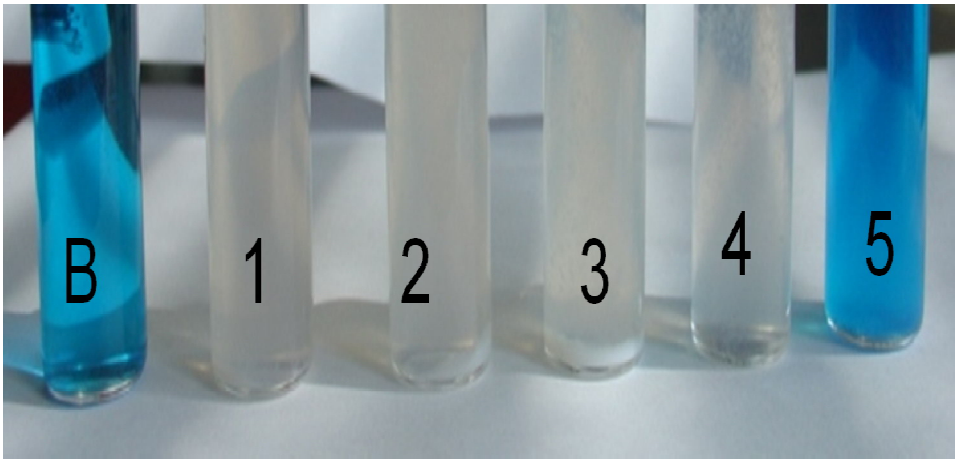


(d) After 20 min UV-irradiation

**Figure 52:** Discoloration efficiency of different concentrations of ZnO nanoparticles under different conditions. Since: B is blank methylene blue (20 mg/l), (1) methylene blue with 0.1 g/l ZnO, (2) methylene blue with 0.5 g/l ZnO, (3) methylene blue with 1 g/l ZnO, (4) methylene blue with 0.5 g/l ZnO and GPTMS; and (5) methylene blue with GPTMS.

Figure 53 shows UV-vis spectrum of decolouration of MB dye using different ZnO nanoparticle concentrations. As a result of the reaction between ZnO nanoparticles (through the reactive oxygen species on its surface) and MB dye, the rate of decolourization was changed as the concentration of ZnO nanoparticles changed. As indicated in the figure the rate of decolourization increased as the concentration of ZnO nanoparticles increased. The rate of decolorization was recorded with respect to the change in the intensity of absorption peak in visible region. The major peak was observed at $\lambda_{max}$, i.e., 645 nm. In the spectrum, the observed peak decrease gradually by increasing the concentration of ZnO nanoparticles and finally disappeared indicating that the MB dye had been completely degraded.

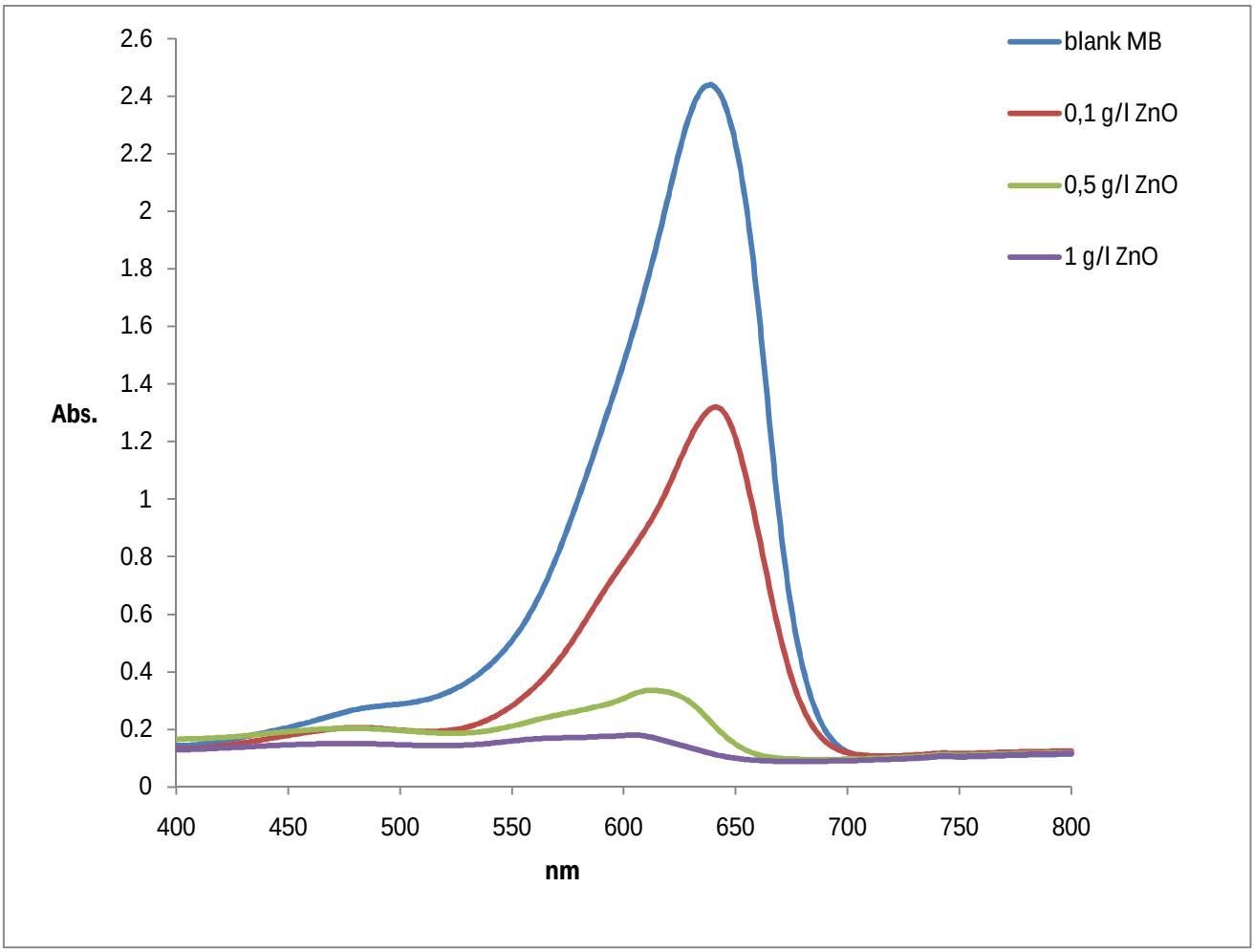


**Figure 53:** UV-Vis absorption spectra of decolourization of methylen blue (20 mg/l) by different concentrations of ZnO (30nm) nanoparticles after 1h in normal laboratory environment.

When the experiments were performed in the normal laboratory environment, after 1h and as a result of using 1 g/l ZnO nanoparticles, 98% decolourization of MB dye was observed compared to 49% and 88% observed when using 0,1 and 0,5 g/l ZnO nanoparticles respectively as shown in figure 54. Figure 54 shows the UV-Vis spectrum of photocatalytic decolourization percent of MB dye by using different concentrations of ZnO nanoparticles (0,1, 0,5 and 1 g/l) after 1h in normal laboratory environment, but when the experiments were performed under the dark condition, the adsorption of the dye by using different concentrations of ZnO nanoparticles (0,1- 1 g/l) was found to be 10–21% respectively and this is may be due to the adsorption of the dye on the ZnO surface which lower the concentration of the dye in the solution.

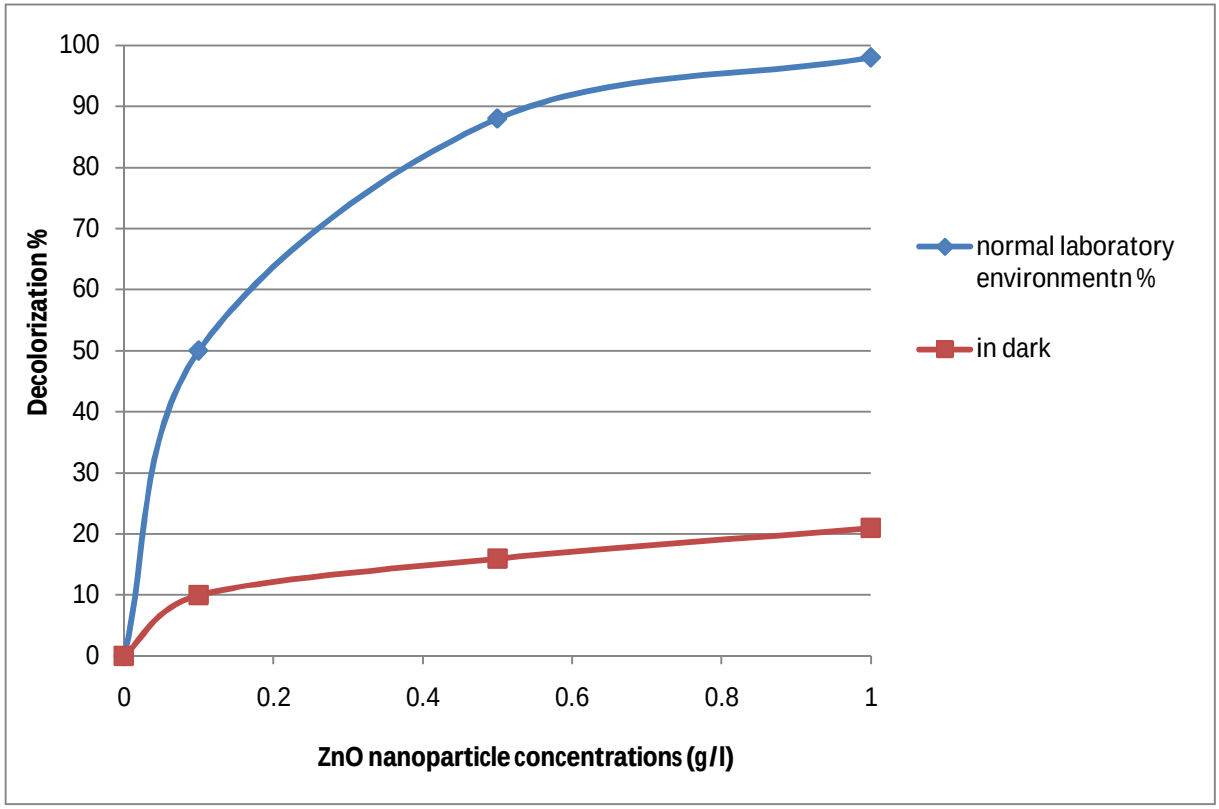


**Figure 54:** UV-Vis spectra of photocatalytic decolourization of MB dye by using different concentrations of ZnO nanoparticles (0,1, 0,5 and 1 g/l) after 1h in (a) normal laboratory environment, and (b) dark.

The photocatalytic processes involve several numbers of possible reactions [133]: photoexcitation of a semiconductor surfaces induces the creation of an electron-hole pair:

$$ZnO + h\nu \rightarrow ZnO\ (e^-_{CB} + h^+_{VB})$$

some electron-hole pairs are recombined, the remaining holes contribute to the oxidation reactions by generating •OH radicals, either by the decomposition of water

$$H_2O + h^+_{VB} \rightarrow H^+ + {}^{\bullet}OH$$

or by the reaction with adsorbed $OH^-$

$$OH^- + h^+_{VB} \rightarrow {}^{\bullet}OH$$

The hydroxyl radical species alone is strong oxidant for the partial or complete degradation of the dye:

$$dye + {}^{\bullet}OH \rightarrow \text{oxidation products}$$

Holes also permit the direct oxidation of the dye to reactive intermediates

$$dye + h^{+}_{VB} \rightarrow dye^{\bullet+} \rightarrow \text{oxidation products}$$

While, on the surface of the catalyst, oxygen is reduced as an electron acceptor to superoxide and this leads to production of $HOO^{\bullet}$ radical which finally plays a strong oxidant role

$$e^{-}_{CB} + O_2 \rightarrow O_2^{-} \rightarrow +H^{+} \rightarrow HO_2^{\bullet}$$
$$HO_2^{\bullet} + O_2^{-} + H^{+} \rightarrow H_2O_2 + O_2$$
$$H_2O_2 + e^{-}_{CB} \rightarrow OH^{-} + {}^{\bullet}OH$$

So, all these possible reactions contribute to increase the degradation and decolorization of MB dye by increasing the concentration of ZnO nanoparticles

### 3.6.2. Photocatalytic activity of ZnO nanoparticles coated fabrics

Photocatalytic activity of fabrics coated with ZnO/GPTMS nanocomposite with different ZnO concentrations (0,1 g/l, 0,5 g/l and 1 g/l)(30 nm) was also evaluated through the fabric self-cleaning of MB dye stains. Self-cleaning takes place at the cotton 100% fabric surface under UV- irradiation as shown in Figure 55.

Figure 55 shows the self-cleaning property of cotton 100% fabrics treated with GPTMS-different ZnO concentrations (30 nm), figure 55a, shows the blank and treated fabrics after staining with 100 µl (20 mg/l) MB dye. On the other hand, figure 55b shows the self-cleaning fabrics after the degradation and decolorization of the dye on the fabric surface after only 10 min UV- irradiation, since under UV-irradiation give more possible reactions between the ZnO surface and MB dye, also as we observed all the treated fabrics give self-cleaning after 10 min UV-irradiation.


(a) Before UV-irradation (0 min)

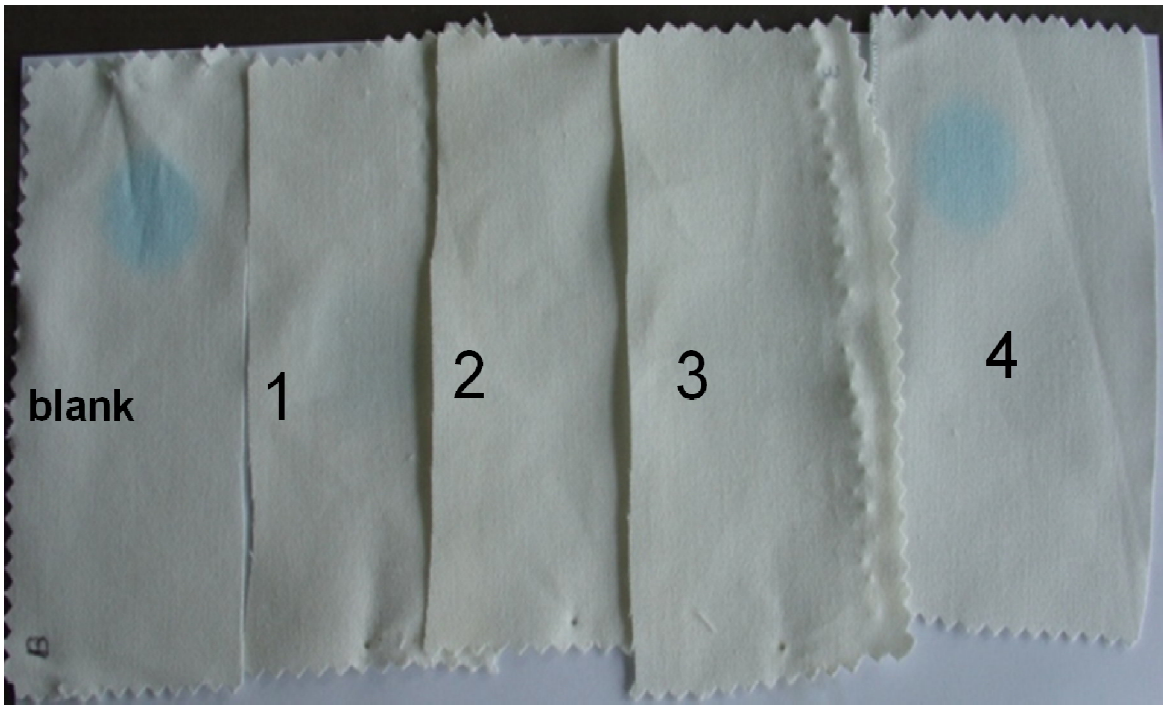


(b) After10 min UV- irradiation

**Figure 55:** Decolorization of MB dye on cotton fabric surface. Since: B is untreated cotton sample, (1) cotton treated with 0.1 g/l ZnO, (2) cotton treated with 0.5 g/l ZnO,(3) cotton treated with 1 g/l ZnO, and (4) cotton treated with only GPTMS.

In the case of cotton coated samples, compared to the non irradiated samples, completely decolourization was achieved when samples were irradiated under UV light for 10 min (ZnO + UV).

## 3.7. Dyeing of nanosol-coated fabrics

### 3.7.1. Introduction

The textile dying technique presents from ancient times. In the dying bath, after immersing the fabric sample the behaviour of the dye depend on the nature of the fabric and the dye molecule, since the dye can transfer from the solution to the fabric surface, then the dye can also diffuse into the inner fibrous.

Dyestuffs which contain only one function group face a low degree of fixation, to solve this problem, bifunctional dyestuff which contain two different reactive groups (i.e. one monochlorotriazin and one vinyl sulfone) were created, since In the field of textile finishing, dyeing process of the finished fabrics is important to make clear and evaluate the effect of these finishing chemicals on the dyeing performance.

ZnO nanosol was used before for enhancing the UV- protective property of cotton fabric and pigment dying in a single bath [134].

### 3.7.2. Dyeing of finished fabrics with reactive dye

Intracron red BF-3RM 150% 1 g was dissolved in 500 ml water, samples treated with different particle size of ZnO /GPTMS were dipped in this solution at temperature 60°C, 1 ml sodium sulphate (50 g/l), 1 ml sodium carbonate (5 g/l) and 1 ml sodium hydroxide (1 M) were added with continues stirring for 30 min. then the samples were washed several times with boiling water and 0.1 % Marlipal, and finally washed with cold water and dried at ambient conditions. Figure 7 shows the chemical structure of the reactive dye.

When ZnO/GPTMS coating of different concentrations and different particle sizes were applied directly to the fabric, and as a result of the ionic interaction between the positive charge on the ZnO surface and the negative charge of the dye molecules, or also due to Van-der-Waals forces an observed improvement in the colour takes place. As the ZnO nanoparticles concentration increase, the positive charges on the ZnO surface increase and this lead to the improvement of the colour as shown in Figure 56. Also by decreasing the particle size of ZnO nanoparticles, the surface

area increased which mean more ZnO-dye interaction which leads to colour strength improvement as shown in figure 57.

Figure 56 shows dyeing of cotton fabrics coated with different concentration of ZnO /GPTMS, as observed the higher the ZnO concentration the higher the depth of the colour.

Figure 57 shows dyeing of cotton fabrics coated with different particle sizes of ZnO /GPTMS, as observed smaller the ZnO concentration (bigger surface) the higher the depth of the colour.

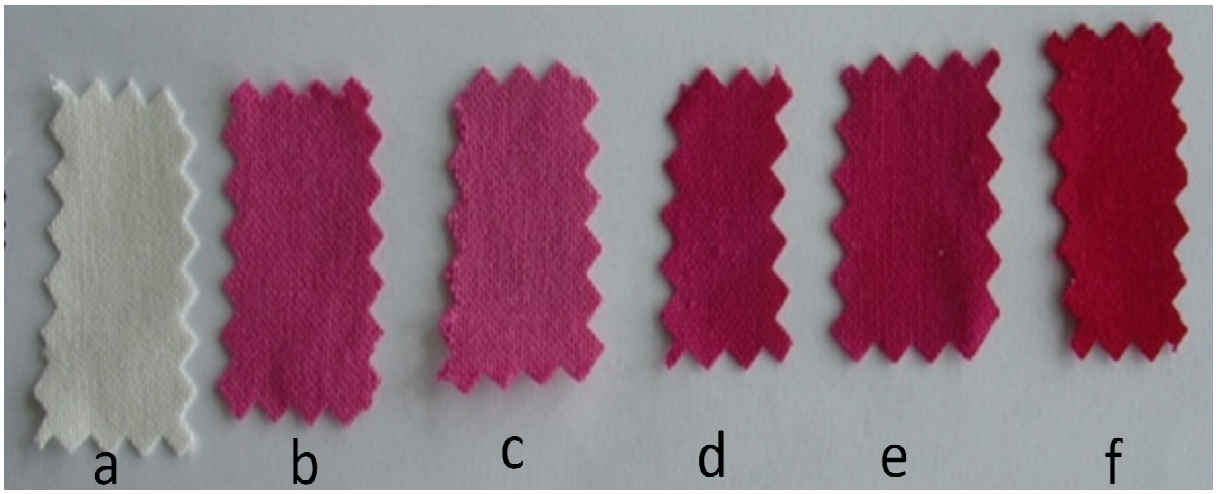


**Figure 56:** Dyeing of finished fabrics with different ZnO concentrations.

Since: (a) Untreated, (b) Dyed of fabric finished with GPTMS, (c) Fabric with only dye, (d) Dyed of fabric finished with 0.1 g/l ZnO, (e) Dyed of fabric finished with 0.5 g/l ZnO, and (f) Dyed of fabric finished with 1 g/l ZnO.

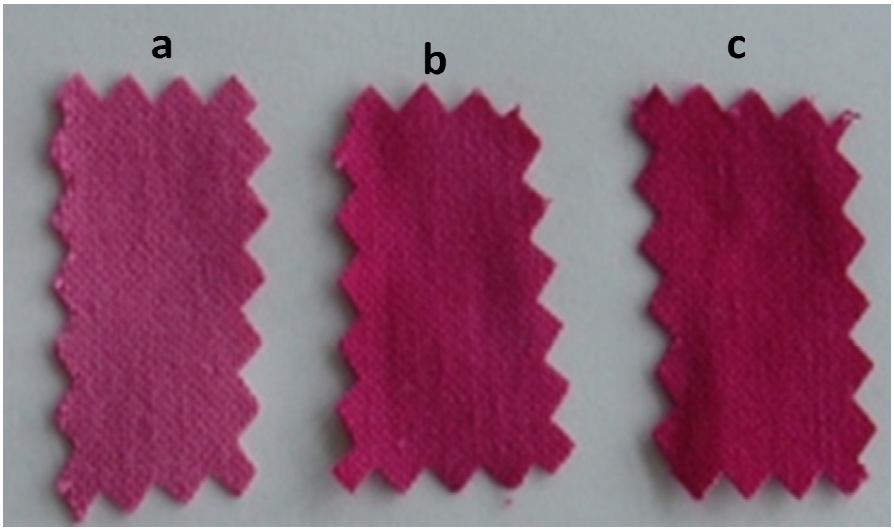


**Figure 57:** Dyeing of finished fabrics with different ZnO particle sizes.

Since: (a) Dyed of fabric finished with ZnO(1g/l) (625 nm) in GPTMS-sol, (b) Dyed of fabric finished with ZnO(1 g/l) (245 nm) in GPTMS-sol, and (c) Dyed of fabric finished with ZnO(1 g/l) (30nm) in GPTMS-sol.

The color properties of the dyed samples were determined using Datacolor spectrophotometer 3880 (cocos Manual Version 2, 3). The relative color strength and staining on white sample were determined with the Kubelka-Munk equations. The color strength was recorded by the K/S value, higher the value of K/S greater is the color strength [135]

$$K/S = (1 - R^2) / 2R$$

Where R is the reflectance of the dyed fabric; K is the absorption coefficient, and S is the scattering coefficient.

Figure 59 shows the color strenght which was recorded by the K/S value for cotton fabrics treated with1 g/l ZnO of different particle size in GPTMS. As observed from the figure, the smaller the particle size of the ZnO treated fabric, the higher the value of K/S which indicates the higher color depth.

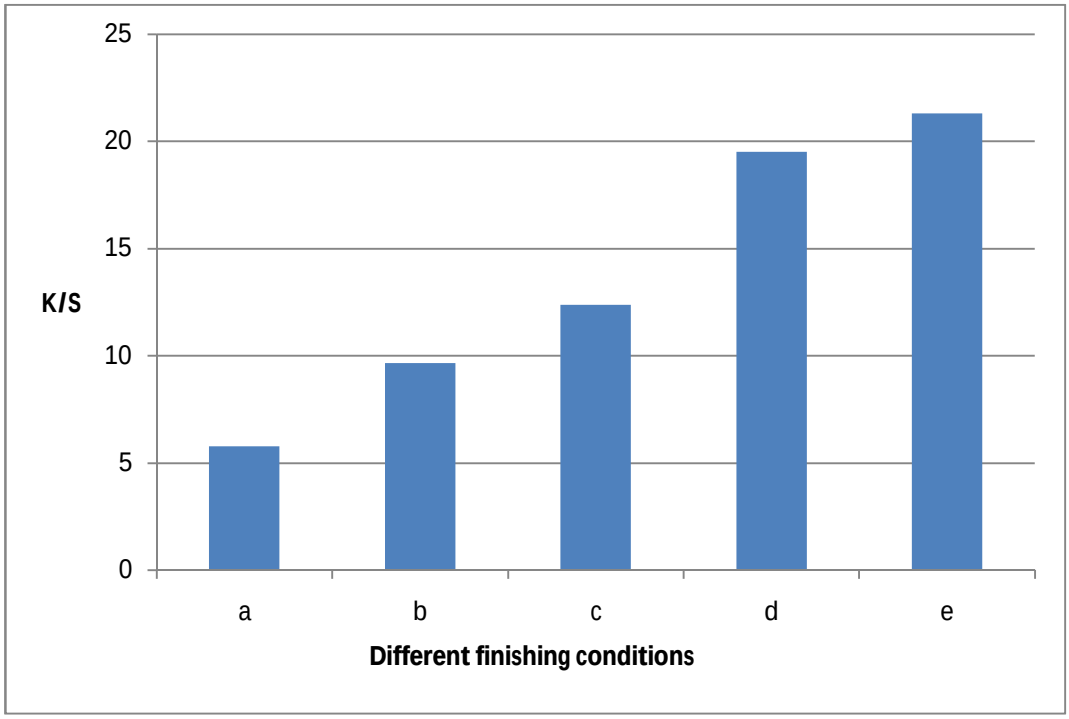


**Figure 58:** Dyeability of finished cotton for reactive dye which expressed by K/S, (a) Untreated (only dye), (b) Dyed of fabric finished with GPTMS, (c) Dyed of fabric finished with ZnO (625 nm) in GPTMS-sol, (d) Dyed of fabric finished with ZnO (245 nm) in GPTMS-sol, and (e) Dyed of fabric finished with ZnO (30nm) in GPTMS-sol May be other experiments should be carried out in the future to be able to understand of the influence of ZnO nanoparticles in the dying process e.g. using cationic dye instead of the anionic.

### 3.7.3. UV-protection property of dyed coated fabrics

Reactive dyes were used to impart UV- Protection to cotton fabric of different construction [136]. Dyes may increase UV Protection depending on their absorption characteristics in the UV- region. UV absorption by dyes depends on the molecular structural of the dye.

The dyes used to stain the fabric can have a great influence of fabric UPF. In order to achieve a color, dyes must selectively absorb visible radiation. The absorption band for some dyes extends into the UVR spectral region so that such dyes act as UVR absorbers. These dyes will therefore increase the fabric UPF value.

The UVR absorption property of each dye is unique to that dye, so it is difficult to generalize. However, for the same fabric construction and dye, darker shades generally increase the fabric UPF value [137,138].

In this study, dying of cotton treated fabrics with the reactive dye improve the UV-protection property of the fabrics. Table 17 shows the effect of dying on the UPF rating of the fabrics treated with ZnO of different particle size. As observed from the table the smaller the particle size of ZnO within the coating layer, the higher the K/S value (higher color strength) as well as the UPF vales, this is may be also due to that the smaller particles mean bigger surface which lead to more ZnO-dye interaction, in this case the absorption of the UV- radiation increase and the transmittance decrease which finally leads to UPF values increased. Compared to the blank sample, all the dyed fabric samples treated with ZnO/GPTMS has an excellent protection.

**Table 17:** Effect of dyeing on the UPF rating of the fabrics treated with different particle size of ZnO.

| Substrate | | K/S | UPF value | | UV Protection |
|---|---|---|---|---|---|
| Untreated | Cotton | 1.53 | 21 | 20 | good |
| Dyed of fabric finished with GPTMS | Cotton | 9.03 | 19 | 15 | good |
| Dyed of fabric finished with ZnO (30nm) in GPTMS-sol | Cotton | 20.16 | 78 | 50+ | excellent |
| Dyed of fabric finished with ZnO (245 nm) in GPTMS-sol | Cotton | 18.80 | 62 | 50+ | excellent |
| Dyed of fabric finished with ZnO (625 nm) in GPTMS-sol | Cotton | 11.89 | 56 | 50+ | excellent |

# Chapter 4

# 4. Conclusion and outlook

## 4.1. Conclusion

The nanosized zinc oxide particles were synthesized and applied for the preparation of functional coating for inorganic-organic hybrid materials. Final coating solutions were stable for several hours showing minimal precipitation which is sufficient for an industrial application. These hybrid materials can be applied to textile materials by a simple pad-cure method at 130°C for 30 min-here shown for cotton (100%) and cotton/polyester (65/35%) fabrics. The sol-gel approach used here for the preparation of the coating materials guarantees a simple processing easily transferred to textile industry. SEM investigations were carried out to investigate changes in the topography of the treated samples compered to the untreated one. Furthermore the principles of sol-gel technique allow combining additional properties in a single coating material. The general results can be concluded as:

i. The resulting treated textile materials achieve significantly improved UV-absorption of high durability, without affecting the textile, changing air permeability and even improving the wear resistance. The use of hybrid polymers modified with ZnO is therefore a promising approach for the development of highly UV-protecting textiles. The inorganic UV-absorber ZnO is highly stable against degradation and it is non-toxic. UV-protection of treated textiles was evaluated by calculating the UPF of the samples. The higher the UPF, the higher the UV-protection of the fabrics. In the coating layer the higher the ZnO concentrations, the higher the UPF of the fabrics. Effect of increasing the concentration of ZnO-sol on some performance properties of cotton and cotton blend fabric samples e.g. tensile strength, air permeability, degree of Whiteness, abrasion resistance and bending stiffness was also studied.

ii. The antibacterial performance of these sol-gel derived hybrid materials is exemplarily investigated against Gram-negative bacterium *E.coli* DSMZ

498 and Gram–positive *Micrococcus lutues* ATCC 9341. The resulting treated textile materials get antibacterial effect and the performance of coated fabrics with different concentrations and different particle sizes of ZnO as an antibacterial agent was investigated. The antibacterial activity of the coated fabrics was tested using some bacteriological tests e.g. zone of inhibition test, AATTC Test Method 100-2004, and tetrazolium/formazan (TTC). The antibacterial activity of fabrics treated with ZnO nanoparticles increases with increasing nanoparticle concentration and also increases with decreasing particle size. The enhanced bioactivity of smaller particles is attributed to the higher surface area to volume ratio. The release of $H_2O_2$ from ZnO surface may contribute to the cell damage of bacteria, but it is not the main mechanism of the antibacterial activity of ZnO nanoparticles; since the generation of oxyradicals or hydroxyl radicals (which investigated by using DPPH radical dye) may also contribute to the antibacterial activity of the prepared ZnO nanoparticles. SEM and the Fluorescence Microscope analyses suggest the direct interaction between ZnO particles surface and the membrane surface of bacteria. One of the probable causes for the break or decomposition of bacteria could be direct interaction between ZnO nanoparticles and the external membrane surface.

iii. As completed part of improving the antibacterial activity of ZnO nanoparticle sol, the antibacterial activity of ZnO sol together with chitosan as composite was also investigated against Gram-negative bacterium *E.coli* DSMZ 498 and Gram–positive *Micrococcus lutues* ATCC 9341. Chitosan of different MW ($1.36.10^5$, $2.2.10^5$ and $3.0.10^5$ Da) and the same degree of deacetylation (85%) were used. From the results we found that ZnO sol/ chitosan (low MW) composite has better antibacterial activity, since the decrease of molecular weight of chitosan increase the antibacterial activity and this phenomenon was explained as the decrease of chitosan molecular weight improves the movement of polymer chains in the solution by decrease the viscosity.

iv. Superhydrophobic surfaces on cellulosic textiles have been successfully prepared. Sol-gel based inorganic-organic hybrid polymers (GPTMS) were modified with ZnO nanoparticles and were applied to cotton (100%) and cotton/polyester (65/35%) fabrics, followed by hydrophobization with

stearic acid, hydrophilic cellulosic fabrics were made superhydrophobic. After the samples modified by stearic acid, the water CA become over 140°. But when ZnO nanoparticles are incorporated onto the fabric surface we had got water CA over 150° depending on the particle size of ZnO. The bigger the particle size, the higher the contact angle. Durability non-wetting of the coated fabrics was investigated using Martindale test.

v. Photocatalytic activity of ZnO nanoparticle resuspended solutions with different concentrations (0,1 g/l, 0,5 g/l and 1 g/l) was evaluated under dark condition, in normal laboratory environment and after UV-irradiation using MB dye, since the decolouration of MB dye using different ZnO nanoparticle concentrations was evaluated. Also photocatalytic activity of fabrics coated with ZnO/GPTMS nanocomposite with different ZnO concentrations (0,1 g/l, 0,5 g/l and 1 g/l) (30 nm) was evaluated through the fabric self-cleaning of MB dye stains. Self-cleaning takes place at the cotton 100% fabric surface under UV- irradiation after only 10 min.

vi. Dyeing of finished fabrics with reactive dye using Intracron red BF-3RM 150% together with the evaluation of the UV-protection property of dyed coated fabrics were also studied. Dyeability and UV-protection of finished cotton for reactive dye which expressed by K/S and UPF values respectively.

## 4.2. Outlook for future work

Application of sol-gel derived inorganic-organic hypride polymer based on other kind of polymer with different amounts could be done. It is also interesting to study the effect of storage on some of the studied properties like antibacterial activity of the textiles to be able to understand the activity of the material against washing of the treated samples. For the reaction between the ZnO nanoparticles and the reactive dye to be clear, other kind of dye could be used e.g. cationic dye with study of some factors which may affect the strength of the color like pH value and temperature used in the dying process.

# References


1- Schindler, W. D.; Hauser, P. J. Chemical Finishing of Textiles, Woodhead publishing Limited, Cambridge England, 2004.

2- Göcek, I.; Kursun, S.; Kücük, G. Applications of Nanotechnology in Textile Industry, Nonwoven Tech. Texti. Techn. Dergisi, 2006.

3- Mahltig, B.; Haufe, H.; Böttcher, H. *J. Mater. Chem.* **2005**,15, 4385-4398.

4- Kathirvelu, S.; Souza, L. D.; Dhurai, B. *Indian J. of Fiber & Textile Res*. **2009** 34, 267-273.

5- Luther, W. Industrial application of nanomaterials-chance and risk, Future Technologies Division, Düsseldorf, 2004.

6- Sharmila, D.; Rameshkumar, C.; Ganeshlbau, C. Nano–Technology: Small Wonders to Textiles 2004.

7- Lapidot, N.; Gans, O.; Biagini, F.; Sosonkin, L.; Rottman, C. *J. Sol–Gel Sci. Technol.,* **2003**, 26, 67–72.

8- Hoffmann, K.; Avermate, A.; Laperr, J.; *Arch dermatol.* **2001**, 137.

9- Parthasarathi, V. Nanotechnology adds value to textile finishing 2008, available from www.fibre2fashion.com.

10- Marc Van Parys, Textile Lamination and coating conference, 2010.

11- AATCC Technical Manual, **2002**, 77, 341-343.

12- Standards Association of Australia, Standard AS/NZS 43399; Australian/New Zealand Standards, Homebush, Australia, 1996.

13- Algaba, I.; Riva, A. *Coloration Technology*, **2002**, 118, 52-58.

14- Farouk, A.; Textor, T.; Schollmeyer, E.; Tarbuk, A.; Marija, A. *AUTEX Research Journal*, **2009**, 9, 4.

15- Papaspyrides, C. D.; Pavlidou, S.; Vouyiouka, S. N. *J. Materials: Design and Applications* 2009.

16- Ramachandran, T.; Rajendrakumar, K.; Rajendran, *R. IE (I) Journal-TX*, **2004**, 84.

17- Sahin, B. 'Fluorochemicals in textile finishing', *International Textile Bulletin – Dyeing/Printing/Finishing,* **1996**, 42, 26–30.

18- Barthlott, W.; Neinhuis, C. *Planta*, **1997**, 202.

19- Wenzel, R. N. *Ind. Eng. Chem.* **1936**, 28, 988.

20- Cassie, A.B. D.; Baxter, S. *Trans. Faraday Soc.* **1944**, 40, 546.

21- Roe, B.; Zhang, X. *Text. Res. J.,* **2009**, 79, 1115–1122.

22- Daoud, W. A.; Xin, J. H.; Tao, X. *J. Am. Ceram. Soc*. **2004**, 87, 1782–1784.

23- Xie, Q. D.; Xu, J.; Feng, L.; Jiang, L.; Tang, W. H.; Luo, X. D.; Han, C.C. *Adv. Mater.* **2004**, 16, 302.

24- Tuteja, A.; Choi, W.; Ma, M. L.; Mabry, J. M.; Mazzella, S. A.; Rutledge, G. C.; McKinley, G. H.; Cohen, R. *E. Science* **2007**, 318, 1618.

25- Zhai, L.; Cebeci, F.C.; Ohen, R. E.; Rubner, F. ano *Lett.* **2004**, 4, 1349.

26- Furstner, R.; Barthlott, W.; Neinhuis, C.; Walzel, P. *Langmuir* **2005**, 21, 956.

27- Han, W.; Wu, D.; Ming, W. H.; Niemantsverdriet, H.; Thune, P. C. Langmuir **2006**, 22, 7956.

28- Kulkarni, S. A.; Ogale, S. B.; Vijayamohanan, K. P. *J. Colloid Interface Sci.* **2008**, 318, 372,.

29- Li, X. M.; Reinhoudt, D.; Crego-Calama, M. *Chem. Soc.Rev.* **2007**, 36, 1350.

30- Gao, L. C.; McCarthy, T. J. *Langmuir* **2006**, 22, 5998.

31- Nystrom, D.; Lindqvist, J.; Ostmark, E.; Hult, A.; Malmstrom, E. *Chem. Commun.* **2006**, 34, 3594.

32- Wang, T.; Hu,X. G.; Dong, S. J *Chem. Commun*. **2007**,1849.

33- Yu, M.; Gu, G. T.; Meng, W. D.; Qing, F. L. *Appl. Surf. Sci.* **2007***,* 253, 3669.

34- Hoefnagels, H. F.; Wu, D.; de With, G.; Ming, W. *Langmuir* **2007**, 23, 13158.

35- Li, Z.; Xing, Y.; Dai, *J. Appl. Surf. Sci*. **2008**, 254, 2131.

36- Michielsen, S.; Lee, H . J. *Langmuir* **2007**, 23, 6004.

37- Satoh, K.; Nakazumi H.; Morita, M. *Text. Res. J.* **2004**, 74, 1079–1084.

38- Textor, T.; Bahners, T.; Schollmeyer, E. *Melliand Textilber. Int.* **1999**, 80, 847–848.

39- Textor, T.; Bahners T.; Schollmeyer, E. *Prog. Colloid Polym. Sci.* **2001**, 117, 76–79.

40- Yeol, G.; Gil, B.; Gyu, Y.; Cheol, S.; Ho, J.; Hoe, G. *J. of Coll. and Inter. Science* **2009**, 337, 170-175.

41- Hsieh, C. T.; Wu, F. L.; Yang, S. Y.; *Surf. Coat. Technol.* **2008**, 202, 6103-6108.

42- Mahltig, B.; Böttcher, H. *J. Sol–Gel Sci. Technol*. **2003**, 27, 43–52.

43- Arbeitsgruppe “Textile Vorbehandlung“ *Melliand Textilber*. **1987**, 8, 581-583.

44- Kathirvelu, S.; Louis, S.; Bhaarathi D. *Indian Journal of Science and Technology* **2008**, 1, 5.

45- Hong, R. Y.; Li, J. H.; Chen, L. L.; Liu, D. Q.; Li, H. Z.; Zheng, Y. *J. Ding, Power Technology* **2009**, 189, 426-432.

46- Luo M., Zhang X. L., Chen S. L. *Coloration Technology* **2003**, 119, 5, 297.

47- Du J.; Zhan L.; Chen S. L.; *Coloration Technology* **2005**, 121, 1, 29.

48- Xiaoyan L.; Wei W.; Peng X. *FIBRES & TEXTILES in Eastern Europe* **2010**,18,1, 93- 96.

49- Wenbin L.; Lingli Z.; Xingpin Z.; Xiaqin W.; Dajun C. *J. of Appli. Poly. Sci.* **2007**, 106, 1670-1676.

50- Yunjie Y.; Chaoxia W.; Chunying W. *J. Sol-Gel Technol.* **2008**, 48, 308-314.

51- Sirachaya K. N. A.; Parawee T.; Okorn M.; Varong P.; Piyasan P. *Crystal Growth & Design* **2006**, 6, 11, 2446-2450.

52- Hay, J. N.; Raval, H. M. *Chem. Mater.* **2001**, 13, 3396.

53- Xin, J. H.; Daoud, W. A.; Kong, Y. Y. *Textile Research Journal* **2004**, 74, 2, 97-100.

54- Hudson, M. J.; Peckett, J. W.; Harris, P. J. F. *J. Mater. Chem.* **2003**, 13, 445.

55- Dire, S.; Campostrini, R.; Ceccato, R. *Chem. Mater.* **1998**, 10, 268.

56- Ksapabutr, B.; Gulari, E.; Wongkasemjit, S. *Mater. Chem. Phys.* **2004**, 83, 34.

57- a) Huang, J.; Matsunaga, N.; Shimanoe, K.; Yamazoe, N.; Kunitake, T. *Chem. Mater.* **2005**, 17, 3513; b) Baumann, T. F.; Kucheyev, S. O.; Gash, A. E.; Satcher, J. H. *Adv. Mater.* **2005**, 17, 1546.

58- Kovtyukhova, N. I.; Mallouk, T. E.; Mayer, T. S. *Adv. Mater.* **2003**, 15, 780.

59- Oral, A. Y.; Mensur, E.; Aslan, M. H.; E.Basaran, E. B. *Mater. Chem. Phys*. **2004**, 83, 140.

60- Ji, L.; Lin, J.; Zeng, H. C. *Chem. Mater*. **2000**, 12, 3466.

61- a) Oliveira, M. M.; Schnitzler, D. C.; Zarbin, A. J. G. *Chem. Mater*. **2003**, 15, 1903; b) Uchiyama, H.; Imai, H. *Chem. Commun*. **2005**, 48, 6014.

62- Niederberger, M.; Garnweitner, G.; Pinna, N.; Antonietti, M. *J. Am.Chem. Soc.* **2004**, 126, 9120; b) Choa, J. H.; Kuwabara, M. *J. Eur. Ceram. Soc.* **2004**, 24, 2959.

63- Veith, M.; Mathur, S.; Lecerf, N.; Huch, V.; Decker, T.; Beck, H. P.; Eiser, W.; Haberkorn, R. *J. Sol-Gel Sci. Technol*. **2000**, 17, 145.

64- Azad, A. M.; Hashim, M.; Baptist, S.; Badri, A.; Haq, A. U. *J. Mater. Sci*. **2000**, 35, 5475.

65- Becheri, A.; Dürr, M.; Baglioni, P. *J. Nanopart. Res*. **2008**, 10, 679-689.

66- Riva, A.; Algaba, I. M.; Pepio, M. *Modelisation of the effect. Cellulose* **2006**, 13, 697–704.

67- Lu, H.; Fei, B.; Xin, J. H.; Wang, R. H.; Li , L. *J Colloid Interface Sci*. **2006** 300, 111–116.

68- Yadav, A.; Prasad, V.; Kathe, A. A.; Raj, S.; Yadav, D.; Sundaramoorthy, C.; Vigneshwaran, N. *Bull Mater Sci*. **2006**, 29, 641–645.

69- Cross, R. B. M.; De Souza, M. M.; Narayanan, E. M. S. *Nanotechnology* **2005**, 16, 2188.

70- Sato, H.; Ikeya, M. *J. Appl. Phys.* **2004**, 95, 3031–3036.

71- Pan, Z. W.; Dai, Z. R.; Wang, Z. L. *Mat. Science* **2001**, 291, 1947–1949.

72- Arnold, M. S.; Avouris, P.; Pan, Z. W.; Wang, Z. L. *J. Phys. Chem*. **2003**, B 107, 659–663.

73- Li , Y. Q.; Fu, S. Y.; Mai, Y. M. *Polymer Scei.* **2006**, 47, 2127–2132,.

74- Sawai, J. *J. Microbiol. Methods* **2003**, 54, 177–182.

75- Bahnemann, D. W.; Kormann, C.; Hoffmann, M. R. *J. Phys. Chem*. **1987**, 91, 3789.

76- Kang, X. Y.; Wang, T. D.; Han, Y.; Tao, M. D.; Tu, M. *J. Mater. Res. Bull*. **1997**, 32,1165.

77- Lokhande, J.; Patil, P. S.; Uplane, M. D. *Mater. Lett*. **2002**, 57, 573.

78- Vayssieres, L.; Keis, K.; Lindquist, S. E.; Hagfeldt, A. *J. Phys. Chem*. **2001**, B 105, 3350.

79- Yu, S. H.; Yoshimora, M. *Adv. Mater*. **2002**, 14, 296.

80- Smith, S. M.; Schlegel, H. B. *Chem. Mater*. **2003**, 15, 162.

81- Music, S.; Dragcevic, D.; Maljkovic, M.; Popovic, S. *Mater. Chem. Phys*. **2002**, 77, 521.

82- Lu, C. H.; Yeh, C. H. *Mater. Lett.* **1997**, 33, 129.

83- Xu, H. Y.; Wang, H.; Zhang, C.; He, W. L.; Zhu, M. K.; Wang, B.; Yan, H. *Ceram. Inter*. **2004**, 30, 93.

84- Kwon, Y. J.; Kima, K. H.; Limb, C. S.; Shim, K. B. *J. Ceram. Proc. Res*. **2002**, 3, 146.

85- Wang, Z. J.; Zhang, H. M.; Zhang, L. G.; Yuan, J. S.; Yan, S. G.; Wang, C. Y. *Nanotechnology* 2003.

86- Komarnenia, S.; Brunoa, M.; Mater, E. M. *Res. Bull*. **2000**, 35, 1843.

87- Rodrıguez-Gattorno, G.; Santiago-Jacinto, P.; Rendon-Vázquez, L.; Nemeth, J.; Dekany, I.; Diaz, D. *J. Phys. Chem*. **2003**, B 107, 12597.

88- Li, Z. Q.; Xiong, Y. J.; Xie, Y. *Inorg. Chem.* **2003**, 42, 8105.

89- Yan, H. Q.; He, R. R.; Johnson, J.; Law, M.; Saykally, R. J.; Yang, P. D. *J. Am.Chem. Soc.* **2003**, 125, 4728.

90- Jie, J. S.; Wang, G. Z.; Han, X. H.; Yu, Q. X.; Liao, Y.; Li, G. P.; Hou, J. G. *Chem. Phys. Lett.* **2004**, 387, 466.

91- Hsu, J. W. P.; Tian, Z. R. R.; Simmons, N. C; Matzke, C. M.; Voigt, J. A.; Liu, J. *Nano Lett.* **2005**, 5, 83.

92- Shen, X. P.; Yuan, A. H.; Hu, Y. M.; Jiang, Y.; Xu, Z.; Hu, Z. *Nanotechnology* **2005**, 16, 2039.

93- Wang, Z. L.; Kong, X. Y.; Zuo, J. M. *Phys. Rev. Lett*. **2003**, 91, 185502.

94- Sawai, J.; Saito, I.; Kanou, F.; Igarashi, H.; Hashimoto, A.; Kokugan T.; Shimizu, M. *J. Chem. Eng. Japan* **1995b**, 28, 352-354.

95- Sawai, J.; Igarashi, H.; Hashimoto, A.; Kokugan, T.; Shimizu, M. *J. Chem. Eng. Japan* **1996a**, 29, 251-256.

96- Sawai, J.; Kawada, E.; Kanou, F.; Igarashi, H.; Hashimoto, A.; Kokugan; T.; Shimizu, M. *J. Chem. Eng. Japan* **1996b**, 29, 627-633.

97- Yamamoto, O.; Hotta, M.; Sawai, J.; Sasamoto, T.; Kojima, H. *J. Ceram. Soc. Japan* **1998**, 106, 1007-1011.

98- Yamamoto, O. *Int. J. Inorgan. Mater*. **2001a**, 3, 643-646.

99- Adams, L. K.; Lyon, D. Y.; Alvarez, J. *J. Water Res* **2006**, 40, 3527–3532.

100- Brayner, R.; Ferrari-lliou, R.; Brivois, N.; Djediat, S.; Benedetti, M. F. *Nano Lett.* **2006**, 6, 866–870.

101- Jeng, H. A.; Swanson, J. J*. Environ Sci Health* **2006**, 41, 2699–2711.

102- Makhluf, S.; Dror, R.; Nitzan, Y.; Abramovich, Y.; Jelinek, R.; Gedanken, A. *Adv. Funct. Mater.* **2005**, 15, 1708–1715.

103- Stoimenov, P. K.; Klinger, R. L.; Marchin, G. L.; Klabunde, K. J. *Langmuir* **2002**, 18, 6679–6686.

104- Zhang, L.; Jiang, Y.; Ding, Y.; Daskalakis, N.; Jeuken, L.; Povey, M.; York,D. *J Nanopart. Res.* **2009**.

105- Zhang, L.; Jiang, Y.; Ding, Y.; Povey, M.; York, D. *J. Nanopart. Res*. **2007**,9, 479-489.

106- Tang, L.; Zhou, B.; Tian, Y.; Bala, H.; Pan, Y.; Ren, S.; Wang, Y.; Lv, X.; Li,M.; Wang, Z. *Colloids Surf.* **2007**, A 296, 92.

107- Wu, X.; Zheng, L.; Wu, D. *Langmuir* **2005**, 21, 2665.

108- Badre, C.; Dubot, P.; Lincot, D.; Pauporte, T.; Turmine, M. *J. Colloid Interface Sci.* **2007**, 316, 233.

109- Badre, C.; Pauporte, T.; Turmine, M.; Lincot, D. *Nanotechnology* **2007**, 18, 365705.

110- Guo, M.; Diao, P.; Cai, S. *Thin Solid Films* **2007**, 515, 7162.

111- Li, M.; Zhai, J.; Liu, H.; Song, Y.; Jiang, L.; Zhu, D. *J. Phys. Chem*. **2003**, 107, 9954.

112- Daoud, W. A.; Xin, J. H.; Tao, X. *J. Am. Ceram. Soc*. **2004**, 87, 1782 – 1784.

113- Spanhel, L.; Anderson, M. A. *J. Am. Chem. Soc*. **1991**, 113, 2826.

114- Xue, C. H.; Jia, S: T.; Chen H. Z.; Wang, M. *Sci. Technol. Adv. Mater*. **2008**, 9.

115- Yamamoto, O.; Hotta, M.; Sawai, J.; Sasamoto, T.; Kojima, H. *J. Ceram. Soc. Japan* **1998**, 106, 1007-1011.

116- Fouda, M.; Knittel, D.; Zimehl, R.; Hipler, C.; Schollmeyer, E. *Adv. Chitin Sci*. **2005**, 8, 418.

117- Seidler, E. The tetrazolium-formazan system: design and histochemistry, Gustav Fischer Verlag, New York, 1991.

118- Vogel AI. Elemental practical inorganic chemistry, part 3, Quantitative inorganic analysis. Longman, 1975.

119- German DIN Book–Methods of Analysis, 53890, 1972.

120- Zhang, J.; Sun, L.; Yin, J.; Su, H.; Liao, C.; Yan, C. *Chem. Mater.* **2002**, 14, 4172.

121- Lee, J. S.; Choi, S. C. *J. Eur. Ceram. Soc.* **2005**, *25*, 14, 3307.

122- Mahltig, B.; Textor, T. Nanosols & Textiles, World Scientific Publishing Co, Singapore, 2008.

123- Wang, H.; Wingett, D.; Engelhard Mark H.; Feris , K. *J. Mater. Sci. Mate.r Med.* **2009**, 20, 11-22.

124- Stoimenov, P.K.; Klinger,R. L; Marchin,G. L.; Klabunde, K. J. *Langmuir*. **2002**, 18, 6679-6686.

125- Jeng, H. A.; Swanson, J. *J Environ Sci. Health* **2006**, 41, 2699-2711.

126- Parks, G. A. The isoelectric points of solid oxides, solid hydroxides, and aqueous hydroxo complex system, *Chem. Rev*. **1965**, 65, 177-198.

127- Dunn, E. T.; Grandmaison, E. W.; Goosen, M. F. A. *J. Bioact. Compat. Poly.***1992**, 7, 370-397.

128- Li-Hua L.; Jian-Cheng D.; Hui-Ren D.; Zi-Ling L.; Ling X. Carbohydrate Res. **2010** 345, 994-998.

129- Salehi, R.; Arami, M.; Mahmoodi, N.; Bahrami, H.; Khorramfar, S. *Colloids Surf B Biointerfaces.* **2010**, 80, 1, 86-93.

130- Karolia, A.; Mendapara, S. *Indian Jour. of Fibre & Text. Res.* **2007**, 32, 99-104.

131- Ruh, U.; Joydeep D. *Journal of Hazardous Material* **2008**, 156, 194-200.

132- Su, S., Lu, S. X.; Xu, W. G. *Material Research Bulletin* **2008**, 43, 2172-2178.

133- Kensal, S. K.; Kaur, N.; Singh, S. *Nanoscale Res. Lett.* **2009**, 4, 709–716.

134- Zheng, L.; Hai, X.; Ke, F.; Lian, W. *AATCC Review* 2007.

135- Sarkar, A. K.; Seal, C. M.; *Clothing and Textiles Research Journal* **2003**, 21,162- 166.

136- Sharma, D. K.; Singh, M. *A study Colourage Annual* **2001**, 69.

137- Curiskis, Pilthorpe, *Textile Magazine* **1996**, 25, 4, 13.

138- Srinivasan, M.; Gatewood, B. M. *AATCC* **2000**, 32, 4, 36.

# 5. Appendix

## 5.1. Abbreviations

| | |
|---|---|
| ATCC | American Type Culture Collection |
| ATR-FTIR | Attenuated total reflection-fourier transform infrared spectroscopy |
| B | Blank |
| CA | Contact angle |
| CFU | Colony forming unit |
| CO | Cotton |
| CO/PET | Cotton/polyester |
| CRA | Crease recovery angle |
| CT | Chitosan |
| DD | Degree of deacetylation |
| DLS | Dynamic light scattering |
| DPPH | 2,2-Diphenyl-1-pikryl hydrazyl |
| E.Coli | Escherichia coli |
| FITC | Fluoresceince isothiocyanate |
| GPTMS | 3-Glycidyloxypropyltrimethoxysilan |
| HPAEC-PAD | High performance anion exchange chromatograph-plused amperometric detection |
| K/S | Color strength |
| M.Lutues | Micrococcus lutues |
| MB | Methylen blue |
| MW | Molecular weight |
| N | Normality |
| NTU | Normal Turbidity Unit |
| PCD | Particle charge detector |
| PDADMAC | Polydiallyl dimethyl ammonium chloride |
| PESNa | Polyethylen sulfonic acid, sodium salt |
| TTC | 2,3,5- Triphenyltetrazolium chloride |
| UPF | Ultraviolet protection factor |

| | |
|---|---|
| UV-vis | Ultraviolet-visible |
| V | Volume |
| Wt | Weight |
| ZnAc | Zinc acetate |

# 5.2. Publications

## List of previous publications

1- N. A. Ibrahim, R. Refai, **A. F. Ahmed**. Proper finishing treatments for sun protective cotton-containing fabrics.
J. of Applied polymer Science, 97, 3, 1024-1030, 2005.

2- N. A. Ibrahim, R. Refai, **A. F. Ahmed**. New approach for improving UV-protecting properties of woven cotton fabrics.
Polymer-Plastic technology and engineering, 44, 5, 919-930, 2005

3- N. A. Ibrahim, R. Refai, **A. F. Ahmed**. Novel approach for attaining cotton fabrics with multi-functional properties.
J. of Industrial Textiles, 40, 1, 2010

## List of publications during doctoral study

1- **A. F. Ahmed Saleh**, T. Textor, E. Schollmeyer, A. tarbak. Sol-gel derived inorganic-organic hybrid polymers filled with ZnO nanoparticles as ultraviolet protection finish for textiles.
AUTEX Research Journal 9, 4, 2009

2- **A. F. Ahmed Saleh**, T. Textor, E. Schollmeyer, S. Moussa. Sol-gel derived inorganic-organic hybrid polymers filled with ZnO nanoparticles as antibacterial finish for textiles.
$10^{th}$ Intternational conference on Applied Surface Engineering, Singapore.
ASIA-PACIFIC INTERFINISH 2010.

## 5.3. Conference proceedings

### Oral Paper in International Conference

1- **A. F. Ahmed Saleh**, T. Textor, E. Schollmeyer, S. Moussa. Sol-gel derived inorganic-organic hybrid polymers filled with ZnO nanoparticles as antibacterial finish for textiles.
10th Intternational conference on Applied Surface Engineering, Singapore.
ASIA-PACIFIC INTERFINISH OCT. 2010.

### Poster Paper in International Conference

1- **A. F. Ahmed Saleh**, T. Textor, E. Schollmeyer, S. Moussa. ZnO nanoparticles-chitosan composite as antibacterial finish for textiles.
4th Aachen-Dresden International Textile
Conference Dresden, November 25-26, 2010.

### Other Posters

1- **A. F. Ahmed Saleh**, T. Textor, E. Schollmeyer, Photocatalytic degradation of methylene blue by ZnO nanoparticles.
CeNiDE (Center for Nanointegration Duisburg-Essen) am 10.11.2010.

2- **A. F. Ahmed Saleh**, T. Textor, E. Schollmeyer, S. Moussa. Sol-gel derived inorganic-organic hybrid polymers filled with ZnO nanoparticles as antibacterial finish for textiles.
Junges Chemie Symposium Ruhr am Jcs-Ruhr am 09.09.2010

## 5.4. Courses

### Course during doctoral study

"Nanosized particles as building blocks for creation of nanostructures"
Erasmus Intensive Program held at Adam Mickiewicz University Poznan, Poland.
$9^{th}$-$22^{th}$ May 2010.

## 5.5. Curriculum Vitae

### Personal Data

**Name:** Asmaa Farouk Ahmed Saleh
**Date of Birth:** 4-3-1978
**Marital Status:** Married
**Nationality:** Egyptian
**Place of birth:** Cairo, Egypt

### Education

**1995-1999** Studied Chemistry in faculty of Science, Helwan University, Egypt.

**2000-2001** Preliminary Master Study courses in Organic Chemistry Department, Helwan University, Egypt.

**2002-2005** Studied for Master degree, Textile Research Division, National Research Center, Cairo, Egypt.

**2007-2011** Studied for Ph.D degree, at German Textile Research Institute, University of Duisburg-Essen; Adlerst.1; 47798-Krefeld, Germany.

### Awards

**May 1999** Bachelor of Science (BSc in Chemistry), (Very good with Honour degree), Chemistry Department, Faculty of Science, Helwan University, Egypt.

**April 2005** Master of Science (MSc in Organic Chemistry, Chemistry Department, Faculty of Science, Helwan University, Egypt.

### Employment and Responsibilities

**2002-2005** Researcher Assistant, Textile Research Division, National Research Center, Cairo, Egypt.

**2005-2006** Assistant Researchers, Textile Research Division, National Research Center, Cairo, Egypt.

**2007-2011** Studies for Ph.D degree at German Textile Research Institute, University of Duisburg-Essen; Krefeld, Germany.

## Permanent address

Asmaa F. A. Saleh

Textile Research Division,

National Research Centre, Tahrir St., Dokki-Cairo 12311-Egypt.

Fax: (+2)-02-3370931

Tele: (+2)-02-3371211, 3371362

e.mail: asmaafarouk2003@yahoo.com